



THE HONG KONG
POLYTECHNIC UNIVERSITY

香港理工大學

Pao Yue-kong Library

包玉剛圖書館

Copyright Undertaking

This thesis is protected by copyright, with all rights reserved.

By reading and using the thesis, the reader understands and agrees to the following terms:

1. The reader will abide by the rules and legal ordinances governing copyright regarding the use of the thesis.
2. The reader will use the thesis for the purpose of research or private study only and not for distribution or further reproduction or any other purpose.
3. The reader agrees to indemnify and hold the University harmless from and against any loss, damage, cost, liability or expenses arising from copyright infringement or unauthorized usage.

IMPORTANT

If you have reasons to believe that any materials in this thesis are deemed not suitable to be distributed in this form, or a copyright owner having difficulty with the material being included in our database, please contact lbsys@polyu.edu.hk providing details. The Library will look into your claim and consider taking remedial action upon receipt of the written requests.

**THE CYTOPROTECTIVE ROLE OF
AUTOPHAGY IN PODOCYTES**

YULIN KANG

Ph.D

The Hong Kong Polytechnic University

2014

The Hong Kong Polytechnic University
Department of Health Technology and Informatics

**THE CYTOPROTECTIVE ROLE OF
AUTOPHAGY IN PODOCYTES**

YULIN KANG

**A thesis submitted in partial fulfilment of the
requirements for the degree of Doctor of Philosophy**

June 2014

CERTIFICATE OF ORIGINALITY

I hereby declare that this thesis is my own work and that, to the best of my knowledge and belief, it reproduces no material previously published or written, nor material that has been accepted for the award of any other degree or diploma, except where due to acknowledgement has been made in the text.

_____ (Signed)

Yulin KANG (Name of student)

Abstract

Podocytes are highly differentiated cells which play an important role in guarding the permeability of the tripartite renal filtration barrier. Many glomerular diseases attribute to podocyte damage including apoptosis, cytoskeleton rearrangement and detachment. The gene mutation of podocyte cytoskeleton proteins has also been acknowledged in the pathogenesis of renal diseases. Thus, podocytes emerge as the therapeutic target of glomerular diseases. However, the strategies for preventing podocyte damage remain insufficient.

Recently autophagy has been described as a ubiquitous catabolic process involving degradation of damaged organelles and protein aggregates. It shows cytoprotective effects in many cell types and helps to maintain cell homeostasis. Autophagy is being kept at basal levels in cells for safeguarding and promoting cell survival. This basal autophagy is one of the major processes that allow cells to respond rapidly to the metabolic stress. Under certain circumstances, autophagy can be induced to a higher level to protect cells. Currently, the better-known potential stimuli inducing autophagy include nutrient starvation, oxidative stress, mitochondrial dysfunction, ischemia-reperfusion and infection.

Puromycin aminonucleoside (PAN) which induces podocyte apoptosis *in vitro* and *in vivo* is widely used for studying the pathophysiology of glomerular diseases. It has been shown that PAN induces autophagy in podocytes. However, the

relationship between autophagy and apoptosis in PAN-treated human podocytes is not known and the role of PAN-induced autophagy in podocyte survival remains unclear. In this thesis, we demonstrated that PAN induced autophagy in human podocytes prior to apoptosis which was featured with the activation of mTOR complex 1 (mTORC1). When the PAN-induced autophagy was inhibited by 3-methyladenine (3-MA) or chloroquine (CQ), podocyte apoptosis increased significantly along with the elevation of active caspase-3. Under such circumstance, the podocyte cytoskeleton was also disrupted. These results suggested that the observed induction of autophagy may be an early adaptive cytoprotective mechanism for podocyte survival after PAN treatment.

Since autophagy induction is beneficial for podocyte survival, it is reasonable to utilize this mechanism to attenuate podocyte injury. Trehalose, a natural disaccharide, is an mTOR independent autophagy inducer. It is unclear whether trehalose alleviates podocyte injury. Therefore, we investigated the efficacy of trehalose in PAN-treated podocytes. Human conditional immortalized podocytes were treated with trehalose with or without PAN. It was shown that trehalose induced podocyte autophagy in an mTOR independent manner and without reactive oxygen species involvement. PAN-induced podocyte apoptosis significantly decreased after trehalose treatment, while the inhibition of trehalose-induced autophagy abolished its protective effect. Additionally, the disrupted actin cytoskeleton of podocytes was partially reversed by trehalose, accompanied by less lamellipodias and diminished motility. These results suggested that trehalose

induced autophagy in human podocytes and showed cytoprotective effects in PAN-treated podocytes.

For confirming the efficacy of trehalose *in vivo*, PAN nephrosis rat model was established and treated with trehalose. It was shown that trehalose induced autophagy in glomeruli with increased LC3-II expression. However, proteinuria and hypoalbuminemia was not alleviated as well as the altered renal ultrastructure. These results suggested PAN-induced podocyte injury *in vivo* was not alleviated by trehalose.

Overall, this thesis showed the cytoprotective role of autophagy *in vitro*. Further investigation is warranted to determine the application of autophagy in the treatment of podocyte related renal diseases.

Publications

Scientific journal papers

1. Kang YL, Saleem MA, Chan KW, Yung BY, Law HK (2014) The cytoprotective role of autophagy in puromycin aminonucleoside treated human podocytes. *Biochemical and Biophysical Research Communications* 443: 628-634.
2. Kang YL, Saleem MA, Chan KW, Yung BY, Law HK. Trehalose, an mTOR independent autophagy inducer, alleviates human podocyte injury after puromycin aminonucleoside treatment. Submitted to *PLOS One* (Manuscript PONE-D-14-17769, under revision)

Conference abstracts

1. Kang YL, Saleem MA, Yung BY, Law HK. Puromycin aminonucleoside induces autophagy in human podocytes. *ISN World Congress of Nephrology, Hong Kong, May 31-June 4, 2013. Published in Conference Abstract SU011: 178. (Poster Presentation)*
2. Kang YL, Law HK, Huang WY, Zhu GH, He WX, Yung BY. The cytoprotective role of autophagy under oxidative stress in human podocytes. *The Sixteenth Congress of International Pediatric Nephrology Association, Shanghai, Aug 30-Sep 3, 2013. Abstract number: 1314. Published in Pediatric Nephrology 2013 28 (8): 1444 (Poster Presentation)*

3. Kang YL, Chan KW, Zhu GH, Huang WY, He WX, Yung BY, Law HK. Puromycin aminonucleoside-induced autophagy affects human podocytes survival. The Second Oriental Congress of Pediatrics (OCP), Shanghai, October 16-20, 2013. (Oral presentation)
4. Kang YL, Saleem MA, Yung BY, Law HK. Trehalose, an mTOR independent autophagy inducer, alleviates human podocyte injury after puromycin aminonucleoside treatment. 10th International Podocyte Conference, Freiburg, Germany, June 4-6, 2014. Abstract number:I12. Published in Nephron Clinical Practice 2014; 126:165. (Poster presentation)

Acknowledgements

I would like to express my sincere gratitude to my chief supervisor Dr. Helen LAW for her guidance, encouragement, patience and enthusiasm throughout my PhD study. I received excellent research training in nephrology and immunology with her help. I also greatly appreciate my co-supervisor Prof. Benjamin Yung for his valuable suggestions and comments in my PhD project and future career.

I sincerely thank Prof. Moin SALEEM and Dr. Lan NI from Academic Renal Unit, University of Bristol for generously providing human podocyte cell line and valuable suggestions in my study. Meanwhile, I sincerely acknowledge Dr. Kwok Wah CHAN from Department of Pathology, Li Ka Shing Faculty of Medicine, University of Hong Kong, as I got precious renal pathology training under his supervision.

My sincere thanks also go to Prof. Gregory STAHL from Harvard Medical School for providing me a precious opportunity to study in his famous laboratory. My knowledge in immunology and nephrology has been strengthened under his guidance. Meanwhile, I appreciate the help from Dr. Margaret MORRISSEY, Dr. Masayuki OZAKI, Dr. Vasile PAVLOV and Ying Siow TAN in Dr. STAHL's Lab. This 4-month study was supported by the Research Student Attachment Program in Hong Kong Polytechnic University.

I thank Prof. Sydney CW TANG, Clinical Professor of Medicine and Yu Professor in Nephrology at the University of Hong Kong, and Prof. HUANG Yu, Professor of Biomedical Sciences, The Chinese University of Hong Kong, for reviewing my thesis and giving me valuable insights into future studies.

Great appreciation is given to Dr. Parco SIU, Prof. Shea-Ping YIP, Dr. Lawrence CHAN, Dr. Daniel SZE, Dr. Michael YING, Dr. Patrick LAI for their helpful suggestions and comments in my PhD study. I also would like to acknowledge Mrs. Brenda WONG, Ms. Sharon HO, Mrs. Grace TANG, Dr. Maran LEUNG, Dr. Blanka LEE for their expert technical assistance. Meanwhile, I express my gratitude to all my classmates and friends in Hong Kong Polytechnic University for their help in my study and life.

Last but not the least, I would like to thank my family for their persistent supports and encouragement throughout my PhD study.

[This work was partially supported by grants to my supervisor Dr. Helen Law (i) Competitive Research Grants for Newly Recruited Junior Academic Staff (NRJS-A-PM13); (ii) Departmental Research Fund, The Hong Kong Polytechnic University and (iii) Early Career Scheme from Research Grants Council of the Hong Kong Special Administrative Region, China (RGC#589413).]

Table of Contents

Certification of Originality.....	i
Abstract.....	ii
Publications.....	v
Acknowledgements.....	vii
Table of contents.....	ix
List of Figures.....	xiii
List of Abbreviations.....	xvii

1. Introduction

1.1 Podocytes emerges as a new therapeutic target of glomerular diseases	
1.1.1 Podocyte structure.....	1
1.1.2 Actin cytoskeleton in podocyte.....	5
1.1.3 Podocyte apoptosis.....	14
1.1.4 Strategies for decreasing podocyte apoptosis.....	20
1.1.5 Podocyte motility.....	23
1.2 Autophagy is a potential therapeutic approach for renal diseases	
1.2.1 Introduction of autophagy.....	24
1.2.2 Mammalian target of rapamycin (mTOR) in autophagy induction.....	28
1.2.3 TOR-autophagy spatial coupling compartment (TASCC) in autophagy induction.....	31
1.2.4 ROS in autophagy induction.....	33
1.2.5 The crosstalk between apoptosis and autophagy.....	34
1.2.6 Autophagy in podocytes.....	36

1.3	Trehalose is an mTOR independent autophagy inducer	
1.3.1	Introduction of trehalose.....	38
1.3.2	Trehalose induces autophagy in mammalian cells.....	39
1.4	Hypothesis and Objectives	
1.4.1	Hypothesis.....	41
1.4.2	Objectives.....	42

2. Methods and materials

2.1	Cell culture.....	43
2.2	Western blotting.....	43
2.3	Immunofluorescence staining.....	47
2.4	Flow cytometry.....	48
2.5	Reactive Oxygen species measurement.....	50
2.6	Necrosis measurement.....	50
2.7	Migration assay.....	50
2.8	Establishment of PAN nephrosis rat model.....	51
2.9	Trehalose treatment in PAN nephrosis rat model.....	51
2.10	Urinalysis and albumin measurement.....	52
2.11	Glomerular isolation.....	52
2.12	Transmission electron microscopy.....	52
2.13	Period Acid-Schiff (PAS) staining.....	54
2.14	Statistical analysis.....	54

3. The cytoprotective role of autophagy in PAN-treated human podocytes

3.1	Introduction.....	56
3.2	Experimental design.....	60
3.3	Results.....	61
3.3.1	PAN induced autophagy prior to apoptosis in human podocytes.....	61

3.3.2	mTORC1 was activated in PAN-treated human podocytes..	68
3.3.3	Inhibition of PAN-induced autophagy increased apoptosis in human podocytes.....	70
3.3.4	Inhibition of PAN-induced autophagy disrupted podocyte cytoskeleton.....	80
3.4	Discussion.....	83

4. Trehalose, an mTOR independent autophagy inducer, alleviated human podocyte injury after PAN treatment

4.1	Introduction.....	87
4.2	Experimental design.....	90
4.3	Results.....	91
4.3.1	Trehalose induced autophagy in human podocytes.....	91
4.3.2	Trehalose induced podocyte autophagy in an mTOR independent manner.....	97
4.3.3	Trehalose-induced autophagy was independent of ROS.....	99
4.3.4	Trehalose decreased PAN-induced apoptosis in human podocytes via the induction of autophagy.....	102
4.3.5	Trehalose alleviated PAN-induced actin cytoskeleton damage in human podocytes.....	113
4.3.6	Trehalose diminished cell motility in PAN-treated human podocytes.....	116
4.4	Discussion.....	119

5. Trehalose induced autophagy but failed to alleviate podocyte injury in PAN nephrosis rat model

5.1	Introduction.....	124
5.2	Experimental design.....	126
5.3	Results.....	127

5.3.1	Trehalose induced autophagy in glomerulus.....	127
5.3.2	Proteinuria was not decreased by trehalose in PAN nephrosis rat model.....	129
5.3.3	Hypoalbuminemia was not alleviated after trehalose treatment in PAN nephrosis rat model.....	131
5.3.4	Renal pathological changes in PAN nephrosis rat model were not alleviated after trehalose treatment.....	133
5.4	Discussion.....	136

6. General discussion and conclusion

6.1	General discussion.....	139
6.2	Conclusion.....	150
	References	151

List of Figures

Chapter 1 Introduction

Figure 1.1	Podocyte structure.....	3
Figure 1.2	Renal filtration barrier.....	4
Figure 1.3	Actin cytoskeleton of podocyte.....	6
Figure 1.4	Nephrin in slit diaphragm.....	8
Figure 1.5	$\alpha3\beta1$ integrin in podocyte.....	12
Figure 1.6	Apoptotic signaling pathways.....	15
Figure 1.7	The stages of autophagy in mammalian.....	27
Figure 1.8	The mTOR signaling pathways.....	30
Figure 1.9	TASCC regulates the activity of catabolic and anabolic processes.....	32
Figure 1.10	The crosstalk between apoptosis and autophagy.....	35
Figure 1.11	The chemical structure of trehalose.....	38

Chapter 2 Methods and materials

Figure 2.1	Representative pictures of YO-PRO-1/PI assay and Active caspase-3 assay.....	49
------------	--	----

Chapter 3 The cytoprotective role of autophagy in PAN-treated human podocytes

Figure 3.1	PAN induced podocyte autophagy in a dose-dependent manner	63
Figure 3.2	PAN induced podocyte autophagy in a time-dependent manner	64
Figure 3.3	LC3 immunostaining in PAN-treated human podocytes.....	65
Figure 3.4	PAN induced apoptosis in human podocytes.....	66

Figure 3.5	PAN increased active caspase-3 positive podocytes.....	67
Figure 3.6	mTORC1 was activated in PAN-treated podocytes.....	69
Figure 3.7	3-MA inhibited PAN-induced autophagy.....	72
Figure 3.8	Morphology changes in human podocytes after 3-MA inhibited PAN-induced autophagy.....	73
Figure 3.9	Podocyte apoptosis increased after 3-MA inhibited PAN- induced autophagy.....	74
Figure 3.10	Active caspase-3 positive podocytes increased after autophagy inhibition by 3-MA.....	75
Figure 3.11	CQ inhibited PAN-induced autophagy.....	76
Figure 3.12	Morphology changes in human podocytes after CQ inhibited PAN-induced autophagy.....	77
Figure 3.13	Podocyte apoptosis increased after CQ inhibited PAN-induced autophagy.....	78
Figure 3.14	Active caspase-3 positive podocytes increased after autophagy inhibition by CQ.....	79
Figure 3.15	The inhibition of PAN-induced autophagy disrupted podocyte cytoskeleton.....	81
Figure 3.16	Podocytes with disrupted actin cytoskeleton increased after autophagy inhibition.....	82

Chapter 4 Trehalose, an mTOR independent autophagy inducer, alleviated human podocyte injury after PAN treatment

Figure 4.1	Trehalose induced autophagy in a dose dependent manner.....	92
Figure 4.2	Trehalose induced autophagy in a time dependent manner.....	93
Figure 4.3	LC3 immunostaining in trehalose-treated human podocytes.....	94
Figure 4.4	LC3 puncta positive podocytes increased after trehalose treatment.....	95
Figure 4.5	Trehalose increased the expression of Atg5.....	96
Figure 4.6	Trehalose induced podocyte autophagy in an mTOR	

	independent manner.....	98
Figure 4.7	Trehalose-induced podocyte autophagy was not associated with energy restriction.....	100
Figure 4.8	Trehalose-induced podocyte autophagy was independent of ROS.....	101
Figure 4.9	Trehalose induced autophagy in PAN-treated human podocytes.....	104
Figure 4.10	LC3 immunostaining in PAN or (and) trehalose-treated human podocytes.....	105
Figure 4.11	No elevated necrosis in PAN or (and) trehalose-treated human podocytes.....	106
Figure 4.12	Trehalose decreased PAN-induced podocyte apoptosis.....	107
Figure 4.13	Trehalose decreased the percentage of active caspase-3 positive podocytes.....	108
Figure 4.14	CQ and WT inhibited trehalose-induced autophagy.....	109
Figure 4.15	Necrosis increased after the inhibition of trehalose-induced autophagy.....	110
Figure 4.16	Podocyte apoptosis increased after the inhibition of trehalose-induced autophagy.....	111
Figure 4.17	Inhibition of trehalose-induced autophagy increased the percentage of active caspase-3 positive podocytes.....	112
Figure 4.18	Trehalose alleviated PAN-induced actin cytoskeleton injury in human podocytes.....	114
Figure 4.19	PAN-induced actin cytoskeleton damage in podocytes was alleviated by trehalose.....	115
Figure 4.20	Trehalose diminished cell motility in PAN-treated human podocytes.....	117
Figure 4.21	PAN-increased motility was suppressed by trehalose.....	118

Chapter 5 Trehalose induced autophagy but failed to alleviate podocyte injury in PAN nephrosis rat model

Figure 5.1	Trehalose induced autophagy in glomerulus.....	128
Figure 5.2	Trehalose fails to decrease proteinuria in PAN nephrosis rat model.....	130
Figure 5.3	Trehalose failed to alleviate hypoalbuminemia in PAN nephrosis rat model.....	132
Figure 5.4	No obvious glomerular lesions were observed in PAN nephrosis rat under PAS staining.....	134
Figure 5.5	Trehalose failed to attenuate renal pathological changes in PAN nephrosis rat model.....	135

List of Abbreviations

3-MA	3-methyladenine
ACEi	Angiotensin converting enzyme inhibitor
Acr	Acrylamide
AIF	Apoptosis-inducing factor
AMPK	AMP-activated protein kinase
APS	Ammonium Persulfate
AT1	Angiotensin-II receptor type 1
Atg	Autophagy-related
Bis	Bisacrylamide
BSA	Bovine serum albumin
CQ	Chloroquine
CRP	C-reactive protein
DAPK	Death-associated protein kinase
DDI	Distilled deionized water
DG	Dystroglycans
ECM	Extracellular matrix proteins
ERK	Extracellular signal-regulated kinase
ESRD	End stage renal disease
F-actin	Filamentous actin
FasL	Fas ligand

FBS	Fetal bovine serum
FP	Foot process
FSGS	Focal segmental glomerulosclerosis
GBM	Glomerular basement membrane
HGF	Hepatocyte growth factor
HMGB1	High mobility group box 1
IL-13	Interleukin-13
IQGAP	IQ motif containing GTPase activating protein
JNK1	c-Jun N terminal kinase 1
LC3-II	Microtubule-associated protein 1 light chain 3-II
LDH	Lactate dehydrogenase
LPS	Lipopolysaccharide
MAPK	p38 mitogen-activated protein kinase
MCNS	Minimal change nephrotic syndrome
MEFs	Embryonic fibroblast cells
MPCs	Mouse podocytes
mTORC1	mTOR complex 1
NAC	Antioxidant N-acetyl-cysteine
NADPH	Nicotinamide adenine dinucleotide phosphate
NK cell	Natural killing cell
OsO4	Osmium tetroxide
p70S6K	p70 S6 Kinase
PAK	p21 activated kinase

PAN	Puromycin aminonucleoside
PE	Phosphatidylethanolamine
PI3K	Class III phosphoinositide 3 kinase
p-mTOR	phospho-mTOR
PPAR γ	Peroxisome proliferator-activated receptor γ
RAS	Renin angiotensin system
ROS	Reactive oxygen species
SD	Slit diaphragm
SH2	Src homology 2
SNP	Single nucleotide polymorphism
SPS	Subpodocyte space
SRNS	Steroid resistant nephrotic syndrome
SSNS	Steroid sensitive nephrotic syndrome
TASCC	TOR-autophagy spatial coupling compartment
TBS	Tris Buffered Saline
TEMED	Tetramethylethylenediamine
TGF- β	Transforming growth factor-beta
TLR	Toll like receptor
TNF	Tumor necrosis factor
TNFR1	Tumor necrosis factor receptor I
TNF α	Necrosis factor alpha
TRAF6	Tumor necrosis factor receptor-associated factor 6
TRAIL-R	TRAIL receptor

TRPC6	Transient receptor potential cation 6
TSC2	Tuberous sclerosis complex 2
UVRAG	UV radiation resistance-associated gene
VEGF	Vascular endothelial growth factor
Vps34	Complex containing class III PI3K
WT	Wortmannin

Chapter 1

Introduction

1.1 Podocyte emerges as a therapeutic target in glomerular diseases

Glomerular diseases are characterized by the disruption of renal filtration barrier which consists of endothelial cell, glomerular basement membrane (GBM) and epithelial cell (also called podocyte) and present with proteinuria. The critical role of podocytes in the pathogenesis of glomerular diseases was revealed after discovering series of podocyte proteins in the past several decades (Reiser and Sever 2013, Saleem 2003, Salomon, Gubler and Niaudet 2000). Evidences accumulate that altered podocyte morphology and protein expression level occur in glomerular diseases such as minimal change nephrotic syndrome (MCNS), focal segmental glomerulosclerosis (FSGS) and diabetic nephropathy (Stitt-Cavanagh, MacLeod and Kennedy 2009, Pollak 2008). *In vivo* studies demonstrated that podocyte injury leads to proteinuria and eventually glomerulosclerosis (Mathieson 2012). Thus, podocyte has emerged as the therapeutic target of glomerular diseases.

1.1.1 Podocyte structure

Podocytes are highly differentiated cells with special morphology. The cell body bulges into major process which extends numerous foot processes encircling capillary loops. Interdigitating foot processes are bridged by slit diaphragm (SD) which can be visualized as a thin lay under electron microscope (Figure1.1-1.2)

(Welsh and Saleem 2012). Podocyte has three domains: apical domain, SD domain and basal membrane domain. The apical and SD domain are coated with negative charge which was produced by sialoglycoproteins such as podocalyxin and podoendin (Faul et al. 2007, Pavenstadt, Kriz and Kretzler 2003). In addition, SD is a zip like structure with small size pores (30-40 nm) so that albumin and other large molecules are prevented from leaking into urine (Grahammer, Schell and Huber 2013). The basal membrane domain is responsible for the adhesion of podocytes. These three domains are connected with actin cytoskeleton which predominates in foot process and maintain the stability of podocytes (Oh, Reiser and Mundel 2004).

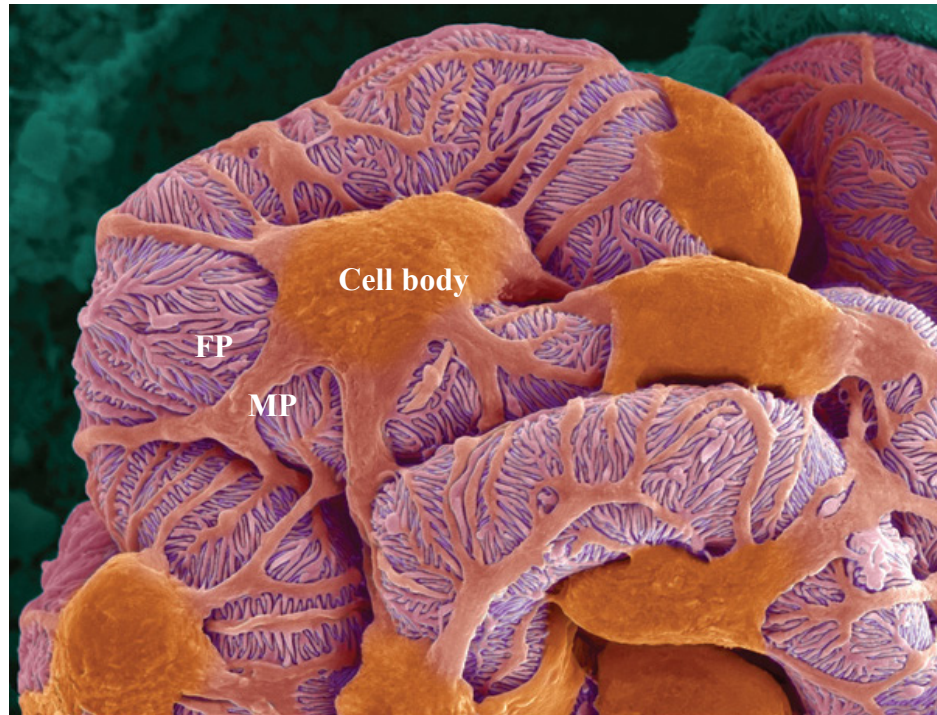


Figure 1.1 Podocyte structure (Welsh and Saleem 2012)

Podocyte consists of cell body, major process (MP) and foot process (FP). Interdigitating foot processes are bridged by SD and encircle capillaries in the glomerulus.

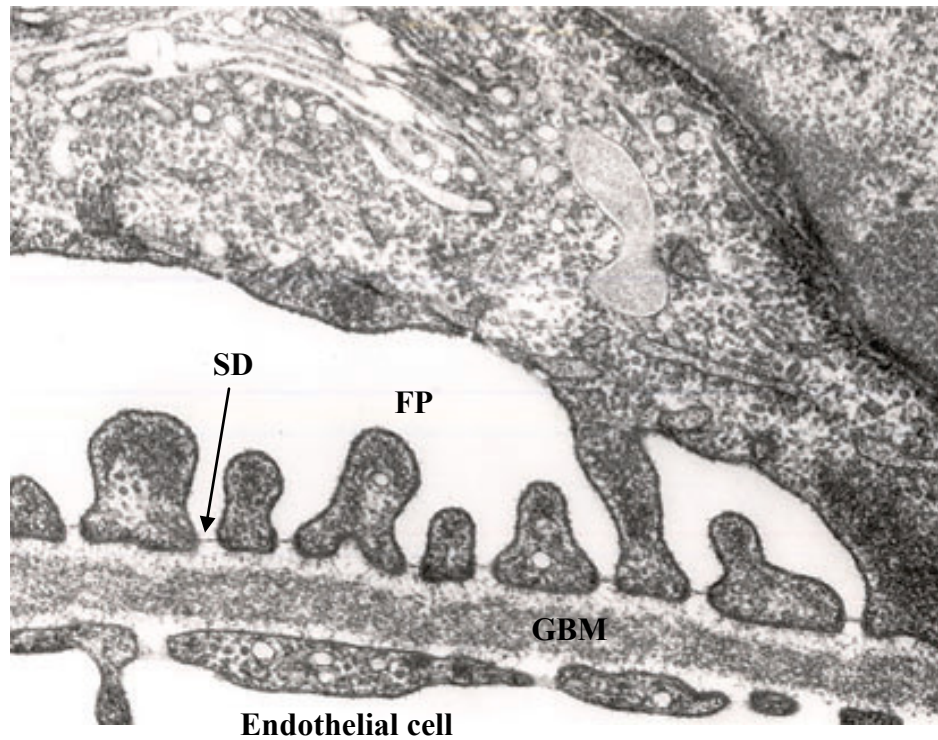


Figure 1.2 Renal filtration barrier (Greka and Mundel 2012)

Renal filtration barrier is composed of endothelial cells, glomerular basement membrane (GBM) and foot processes (FP). Slit diaphragm (SD) connects the FP and serves as filtration sieve.

1.1.2 Actin cytoskeleton in podocyte

Filamentous actin (F-actin), the backbone of podocyte cytoskeleton, is bundled by α -actinin-4 and synaptopodin (Figure 1.3) (Scharpe, Maes and Van Damme 2005). The morphology and movement of podocytes is mechanically supported by actin cytoskeleton. The disruption of actin cytoskeleton leads to glomerular diseases presenting with proteinuria (He et al. 2013). The advances in single gene mutation enhance our understanding of podocyte biology. These proteins discussed below are physically or functionally associated with actin cytoskeleton.

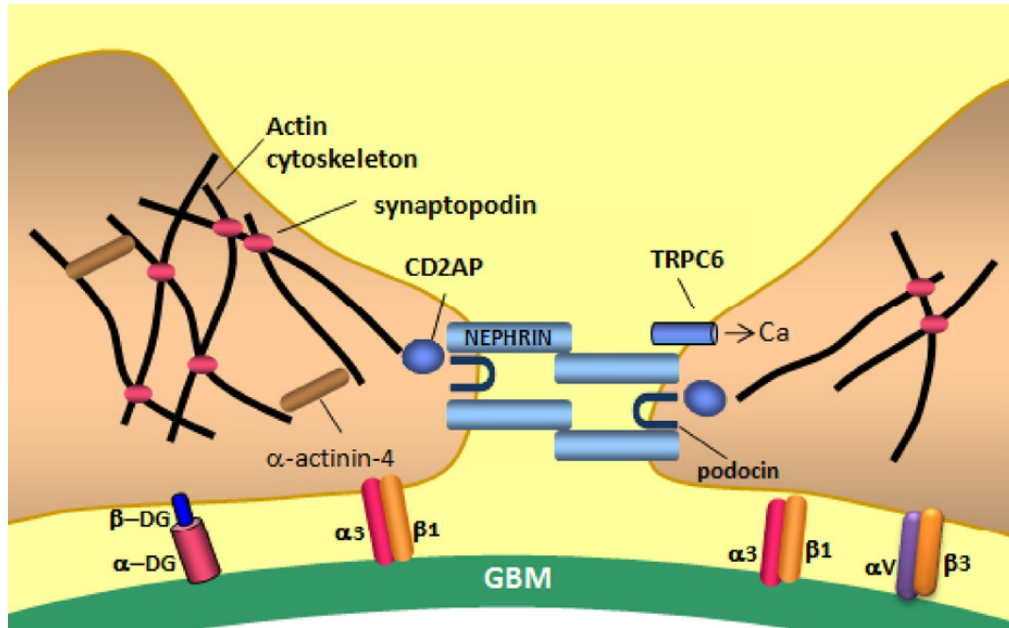


Figure 1.3 Actin cytoskeleton of podocyte (Scharpe et al. 2005)

The actin cytoskeleton of podocyte has a complex relationship with other molecules. F-actin is bundled by α -actinin-4 and synaptopodin to form actin cytoskeleton. CD2AP and podocin link Nephrin with actin cytoskeleton. Podocyte attachment relies on adhesion proteins including $\alpha 3\beta 1$ integrin and α - and β -dystroglycans (DG).

Nephrin

Nephrin is a transmembrane protein which belongs to the immunoglobulin family (Holthofer et al. 1999). In renal tissue, nephrin is uniquely expressed in podocytes, and its encoding gene NPHS1 mutates in Finnish type-congenital nephrotic syndrome which presents with heavy proteinuria (Salomon et al. 2000, Jalanko et al. 2001). As depicted in Figure 1.3-1.4, the extracellular domain of nephrin involves the formation of SD, while the intracellular part combines with CD2AP, podocin and indirectly binds to actin cytoskeleton (Scharpe et al. 2005, Ruotsalainen et al. 1999). In addition, Nephrin also functions as signal transduction scaffold to regulate the actin cytoskeleton dynamics (Patrakka and Tryggvason 2007). When tyrosine residues in cytoplasmic domain of nephrin are phosphorylated by Fyn, the docking sites (such as multiple YDxV site) of nephrin interact with Src homology 2 (SH2) domains of Nck adaptor proteins. Subsequently, SH3 domains of nephrin regulate actin polymerization and cell shape by summoning p21 activated kinase (PAK) and N-WASp (Jones et al. 2006, Blasutig et al. 2008). Phosphorylated nephrin interacts with the IQ motif containing GTPase activating protein (IQGAP) and phospholipase C γ 1 to regulate actin cytoskeleton dynamics in response to high pressure from glomerular capillary or insults (Brandt and Grosse 2007). It has also been reported that binding of Nephrin to Nck desphosphorylates and activates cofilin which plays a key role in maintaining the normal function of actin cytoskeleton (Garg et al. 2010, Teng, Lukasz and Schiffer 2012).

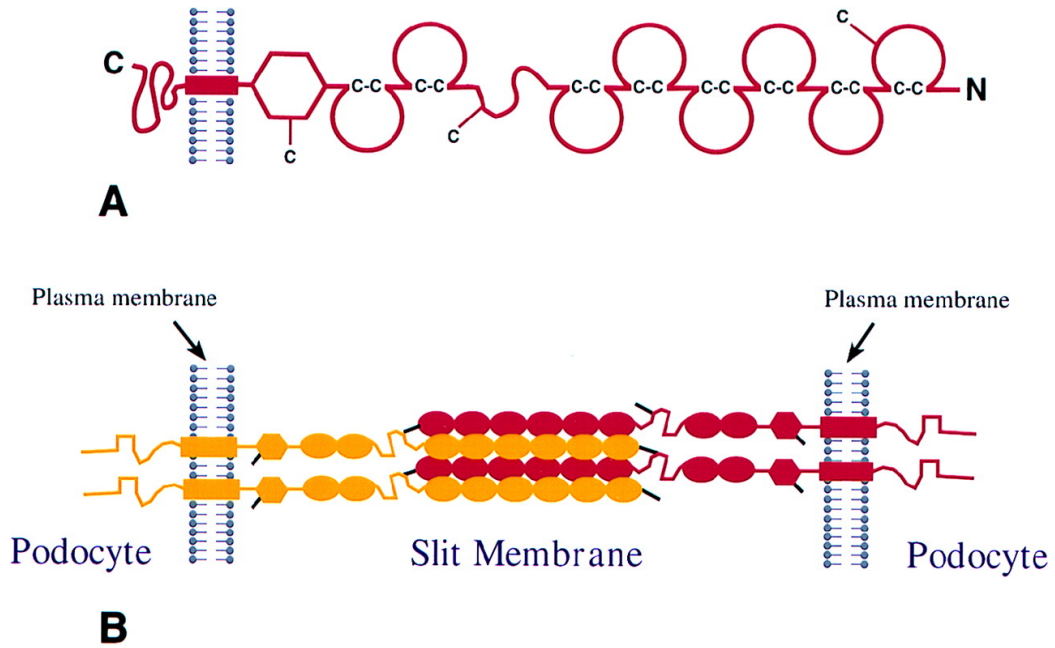


Figure 1.4 Nephrin in slit diaphragm (Ruotsalainen et al. 1999)

(A) Schematic domain structure of nephrin. (B) Interdigitating association of nephrin molecules in SD between two-foot processes. The zipper-like structure in the slit diaphragm is the backbone of the filtration sieve.

CD2AP

CD2AP is originally recognized as the protein that interacts with CD2 of T cell and natural killing cell (NK cell). It is widely expressed in all tissues apart from the brain. CD2AP is composed of three SH3 domains at N terminus and a coiled coil domains at C terminus. In renal tissue, CD2AP predominantly distributes in podocytes, and associates with other proteins in slit diaphragm to maintain the normal permeability of filtration barrier (Li et al. 2000, Shih et al. 2001). Additionally, CD2AP combines to actin cytoskeleton directly through its actin binding sites in C terminus, and is involved in actin cytoskeleton dynamics to resist physiological and pathological stimuli (Yuan, Takeuchi and Salant 2002). It was demonstrated that CD2AP deficient mice presented with renal dysfunction and deteriorated into nephrotic syndrome at 4 weeks after birth, died at sixth week of age. Mutation has also been detected in some FSGS patients (Kim et al. 2003).

Podocin

Podocin is encoded by NPHS2 and belongs to the stomatin family. NPHS2 mutations result in childhood autosomal recessive steroid resistant nephrotic syndrome (SRNS) (Boute et al. 2000, Jaffer et al. 2011, Otukesh et al. 2009). Podocin has a hairpin-like structure which is composed of 383 amino acids. In kidney, podocin is exclusively expressed in podocytes and localizes at the anchor site of slit diaphragm. Podocin co-localizes with CD2AP and nephrin at its C-terminal domain, and serves as a scaffold for the binding of tight junction proteins to actin cytoskeleton. Podocin enables the signaling transduction through SD and

remodels podocyte cytoskeleton in response to mechanical stimuli (Wolf and Stahl 2003).

α -actinin-4

α -actinin-4, a 100 KDa encoding protein of ACTN4, is a homodimer from spectrin superfamily. ACTN4 mutations have been indentified in autosomal dominant FSGS patients who are resistant to the steroid therapy (Kaplan et al. 2000). The N-terminal of α -actinin-4 contains two calponin homology domains (CH1 and CH2) which function as actin binding site where actin filaments are crosslinked and bundled. Two EF hand motifs of α -actinin-4 in the C-terminal serve as sensing sites of calcium, while CH2 serves as the phosphoinositides binding site. It has been suggested that α -actinin-4/actin interaction is controlled by phosphoinositides and calcium. For instance, the elevated calcium suppresses the affinity between α -actinin-4 and actin (Michaud et al. 2009). Moreover, the number of podocytes decreased significantly in α -actinin-4 deficiency mouse model than that in wild type model and podocytes easily detach from GBM as α -actinin-4 is required for podocyte adhesion (Dandapani et al. 2007).

TRPC6

Transient receptor potential cation (TRPC) family contains seven subtypes (TRPC1 to TRPC7) which are crucial for elevating intracellular calcium concentration. TRPC6 gene locates in chromosome 11q21-22 and around 75% identity exists among TRPC6, TRPC3 and TRPC7 (Faul et al. 2007). TRPC6 expresses in

podocytes and co-localizes with nephrin and podocin. Nephrin deficiency in podocytes leads to high expression and accumulation of TRPC6 (Reiser et al. 2005). TRPC6 is an important component for signal transduction, as it can sense the variable mechanical stimuli from filtration and regulate actin cytoskeleton dynamics by altering calcium flux. Additionally, TRPC6 mutation is related to hereditary FSGS and some acquired renal diseases (Mukerji, Damodaran and Winn 2007). Glomerular diseases can also be induced by over-expression of TRPC6 (Yu and Yu 2012). Therefore, renal injury may be alleviated by blocking TRPC6 channel. However, there is lack of ways for specifically blocking TRPC6 channel, as TRPC3 and TRPC 7 share 75% of the same sequence with TRPC6. Furthermore, TRPC6 expression is not restricted to podocytes. The management of global side effects would be a big challenge (Mukerji et al. 2007).

$\alpha 3\beta 1$ integrin

$\alpha 3\beta 1$ integrin is heterodimeric transmembrane receptors and interacts with collagen IV and lamin of GBM, suggesting that $\alpha 3\beta 1$ integrin is essential for podocyte adhesion (Dessapt et al. 2009). $\alpha 3\beta 1$ integrin also indirectly connects with nephrin and α -actinin-4, and is involved in regulating actin cytoskeleton dynamics and signaling transduction (Figure 1.5) (Quaggin and Kreidberg 2008).

Other cytoskeleton proteins

Besides molecules mentioned above, a number of proteins have been discovered in slit diaphragm and actin cytoskeleton in podocytes, such as ZO-1, FAT, NEPH1, synaptopodin and P-cadherin (Greka and Mundel 2012, Fukasawa et al. 2009, Heikkila et al. 2011, Yanagida-Asanuma et al. 2007, Rinta-Valkama et al. 2007).

1.1.3 Podocyte apoptosis

Signaling pathways of apoptosis

Cell undergoes series of changes in morphology after being triggered by death signals, including blebbing, cell shrinkage, nuclear fragmentation, chromatin condensation and chromosomal DNA fragmentation. Currently two major cell death pathways have been identified (Elmore 2007) (Figure 1.6):

- (1) Cell surface death receptor pathways: Apoptosis may be triggered by death ligands, such as Fas/FasL, TNF-R-I or -II/TNF α and TRAIL-R/TRAIL. When death ligand binds with extracellular death binding domain of death receptor, death signal will be transduced into cell, then Caspase-8 and (or) Caspase-10 is activated to promote apoptosis.

- (2) Mitochondrial death pathway: Intracellular death signals may also initiate this program death pathway. At the early stage, mitochondria release apoptotic proteins such as cytochrome C, Procaspase 3, Apoptosis-inducing factor (AIF) and Smac/Diablo. Subsequently, the formation of apoptosomes containing Caspase 9 and Apaf-1 results in the activation of caspase cascade.

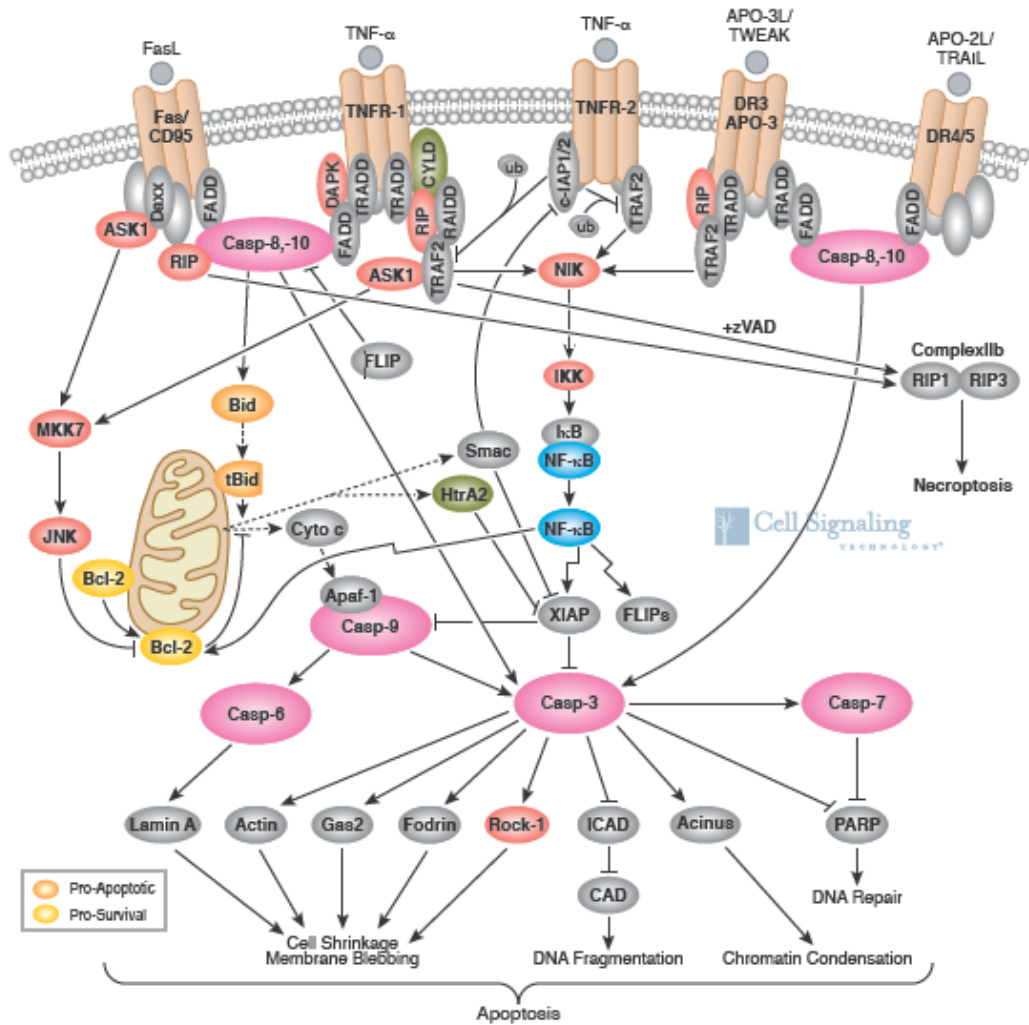


Figure 1.6 Apoptotic signaling pathways (http://www.cellsignal.com/reference/pathway/Death_Receptor.html)

Podocyte apoptosis may be mediated by different signaling pathways. Cell surface death receptor pathways include Fas/FasL, TNF-R-I or -II/TNF α and TRAIL-R/TRAIL pathways. Whereas, the mitochondrial death pathway is activated by intracellular death signals.

Causes of podocyte injury

The advances in the knowledge of podocyte injury enhance our understanding of glomerular diseases and are also critical for the development of therapeutic strategies. It has been known that podocyte apoptosis is driven by a number of stimuli, such as transforming growth factor-beta (TGF- β), cytokines, chemokines, mechanical stress, toxin, reactive oxygen species (ROS) and complement factors.

TGF- β

The physiological level of TGF- β is essential for tissue repair due to its anti-inflammation features, whereas over-expression of TGF- β contributes to glomerulosclerosis (Loeffler and Wolf 2014). Most cell types including activated T and B cell, dendritic cells, and neutrophil are able to produce TGF- β . It has been demonstrated that the expression of three TGF- β forms (TGF- β 1, TGF- β 2 and TGF- β 3) and their receptors increased in glomerular diseases, such as IgA nephropathy, FSGS, lupus nephritis and diabetic nephropathy which present with excessive extracellular matrix (ECM) proteins (Pohlert et al. 2009, Yamamoto et al. 1996, Yamamoto et al. 1998). Increased podocyte apoptosis was demonstrated in TGF- β over-expression transgenic mouse model as well as in murine podocyte cell line after TGF- β treatment (Schiffer et al. 2001). TGF- β -induced podocyte apoptosis is mediated by p38 mitogen-activated protein kinase (MAPK) and caspase 3 (Lopez-Hernandez and Lopez-Novoa 2012).

Cytokines and chemokines

Inflammation plays an important role in the pathogenesis of podocyte injury. For instance, serum interleukin-13 (IL-13) is elevated in children with steroid sensitive nephrotic syndrome (SSNS) (Tain, Chen and Yang 2003). It has been known that rats with over-expression of IL-13 are characterized by foot process effacement and proteinuria (Lai et al. 2007). In addition, IL-4 and Interferon (IFN)- γ exhibit toxic effects to podocytes (Coers et al. 1995). Consistently, another study shows that IFN- γ treatment also leads to podocyte collapse in FSGS (Markowitz et al. 2010).

Chemokines not only recruited inflammation cells to the infected sites, but also affect the function of podocytes. It has been reported that CCR4, CCR8, CCR9, CCR10, CXCR1, CXCR3, CXCR4, CXCR5 and CXCR7 are expressed in podocytes (Pavenstadt et al. 2003). The activation of these receptors results in podocyte injury by increasing calcium concentration and activity of nicotinamide adenine dinucleotide phosphate (NADPH)-oxidase (Huber et al. 2002).

ROS

Oxidative stress is known as a key mediator of cell injury. It was reported that NADPH oxidase-derived ROS induces podocyte injury after PAN treatment via up-regulating TRPC6 expression (Wang et al. 2009). ROS also leads to deglycosilation of alpha-DG which results in podocyte detachment (Vogtlander et al. 2006). In addition, high glucose and angiotensin II elevate ROS which induces podocyte apoptosis (Liu et al. 2013, Anderson et al. 2014).

Mechanical stress

Numerous foot processes extending from cell body of podocytes surround glomerular capillary to withstand hydrostatic pressure. Shear stress alters actin cytoskeleton dynamics and cell adherence. As a result, podocytes detach from GBM into urine (Endlich and Endlich 2012, Friedrich et al. 2006). Furthermore, hemodynamic stress disrupts the structure of slit diaphragm by decreasing the expression of nephrin and $\alpha3\beta1$ integrin (Miceli et al. 2010, Dessapt et al. 2009) . Podocyte apoptosis also can be induced by shear stress via a c-Src-phospholipase D-mTOR signaling pathway (Huang et al. 2012).

Hyperglycaemia

Strong evidence revealed that the number of podocytes decreases significantly in diabetic nephropathy (Petermann et al. 2004, Weil et al. 2012). Recently some studies have provided more insights into its mechanism. Data showed that hyperglycaemia activates P38/MAPK and caspase cascade, then lead to podocyte injury (Sakai et al. 2005). Meanwhile, the expression of cyclin dependent kinase P27KiP1 and angiotensin II are up-regulated by hyperglycaemia and induce podocyte apoptosis (Merline et al. 2009, Gagliardini et al. 2013). In diabetes, another group demonstrated that forkhead binding box O4 (FoxO4) transcription factor leads to podocyte apoptosis (Chuang et al. 2011).

Angiotensin II

The rennin angiotensin system (RAS) is known for regulating fluid and electrolyte balance. However, abnormal RAS activation plays a pathological role in the progression of chronic kidney disease (Mao et al. 2013). Angiotensin II decreases the expression of α -actinin-4 and remodels podocyte actin cytoskeleton (Hsu et al. 2008). Moreover, podocyte apoptosis is induced by angiotensin II via dephosphorylating nephrin (Ren et al. 2012). It was also reported that angiotensin II lead to podocytes injury by increasing the production of TNF-alpha (Rosa et al. 2012). Thus, angiotensin II type I antagonists and angiotensin converting enzyme inhibitors (ACEi) have been using to reduce proteinuria (Nakamura et al. 2000, Bolignano et al. 2014).

1.1.4 Strategies for decreasing podocyte apoptosis

Since podocyte apoptosis is a major cause of glomerular diseases, studies focus on developing therapeutic approaches of decreasing apoptotic podocytes have been carried out in recent years. A number of potential strategies alleviating podocyte injury are listed below.

Heparin, an anticoagulant, significantly decreases podocyte apoptosis induced by H₂O₂, staurosporine and ultraviolet light (Ishikawa and Kitamura 1999).

Rosuvastatin is commonly used for the treatment of hyperlipidemia. However, it also can reduce proteinuria by protecting podocytes against apoptosis via up-regulating P21 which is a cell cycle protein (Cormack-Aboud et al. 2009).

Adrenomedullin, an antioxidant, decreases podocyte apoptosis in the PAN-treated podocytes (Oba, Hino and Fujita 2008).

Hepatocyte growth factor (HGF) alleviates proteinuria by down-regulating podocyte apoptosis. It was revealed that HGF preserves nephrin and WT1 expression (Fornoni et al. 2001, Dai et al. 2010).

Pioglitazone is a peroxisome proliferator-activated receptor γ (PPAR γ) agonist. It has been showed that pioglitazone maintains normal expression of nephrin and α -actinin-4 (Zuo et al. 2012).

Estradiol is considered to be an anti-apoptotic agent for podocytes because women are found to have a better prognosis than men in some certain chronic kidney diseases. The mechanism involves the activation of MAPK and the stabilization of mitochondrial membrane potential (Kummer et al. 2011).

1,25-dihydroxyvitamin D3 protects podocytes against apoptosis by down-regulating the expression of Fas, FADD, P-Smad3, Bax and active caspase-3 (Zou et al. 2010).

Angiotensin-II receptor type 1 (AT1) blocker is used for the treatment of proteinuria diseases. Caspase 3 and Bax can be down-regulated by AT1 blocker to decrease podocyte apoptosis (Tuncdemir and Ozturk 2011).

Unsaturated free fatty acid delays diabetic nephropathy by decreasing podocyte apoptosis which was induced by palmitic acid (Sieber et al. 2010).

Cyclin 1 safeguards against podocyte apoptosis by bounding and activating cyclin-dependent kinase 5 (Cdk5). It also maintains the normal expression level of pro-survival proteins Bcl-2 and Bcl-XL (Brinkkoetter et al. 2009).

HSPB1, a member of heat shock protein family proteins, is involved in regulating actin cytoskeleton dynamics. In diabetic nephropathy, HSPB1 showed protective effect to podocytes (Sanchez-Nino et al. 2012).

C-reactive protein (CRP) promotes podocyte survival by elevating Bcl-2 expression and decreasing Caspase 3 activity. Furthermore, it maintains the integrity of slit diaphragm by up-regulating nephrin and CD2AP expression as well as the structure proteins ezrin and podocalyxin-like protein-1 (Pawluczyk et al. 2011).

Vascular endothelial growth factor (VEGF) in glomerulus is mainly generated from podocytes. VEGF-A (the main form of VEGF) regulates cellular processes in podocytes by binding with vascular endothelial growth factor receptor-2 (VEGFR-2) (Hohenstein et al. 2010). It was reported that VEGF phosphorylates nephrin and prevents podocyte apoptosis (Foster et al. 2005).

1.1.5 Podocyte motility

In glomerulus, it has been demonstrated that podocyte motility is kept at a considerable level (Welsh and Saleem 2012). It is an essential process for cleaning proteins deposit in subpodocyte space (SPS) which covered around 60% of GBM (Neal et al. 2005, Neal et al. 2007). Thus, podocyte motility serves as a self-cleaning mechanism to ensure the normal filtration. Altered podocyte motility results in foot process dysfunction including effacement. Migration assay reveals that podocyte motility increased dramatically by PAN, suPAR, Angptl4, synaptopodin loss, proteases, integrin and cathepsin L activation (Jeruschke et al. 2013, Welsh and Saleem 2012, Mundel and Reiser 2010, Wei et al. 2008a, Asanuma et al. 2006). On the contrary, decreased migratory phenotype can be observed when the expression of TRPC6 or RhoA activity is down-regulated as well as ACTN4 mutations (Tian et al. 2010, Shao et al. 2010).

Actin cytoskeleton predominates in foot process. The factors which affect actin structure may alter podocyte motility. Three small GTPases RhoA, Cdc42 and Rac1 are the core regulators of actin cytoskeleton dynamics (Lin et al. 2013). RhoA is vital for the formation of stress fiber, while Cdc42 and Rac 1 regulate the formation of lamellipodia and filopodia (Gao et al. 2007, Mouawad, Tsui and Takano 2013). It has been reported that synaptopodin can inhibit the degradation of RhoA to promote the formation of stress fibers (Asanuma et al. 2006). Therefore, it would be a new approach for the treatment of glomerular diseases by targeting podocyte actin dynamics.

1.2 Autophagy is a potential therapeutic approach for renal diseases

1.2.1 Introduction of autophagy

Macroautophagy (hereafter referred to as autophagy) is a ubiquitous catabolic process of which misfolded proteins and damaged organelles are degraded in response to starvation and cell stress. An isolated membrane structure, phagophore, sequesters cytoplasmic contents such as damaged mitochondria to form autophagosome which fuses with lysosome to digest the cellular components (Kang et al. 2011). These metabolic products including nucleotide acid are recycled for cell survival. Therefore, autophagy plays a critical role in keeping cell homeostasis.

Autophagy is governed by the complex systems in which more than 30 Atg (autophagy related) proteins have been identified in yeast and at least 11 orthologs in mammals (Thorburn 2008). The initiation of autophagy is controlled by the class I and class III phosphoinositide 3 kinases (PI3K) (Figure 1.7). The class I PI3K-AKT-mTOR is generally considered as the critical pathway to regulate the whole process, majority of the stimuli inactivate mTOR by phosphorylation to induce autophagy (Hsieh, Athar and Chaudry 2009). For example, Rapamycin induces autophagy because of the inhibition of mTOR (Cina et al. 2012a).

The initiation of autophagy requires the core complex containing class III PI3K (Vps34), Vps 15 and Beclin-1. Thus, the opposite consequence can be achieved by the disruption of any member of this core complex. Base on the above knowledge,

3-methyladenine (3-MA) was developed to inhibit the class III PI3K to suppress autophagy (Klionsky et al. 2012). Beclin-1, interacting with Bcl-2 via its BH3 domain, plays a central role in autophagy through diverse regulating mechanisms. Some studies suggested that transcriptional factors, such as NF κ B, E2F1, c-Jun and H1F1 α , are involved in the regulation of Beclin-1 expression (Wirawan et al. 2012, Li et al. 2009, Djavaheri-Mergny et al. 2007). Post transcriptional factors, such as mi-RNA 30a, decrease the Beclin-1 mRNA by binding to its three prime untranslated regions (Zhu et al. 2009).

Notably, the dissociation of Beclin-1 and Bcl-2 contributes to the activation of autophagy (Kang et al. 2011). For instance, death-associated protein kinase (DAPK) can induce the autophagic process by separating the Beclin-1/Bcl-2 complex via the phosphorylation of Beclin-1 on Thr 119 as well as extracellular signal-regulated kinase (ERK) or c-Jun N terminal kinase 1 (JNK1) (Zalckvar et al. 2009, Wei et al. 2008b, Tang et al. 2010). Similarly, the tumor necrosis factor receptor-associated factor 6 (TRAF6) can achieve the same goal by ubiquitination of Beclin-1, by contrast, the deubiquitinating enzyme A20 which decreases the ubiquitination of Beclin-1 stable the interaction between Bcl-2 and Beclin-1 to suppress autophagy (Shi and Kehrl 2010) . When other Bcl-2 family members such as Bad, tBid and BNIP competitively replaced of Bcl-2 to dominate in the BH3 domain of Beclin-1, autophagy would also be triggered (Sinha and Levine 2008). Likewise, the substitution of Bcl-2 by high mobility group box 1 (HMGB1), UV radiation

resistance-associated gene (UVRAG) or Atg14L/Barkor results in the formation of autophagosome for protecting cells under cell stress (Kang et al. 2011).

After the initiation of autophagy, the elongation of the phagophore requires two ubiquitin-like conjugation systems to recruit more Atg proteins (Hsieh et al. 2009). One is responsible for the assembly of the Atg12-Atg5-Atg16 complex which is essential for the microtubule-associated protein 1 light chain 3-II (LC3-II) attachment. The other one is related to the formation of LC3-II which originates from LC3-I conjugating with phosphatidylethanolamine (PE) with the involvement of ATG7 and ATG3. In addition, LC3-I is generated from the cleavage of LC3 by Atg4 (Figure 1.7) (Hsieh et al. 2009). Thus, the expression of LC3-II normalized to housekeeping proteins such as beta-actin or GAPDH is universally used as the marker of autophagosome formation.

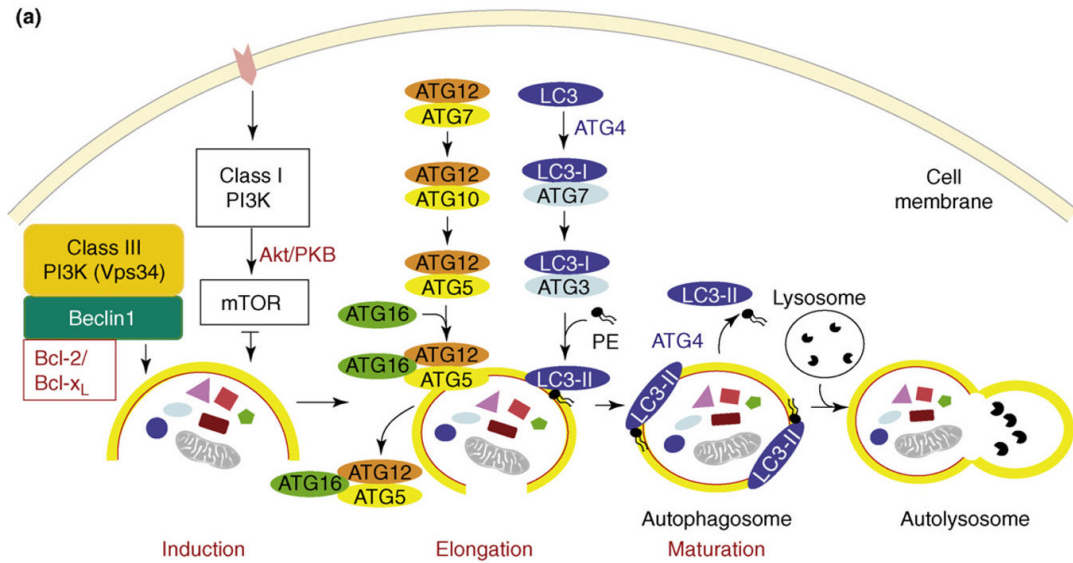


Figure 1.7 The stages of autophagy in mammalian (Hsieh et al. 2009)

Four stages of autophagic flux have been reported, including induction, elongation, maturation and formation of autolysosome. Initially, a double membrane (named phagophore) sequesters unwanted cellular components such as misfold proteins and damaged organelles. Subsequently, phagophore elongates and turns into autophagosome which fuses with lysosome. Sequestered components were digested in autolysosome and recycled as nutrients for cell survival.

1.2.2 Mammalian target of rapamycin (mTOR) in autophagy induction

mTOR, a serine/threonine protein kinase, is the key subunit of mTOR complex 1 (mTORC1) and mTORC2. mTOR binds with Raptor in mTORC1 and Rictor in mTORC2. mLST8 and Deptor are contained in both mTOR complexes (Wang and Proud 2011). It is well known that mTORC1 negatively regulates autophagy (Cina et al. 2012b). For instance, rapamycin binds with FKBP12 to inactivate mTORC1 and induces autophagy (Inoki and Huber 2012).

mTORC1 is regulated by series of upstream proteins (Huber, Walz and Kuehn 2011). As shown in Figure 1.8, mTOR is directly activated by Rheb and Rag, whereas FKBP12, Deptor and PRAS40 inhibit the function of mTOR (Sancak et al. 2008, Sancak et al. 2007, Wang et al. 2012b). Under the condition of abundant nutrition, PI3K-AKT, ERK and RSK phosphorylate tuberous sclerosis complex 2 (TSC2) at specific sites and inhibit the TSC, allowing Rheb to activate mTORC1 (Yang and Guan 2007, Pradhan et al. 2014). In addition, upon the stimulation of growth factors, the PI3K/AKT dissociates PRAS40 from mTORC1, ultimately leading to the inhibition of autophagy. Eventually, two downstream markers of mTOR (p70S6K and p-4E-BP-1) are activated and play a vital role in ribosome biogenesis and cell proliferation (Xiong et al. 2014, Wiza, Nascimento and Ouwens 2012). On the contrary, when AMPK senses energy stress such as starvation, it phosphorylates TSC2 to inhibit Rheb so that the mTOR is inactivated and autophagy is induced (Lee et al. 2010). AMPK also can directly inhibit Raptor and result in induction of autophagy (Gwinn et al. 2008). Additionally, TSC2 can be

activated by GSK3 which is inhibited by Wnt signaling (Inoki et al. 2006). Comparing with mTORC1, the knowledge of mTORC2 is limited, but it has been reported that mTORC2 is involved in organizing actin cytoskeleton (Josselyn and Frankland 2013, Angliker and Ruegg 2013).

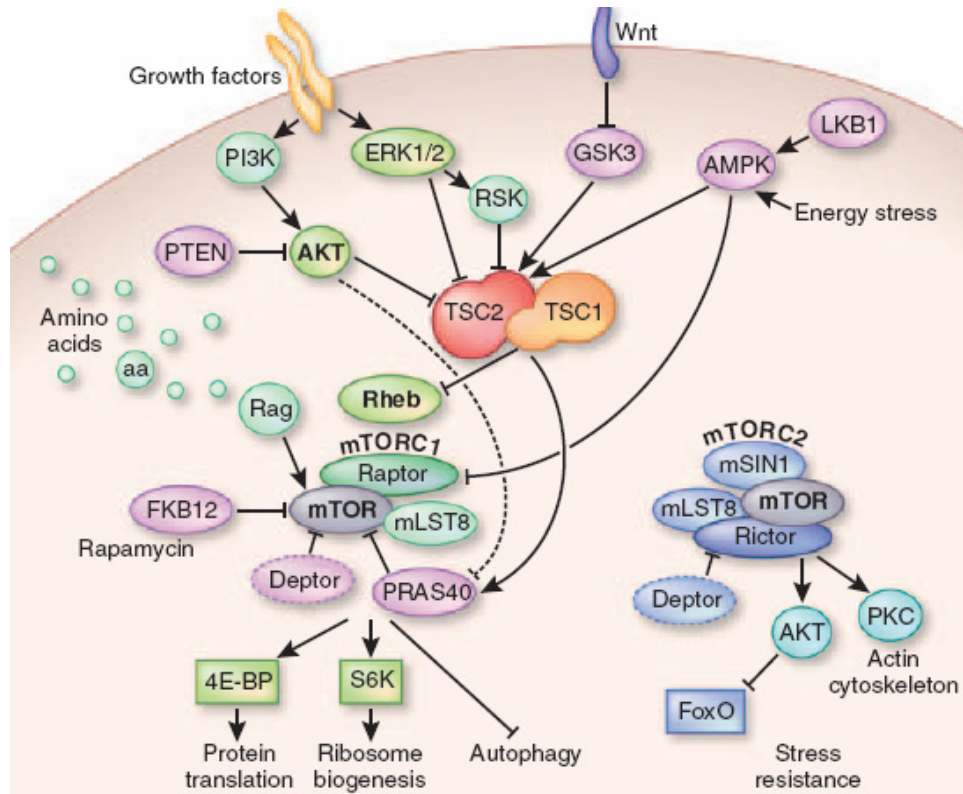


Figure 1.8 The mTOR signaling pathways (Huber et al. 2011)

The upstream signalling proteins AMPK and TSC negatively regulate mTOR activity. Activated mTORC1 inhibits autophagy, while the inhibition of mTORC1 induces autophagy. In addition, mTORC2 participates in regulating the stability of actin cytoskeleton.

TOR-autophagy spatial coupling compartment (TASCC) in autophagy induction

Catabolic and anabolic processes are regulated by mTOR in an opposite manner. However, recent findings demonstrated that both of these cellular activities can occur simultaneously in macrophages and podocytes due to the formation of TASCC (Young and Narita 2011, Narita et al. 2011). Under certain circumstance, it is beneficial for cell survival as protein turnover is being accelerated. TASCC enriches autolysosomes and mTOR in a distinct cellular compartment which located at the trans site of Golgi apparatus (Figure 1.9) (Huber et al. 2012). Thus, the space with a lower concentration of mTOR in cytoplasm is created by TASCC and enables the induction of autophagy. Meanwhile, the mass synthesis of secretory proteins becomes available. Since podocytes are post-mitotic cells and are associated with the turnover of GBM and endothelium, TASCC is vital for keeping podocyte homeostasis.

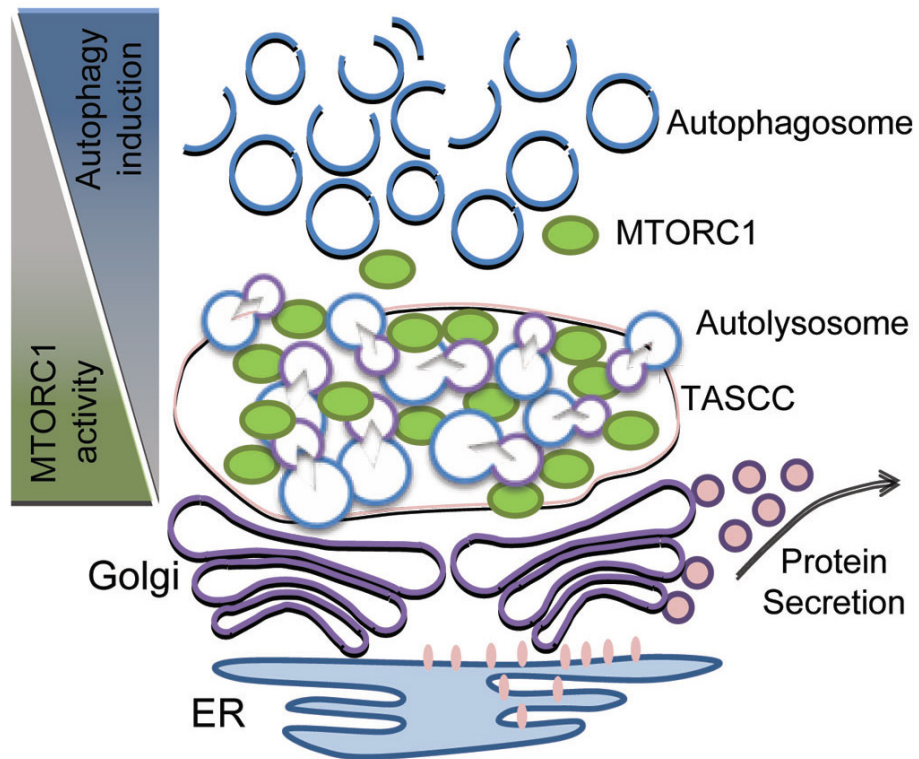


Figure 1.9 TASCC regulates the activity of catabolic and anabolic processes

(Huber et al. 2012)

TASCC enriches autophagosome and mTORC1 at the trans site of Golgi apparatus. Environment with a low concentration of mTOR in cytoplasm is created for autophagy induction.

1.2.3 ROS in autophagy induction

ROS not only serves as a pro-apoptotic stimulus, but also plays a role in inducing autophagy. Scherz-Shouval *et al.* showed ROS functions as a signaling molecular in starvation-induced autophagy which can be abolished by anti-oxidative agents. Inactivation of Atg4 and lipidation of Atg8 may attribute to ROS-induced autophagy (Scherz-Shouval *et al.* 2007b). Consistently, it has been demonstrated that angiotensin-II induces podocyte autophagy via the production of ROS, as antioxidant N-acetyl-cysteine (NAC) or catalase inhibit autophagy (Yadav *et al.* 2010). Taken together, it suggested that ROS may adaptively induce autophagy to alleviate cell damage in response to cell stress.

1.2.4 The crosstalk between apoptosis and autophagy

Autophagy is kept at a low basal level for maintaining cell homeostasis. Upon cell stress, autophagy increases rapidly to remove dysfunction organelles and misfold proteins. The cytoprotective role of autophagy has been highlighted in a variety of disciplines. However, autophagy is also recognized as Type II programmed cell death. A mind-boggling question about cell fate is that after the initiation of autophagy, what mechanisms govern the decision of the cells to survival or to die?

The crosstalk between apoptosis and autophagy remains unclear because the relationship between the two mechanisms is complicated. It has been revealed that autophagy can decrease apoptosis by inhibiting the production of active caspase 8 and tBid (Figure 1.10) (Hou et al. 2010). Moreover, autophagy eliminated dysfunctional mitochondria to decrease the generation of cytochrome C which activates apoptosis. On the other hand, apoptosis also suppresses autophagy by cleaving Beclin 1 and Atg 5. Therefore, intrinsic relation exists between apoptosis and autophagy. It would be reasonable to utilize autophagy for decreasing cell apoptosis (Djavaheri-Mergny, Maiuri and Kroemer 2010, Luo and Rubinsztein 2010).

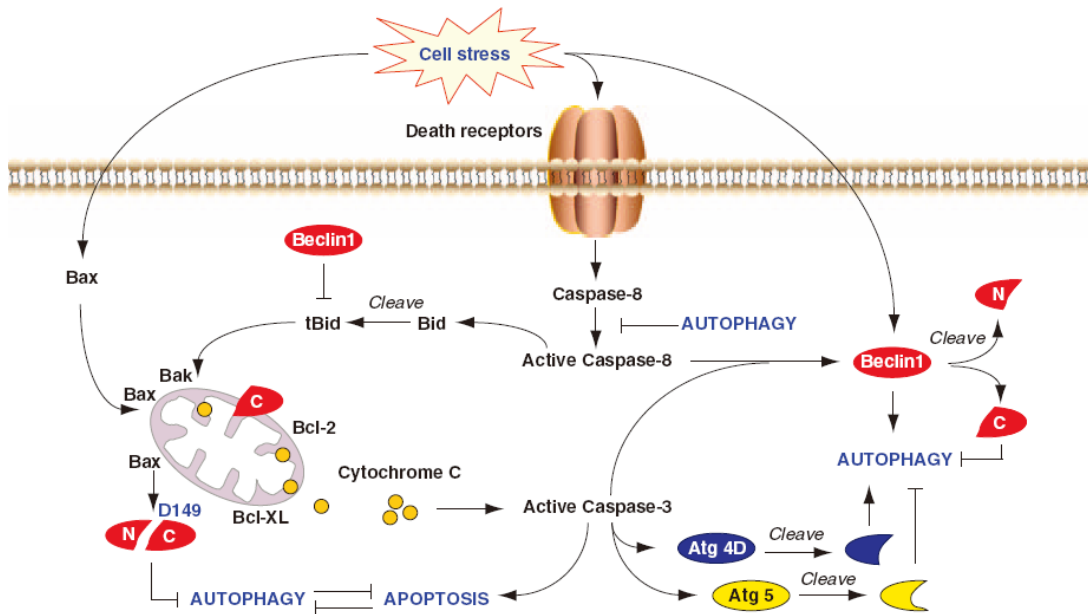


Figure 1.10 The crosstalk between apoptosis and autophagy (Kang et al. 2011)

Autophagy decreases cell apoptosis by inhibiting apoptotic proteins such as tBid and caspase-8. On the contrary, apoptosis inhibits autophagy. The cleavage of Beclin1 and Atg5 by apoptotic proteins blocks the induction of autophagy.

Autophagy in podocytes

Podocytes are highly differentiated cells withstanding hydrostatic pressure to maintain normal renal filtration. Thus, cellular protective mechanisms such as autophagy and ubiquity-proteasome system are critical for podocyte survival. Asanuma *et al.* firstly described autophagy in podocytes and demonstrated that autophagic marker LC3-II increases at the stage of podocyte differentiation, and autophagy is induced during the recovery stage of PAN-induced nephrosis. It suggests that autophagy is involved in alleviating podocyte injury (Asanuma *et al.* 2003). Another elegant study showed that podocytes exhibit a high level of basal autophagy when comparing with other cell types such as renal tubular cells, suggesting that podocyte need a stronger cytoprotective mechanism to maintain cellular metabolism (Hartleben *et al.* 2010). Podocyte-specific Atg5 knockout mice are characterized by elevated oxidized and ubiquitinated proteins, endoplasmic reticulum (ER) stress and proteinuria. Moreover, this mouse is susceptible to models of glomerular diseases including PAN and lipopolysaccharide (LPS) nephritis (Hartleben *et al.* 2010). It was also reported that autophagy can repair podocyte damage caused by ER stress in passive Heymann nephritis model (Wang *et al.* 2012a). In addition, rapamycin attenuates podocyte injury by inducing autophagy via the inhibition of mTOR-ULK1 pathway (Wu *et al.* 2013) . Therefore, it suggests that basal and induced autophagy are critical quality control mechanism for keeping podocyte homeostasis.

Autophagy was also described in human renal diseases. For instance, down-regulated autophagy attributes to podocyte damage in Fabry's disease (Chevrier et al. 2010, Liebau et al. 2013). In renal biopsy specimens, two types of autophagy were described. No autophagosomes are formed in type I autophagy, while type II plays an important role in cleaning dysfunction proteins and lipid. Thus, In IgA nephropathy, it has been reported that type I autophagy is associated with the poor prognosis (Sato et al. 2006, Sato et al. 2009). Currently the protective mechanism of autophagy has been partially revealed, but it still lack of strategies to harness autophagy for protecting podocyte against injury. Therefore, in the present study, we aimed to make use of autophagy for alleviating podocyte damage.

1.3 Trehalose is an mTOR independent autophagy inducer

1.3.1 Introduction of trehalose

Trehalose (C₁₂H₂₂O₁₁) is an alpha-linked disaccharide with the molecular weight of 342.31 (Figure 1.11). α,α -trehalose (hereafter refer to trehalose) is the most common form founded in nature. For instance, it exists in animals, plants and microorganisms. α,β and β,β forms of trehalose are named neotrehalose and isotrehalose respectively, both of them have been synthesized but rare in nature. The solubility and osmotic features of trehalose is similar to maltose, it is stable in series of pH and temperature (Richards et al. 2002).

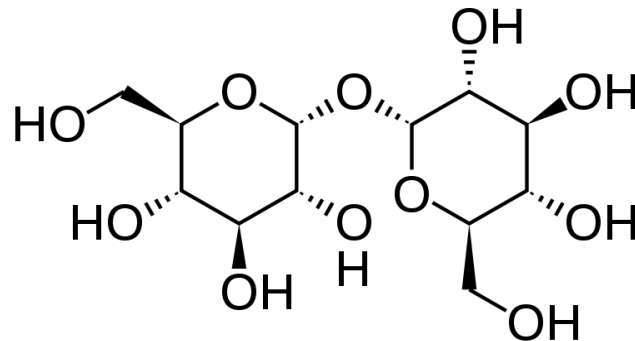


Figure 1.11 The chemical structure of trehalose (<http://en.wikipedia.org/wiki/Trehalose>)

In low organisms, trehalose is believed to be energy resource, whereas in other species, trehalose protects living systems from the injury of freeze-thaw, heating-cooling and dehydration-rehydration (Ohtake and Wang 2011, Crowe 2007). It has

been also reported that trehalose can stabilize the proteins and lipid membrane during the drying process (Kaushik and Bhat 2003). The potential mechanisms include water replacement, glass transformation instead of crystallizing and chemical stability. As a result, trehalose has been used as a cryoprotectant (Erdag et al. 2002).

The metabolism of trehalose is associated with trehalase which is primarily founded in intestine. Trehalose is assimilated after hydrolysis in intestine (Richards et al. 2002, Elbein et al. 2003). However, it is still unknown why trehalase is also enriched in renal tissue (Skoczynska et al. 2001, Sasai-Takedatsu et al. 1996). It may suggest that trehalose is important for keeping normal renal function. In addition, trehalose has no mutagenicity and genotoxicity. Thus, trehalose is considered to be a safe agent and accepted as an additive in food and cosmetic.

1.3.2 Trehalose induces autophagy in mammalian cells

The new role of trehalose has been explored in neurodegenerative diseases such as Alzheimer's disease, frontotemporal dementia, progressive supranuclear palsy and corticobasal degeneration (Fernandez-Estevez et al. 2014, Emanuele 2014). It has been reported that trehalose degrades mutant proteins such as mutants of α -synuclein by inducing autophagy in an mTOR independent manner and protects neurons against pro-apoptotic insults via the mitochondrial pathway (Sarkar et al. 2007). In addition, trehalose counteracts cellular prion infection which is a fatal neurodegenerative and infectious disease, as it induces autophagy to

degrade intracellular pathological prion protein (Aguib et al. 2009) . In contrast to starvation-induced autophagy, trehalose induces autophagy without the generation of ROS (Sarkar and Rubinsztein 2008).

1.4

Hypothesis and Objectives

1.4.1 Hypothesis

Autophagy plays a cytoprotective role in podocytes under cell stress

It has been known that puromycin aminonucleoside (PAN) induces autophagy in podocytes. However, the role of PAN-induced autophagy remains elusive. Autophagy is a catabolic process which degrades misfold proteins and organelles. Thus, we hypothesized that PAN-induced autophagy plays a cytoprotective role in podocytes in response to cell stress.

Autophagy can be harnessed to attenuate podocyte injury *in vivo* and *in vitro*

Since autophagy is a stress response and cellular quality-control mechanism, it is reasonable to harness autophagy for attenuating podocyte injury. Trehalose, an mTOR independent autophagy inducer, has showed cytoprotective effects in neurodegenerative diseases. Thus, we hypothesized that trehalose alleviated podocyte injury by inducing autophagy *in vivo* and *in vitro*.

1.4.2

Objectives

Elucidating the cytoprotective role of autophagy under cell stress in human podocytes

To reveal the cytoprotective role of autophagy in response to cell stress. The relationship between autophagy and apoptosis was investigated in PAN-treated human podocytes. Podocyte apoptosis and actin cytoskeleton rearrangement were evaluated after PAN-induced autophagy was pharmacologically blocked.

Test the efficacy of trehalose in podocyte injury model *in vitro* and *in vivo*.

To test the efficacy of trehalose, firstly the ability of autophagy induction by trehalose was investigated in human podocytes. The efficacy of trehalose was evaluated by measuring apoptosis, necrosis, actin cytoskeleton rearrangement and motility in PAN-treated podocytes. *In vivo* model, proteinuria, hypoalbuminemia and renal ultrastructure were investigated for demonstrating the benefits of trehalose treatment.

Chapter 2

Materials and Methods

2.1 Cell culture

Conditionally immortalized human podocytes AB8/13 were cultured in RPMI 1640 supplemented with 10% fetal bovine serum (FBS) (Life Technologies). This conditionally immortalized human podocyte cell line has been developed by transfection with the temperature-sensitive SV40-T gene and a telomerase gene (Saleem et al. 2002). The human podocytes proliferated at 33°C, with the addition of Insulin-Transferrin-Selenium (Life Technologies). After growing to 50-60% confluency, cells were transferred to 37 °C for stopping proliferation and achieving full differentiation in 10-14 days. Fully differentiated human podocytes were treated with different reagents, such as PAN, in RPMI 1640 medium plus 10% FBS at 37 °C in a humidified atmosphere containing 5% CO₂.

2.2 Western blotting

Preparation of lysis buffer: A tablet of protein inhibitor (cOmplete ULTRA Tablets, mini, EDTA free, Roche Applied Science) was dissolved in 10ml RIPA buffer. Additionally, phosphatase inhibitor (Calbiochem) was added into RIPA buffer, when measuring phosphorylated proteins. The lysis buffer was aliquoted into small vials and stored in -20°C.

Extracting total proteins: Podocytes were harvested with trypsin and washed in ice-cold PBS two times. Ice-cold lysis buffer (0.5ml per 5×10^6 cells) was added to cells and maintained constant agitation for 30 minutes at 4°C. The lysis solution was centrifuged in a microcentrifuge at 12,000 rpm in 4°C. The supernatant was collected and stored in -80°C.

Determination of protein concentration: Bradford assay was performed for measuring protein concentration. Bovine serum albumin (BSA) was used for making protein standard curve. Proteins sample was diluted in milliQ water (1µl Sample+49 µl milliQ water). 10 µl of each standard and sample solution were added into separate microtiter plate wells. Protein solutions are assayed in duplicate. 200 µl of diluted dye reagent (Bio-Rad) was mixed with the sample thoroughly using a microplate mixer and incubated at room temperature for at least 5 minutes. Absorbance was measured at 595 nm. Eventually protein concentration was calculated using PRISM software.

Protein denaturation: 6 µl sample buffer (6×) with the anionic denaturing detergent SDS was mixed with 30 µl sample. The mixture was boiled at 95°C for 5 minutes.

Preparation of SDS-PAGE gels: The concentration of stacking gel is commonly set at 4%, while the concentration of resolving gel depends on the molecular weight of target protein. The following information is recommended by Bio-RAD:

Protein size (kDa)	Gel percentage (%)
4-40	20
12-45	15
10-70	12.5
15-100	10
25-200	8

Gel formulations (10 ml):

Percent Gel	DDI H ₂ O (ml)	30% Degassed Acr/Bis (ml)	Gel Buffer (ml)	10% SDS (ml)
4%	6.1	1.3	2.5	0.1
5%	5.7	1.7	2.5	0.1
6%	5.4	2.0	2.5	0.1
7%	5.1	2.3	2.5	0.1
8%	4.7	2.7	2.5	0.1
9%	4.4	3.0	2.5	0.1
10%	4.1	3.3	2.5	0.1
11%	3.7	3.7	2.5	0.1
12%	3.4	4.0	2.5	0.1
13%	3.1	4.3	2.5	0.1
14%	2.7	4.7	2.5	0.1
15%	2.4	5.0	2.5	0.1

Prior to pouring the gel, 50µl 10% ammonium Persulfate (APS) and 35µl Tetramethylethylenediamine (TEMED) were added to 10 ml gel solution to accelerate depolymerization. Mini-PROTEAN Tetra cell (Bio-Rad) was assembled for casting gel according to the manufacture's protocol. The resolving gel solution was poured at a corner of glass plate, and sufficient space was ensured for the stacking gel (the length of the teeth of comb plus 1cm). Distilled water was

overlayed the Acr/Bis solution and left the gel in a vertical position at room temperature. After 1 hour-polymerization, the overlay was discarded and the top of resolving gel was washed 3 times with deionized water to remove unpolymerized acrylamide. When polymerization of the stacking gel was completed, the comb should be removed carefully. Before loading samples, the wells were recommended to wash with deionized water 3 times.

Loading samples and gel running: 20-40 μg total protein was loaded in each well and a voltage of 80V was applied initially. When the dye front moved to the resolving gel, the voltage was increased to 120V. When gel running was completed, the gel was removed from electrophoresis apparatus and incubated it in transfer Buffer for 5min. The PVDF membrane should be immersed in 100% methanol for 2 min and in cold transfer buffer for 5 min. The gel sandwich should be free of air bubbles, and then the cassette was placed in module. The frozen cooling unit was added for lowering the temperature. If necessary, a stir bar can be place at the bottom of module to help maintain even buffer temperature and ion distribution. The transfer time depends on the molecular weight of target protein. For instance, 70 minutes were set for separating LC3.

BSA blocking: The PVDF membrane was incubated in BSA blocking buffer for 1 hour at room temperature.

Antibody incubation: Primary antibody was diluted in antibody dilution buffer according to the manufacturer's instruction. The PVDF membrane was incubated in primary antibody solution overnight (16-20h). Before the incubation with secondary

antibody, the membrane was washed 3 times with TBST. The second antibody incubation took 2 h at room temperature.

Protein visualization: Prepare chemiluminescence reagent (Perkinelmer) working solution was composed of equal volume of the enhanced luminal reagent and the oxidizing reagent. The membrane was incubated in this chemiluminescence reagent for 1min. The image was captured by the ChemiDoc MP system (Bio-Rad) and analyzed with the Image J software (NIH, USA). LC3, p62, p-mTOR (Ser2448), T-mTOR, p-p70S6K (Thr389), p70S6K, p-4E-BP-1, T-4E-BP-1, p-AMPK, AMPK, β -actin antibodies, anti-rabbit IgG, HRP linked antibody (Cell Signaling Technology) have been used.

2.3 Immunofluorescence staining

Podocytes were fixed with 4% paraformaldehyde, blocked with PBS+2% BSA and incubated with anti-LC3 antibody (4 °C, 12h). Then, Alexa Fluor 488 goat anti-rabbit IgG antibody (Life Technologies) was added (room temperature, 2h) and washed. After being mounted with the ProLong® Gold Antifade Reagent with DAPI (Life Technologies), cells were visualized by confocal microscopy (EZ-C1, Nikon Instrument, Japan). In addition, Alexa Fluor 594 Phalloidin (Life Technologies) was used to stain F-actin. The percentage of podocytes showing accumulation of LC3 puncta (that is with at least five puncta per podocyte) were counted and podocyte with disrupted cytoskeleton was quantified as the previous study described (Wong et al. 2011, Kang et al. 2014). The lamellipodias per cell

were calculated following the method described before (Lin et al. 2013). At least 100 cells were scored in each of the six independent experiments.

2.4 Flow cytometry

The treated podocytes were harvested and the cell density was adjusted to 1×10^6 /ml for YO-PRO-1/PI assay (Life Technologies) and active caspase-3 assay (BD Pharmingen) according to manufacturers' recommendation. Apoptotic cells were measured by the flow cytometry (FC500, Beckman Coulter) and expressed as a percentage of total cells. Examples of plots and analysis are shown in Figure 2.1.

Yo-pro-1/PI assay: 1ml harvested podocytes were incubated with 1 μ l YO-PRO-1 stock solution and 1 μ l PI stock solution for 20–30 min on ice. 488 nm excitation of green fluorescence emission was used for YO-PRO-1, while red fluorescence emission was used for propidium iodide. Cells were stained with single colour to perform standard compensation. As a result, live cells presented with a low level of green fluorescence, while apoptotic cells showed an incrementally higher level of green fluorescence, dead cells showed both red and green fluorescence.

Active caspase 3 assay: Harvested podocytes were resuspended and fixed in 250 μ l Cytofix/Cytoperm solution (1 million cells/0.5 ml) for 20 min (ice). Then, cells were washed twice with 1 ml Perm/Wash solution and incubated with the active caspase 3 antibody solution. Eventually cells were resuspended in 250 μ l Perm/Wash solution for flow cytometry.

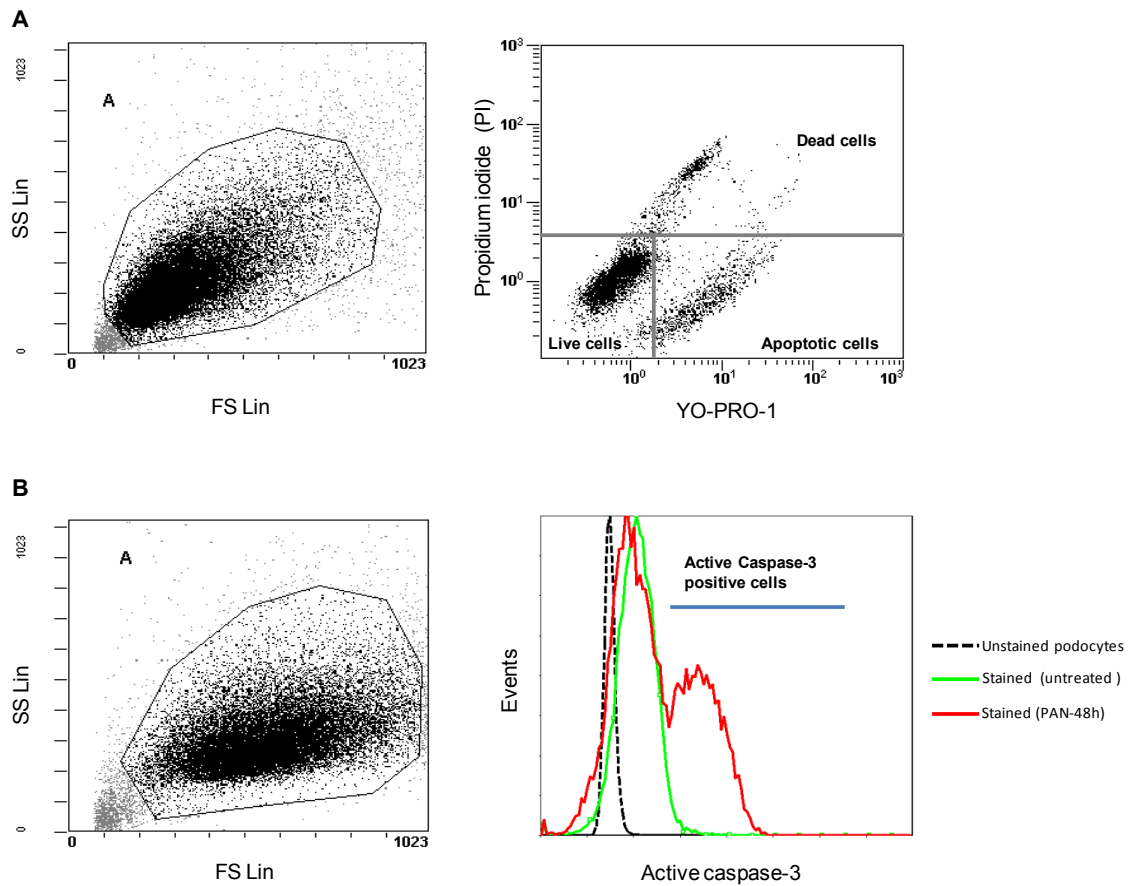


Figure 2.1 Representative pictures of YO-PRO-1/PI assay and Active caspase-3 assay

(A) Representative plots of YO-PRO-1/PI assay (flow cytometry). Apoptotic podocytes are defined as YO-PRO-1 positive and PI negative in this study.

(B) Representative plots of active caspase-3 assay (flow cytometry). Well-defined peak of active caspase-3 positive podocytes were detected after PAN treatment.

2.5 Reactive oxygen species (ROS) measurement

Podocytes were cultured in RPMI 1640 free of phenol red (Life Technologies) in black 96-well plates (Perkin Elmer). Differentiated podocytes were incubated with 10 μ M CM-H₂DCFDA (Life Technologies) or vehicle alone (20 min), followed with trehalose treatment (50mM). After recovering for 0.5 hour (37°C), immunofluorescence was recorded using the VICTOR 3 plate reader (Perkin Elmer). The fluorescence intensity was calculated and analyzed as described previously (Yadav et al. 2010).

2.6 Necrosis measurement

Equal number of podocytes was seeded in 6-well plates. Podocyte necrosis was evaluated by measuring lactate dehydrogenase (LDH) activity in culture medium. The CytoTox 96® Non-Radioactive Cytotoxicity Assay (Promega) was used for assessing LDH activity. The manufacture's protocol was strictly followed (Vollenbroeker et al. 2009).

2.7 Migration assay

Fully differentiated podocytes in 6-well plates were wounded by marking two strokes with a sterile 0.4mm 200 μ l Gilson style extension length tip. Podocytes were treated by PAN and/or trehalose for 12h. The number of podocytes migrating into the gap was counted as described before (Vollenbroeker et al. 2009).

2.8 Establishment of PAN nephrosis rat model

All animal procedures were conducted in accordance with the Guide for Animal Experimentation of the Hong Kong Polytechnic University (Ethics approval 12-24) and Animal licence from the Department of Health, Food and Environment Bureau, Hong Kong SAR Government. Male Sprague-Dawley rats were purchased from the Central Animal Facility, Hong Kong Polytechnic University, Hong Kong. The animals were kept under controlled environmental conditions (12:12h light/dark cycle and room temperature $22\pm 2^{\circ}\text{C}$). The rats had free access to UV-treated tap water and were fed ad libitum throughout the study with ordinary rat chow (LabDiet, Indiana, USA). They were acclimatized to metabolic cages (Techniplast, Nalgene, USA) for at least two days before experiments. Twenty-four hour urine was collected for determinations of urine protein and creatinine. The rats received a single intraperitoneal injection of PAN (15mg/100g body weight in 1.5 ml NaCl 0.9%) or equal volume of the vehicle (1.5ml NaCl 0.9%). Injection of PAN results in the development of heavy proteinuria as confirmed by urinalysis.

2.9 Trehalose treatment in PAN nephrosis rat model

Trehalose (Sigma) was dissolved in drink water for inducing autophagy. The rats have free access to the drinks throughout the experiment. Rat groups were set up as follows:

Groups	Treatment
Control	No treatment
PAN group	IP injected with PAN
Trehalose group	Pretreated with trehalose (2%) for 3 weeks
Trehalose+PAN group	Pretreated with trehalose (2%) for 3 weeks IP injected with PAN

2.10 Urinalysis and serum albumin measurement

The urinary protein, creatinine and serum albumin levels were determined by automated clinical chemistry analyzer (AU480 Chemistry System, Beckman Coulter, USA) using reagent cartridges recommended by the manufacturer. The operators were blinded to the rat grouping information.

2.11 Glomerulus isolation

Renal cortex was separated from kidneys and cut into small pieces. Renal tissues were grinded with 1640 solution on the grade sieves of which the pore sizes are 250mm, 110mm and 70mm respectively. Glomerulus solution was centrifuged, and the purity of glomerulus was checked under inverted microscope.

2.12 Transmission electron microscopy

Animals were sacrificed by an overdose of pentobarbital sodium (50mg/kg body weight; i.p.). 2 mm x 2 mm columns of tissues were taken from the right kidney. The samples were fixed with 2.5% glutaraldehyde in cacodylate buffer (0.1M

sodium cacodylate-HCl buffer pH 7.4) overnight and stored at 4°C before processing. Fixation was stopped by changing cacodylate buffer with 0.1 M sucrose to stop fixation. Tissue blocks were put into the processing glass vial and washed the tissue blocks with several changes of cacodylate buffer. Samples were post-fixed in 1% osmium tetroxide (OsO₄) in cacodylate buffer for 1 hour at R.T. The used OsO₄ was discarded into the waste container. The tissue blocks were washed thoroughly in several changes of cacodylate buffer. Dehydration was completed on a rotary shaker as follows:

50% ethanol, 5 min

70% ethanol, 5 min

90% ethanol, 5 min

100% ethanol, 3 times, 10 min for each time

Propylene oxide, 2 times, 5 min for each time

The tissue blocks were infiltrated with epoxy resin/propylene oxide 1:1 mixture for 1 hour 30min at 37 °C and epoxy resin for another 1 hour at 37 °C. Tissue blocks were embedded in epoxy resin containing in dried, labeled plastic capsules (Micron Moulds). After polymerizing at 60 °C overnight, the plastic capsules with blades can be removed. One-micron sections were cut from tissue blocks and stained with toluidine blue. These sections were used for selection of the centermost glomerulus whose entire profile was present and which was at least one tubular diameter distant from the edge of the section. Thin sections of this central glomerulus were cut, stained with uranyl acetate and lead citrate, and viewed on a Philips CM100

transmission electron microscope (Philips Electron Optics, Eindhoven, The Netherlands) at an accelerating voltage of 80 kV. Micrographs from each glomerulus were obtained by random sampling.

2.13 Period Acid-Schiff (PAS) staining

Renal tissue was fixed in formalin and embedded with paraffin. Before staining, the tissues were dewaxed as following: xylene1 (3-5min) - xylene2 (30s) - xylene3 (30s)-100% ethanol (30s) -95% ethanol (30s)-70% ethanol (30s). Then, samples were washed with tap water and distilled water 3 times respectively. 1% periodic acid solution (PAS) was added to samples for 5 minutes, then, slides were rinsed in distilled water 3 times and treated with Schiff's reagent for 15 minutes. After washing in running tap water for 5-10 minutes (place the slides horizontally), cell nuclei were stained with Mayer's haematoxylin for 10 minutes. Slides were rinsed with tap water and sprayed with 1% acid alcohol. Furthermore, slides were quickly rinsed well with tap water and added Scott's tap water. After rinsing slides with tap water, samples were dehydrated by the following treatment: 70 % ethanol (5s)-95% ethanol (5s)-100% ethanol (5s)-xylene3 (5s)-xylene2 (5s)-xylene1 (5s). Ultimately, slides were mounted and observed under microscope.

2.14 Statistical Analysis

Data were expressed as mean \pm SEM. T-test was used for two group's comparison. Multiple groups were analyzed by Kruskal-Wallis test with post hoc procedures

using the Prism 5.0 Software (GraphPad, San Diego, CA, USA). A p value <0.05 was considered to be statistically significant.

Chapter 3

The cytoprotective role of autophagy in PAN-treated human podocytes

(This chapter has been published in Biochemical and Biophysical Research Communications.2014 Jan; 443(2): 628-634)

3.1 Introduction

Podocytes are highly differentiated cells which play an extremely important role in guarding the permeability of the tripartite renal filtration barrier. Many glomerular diseases attribute to podocyte damage including apoptosis, cytoskeleton rearrangement and detachment (D'Agati 2008, Greka and Mundel 2012). Single gene mutations, such as those affecting nephrin and podocin, in podocytes have also been acknowledged in the pathogenesis of renal diseases (Ruotsalainen et al. 1999, Welsh and Saleem 2012). Therefore, podocytes emerge as the therapeutic target of glomerular diseases. Since podocytes are terminally differentiated cells, they are able to cope with various adverse stimuli and repair themselves efficiently. The question of “How do podocytes survive longly?” initiated our investigation into the cellular protective mechanisms.

Autophagy is an evolutionary conserved catabolic process (Mizushima et al. 2008). It is involved in processing unwanted cellular materials including misfold proteins,

damaged organelles and invasive microorganisms to the lysosomes for degradation. The degraded products can be recycled for maintaining energy homeostasis (Periyasamy-Thandavan et al. 2009). Autophagy is being kept at basal levels in cells for safeguarding and promoting cell survival. It is one of the major processes that allow cells to respond rapidly to the metabolic stress. Under certain circumstances, autophagy can be induced to a higher level to protect cells. For instance, the induction of autophagy under ischemia in neurons protects them from apoptosis (Zhang et al. 2013). Currently, the better known potential stimuli inducing autophagy include nutrient starvation, oxidative stress, mitochondrial dysfunction, ischemia-reperfusion and infection (Jiang et al. 2010, Hsieh et al. 2009).

mTOR is an evolutionarily conserved serine/threonine kinase which is the core part of two complexes: mTORC1 and mTORC2. Besides mTOR, mTORC1 also contains mLST8 and Raptor which recruits substrates such as p70 S6 Kinase (p70S6K) for the phosphorylation by the kinase domain of mTOR. mTORC1 plays multiple roles in regulating ribosome biogenesis, protein synthesis and tissue hypertrophy (Wang and Proud 2011). More importantly, the activation of mTORC1 inhibits autophagy. On the contrary, autophagy can be induced when mTORC1 is inhibited by the decreased growth factors and amino acids during starvation as well as some agents such as rapamycin (Jung et al. 2010, Yu et al. 2010).

Puromycin aminonucleoside (PAN) is widely used for studying glomerular diseases as it induces podocyte injury mimicking nephrotic syndrome *in vitro* and *in vivo*

(Lowenborg, Jaremko and Berg 2000, Wada et al. 2005). Rats after a single dose of PAN injection will present with heavy proteinuria, effacement of foot processes and podocyte loss (Pippin et al. 2009). Thus, valuable knowledge for understanding the pathophysiology of renal diseases has been generated based on this reagent. Recently, it has been reported that PAN can induce autophagy in podocytes *in vitro* and *in vivo*. For instance, Asanuma *et al.* found that autophagy was induced in PAN treated conditionally immortalized mouse podocytes (MPCs) and in PAN nephrosis rat model (Asanuma et al. 2003). Another study showed that mTOR-ULK1 pathway was involved in PAN-induced autophagy in MPCs (Wu et al. 2013). In addition, Hartleben *et al.* demonstrated that autophagy deficient mice exhibited more severe albuminuria after PAN treatment than the wild type (Hartleben et al. 2010). Taken together, these studies demonstrate that autophagy is essential for podocytes to maintain normal function. Even though PAN is known to induce podocyte apoptosis, cytoskeleton damage and autophagy, the relationship between these important processes remains unclear. In particular, the role of PAN-induced autophagy in podocyte survival has not been elucidated.

In the present study, we found that PAN induced autophagy prior to apoptosis which was featured with the activation of mTORC1 in human podocytes. Moreover, when the PAN-induced autophagy was being blocked by autophagy inhibitors, podocyte apoptosis increased significantly. In addition, we revealed that the proportion of podocytes with disrupted cytoskeleton dramatically increased after autophagy

inhibition. These results suggested that the induced autophagy may be an early adaptive cytoprotective mechanism for podocyte survival after PAN treatment.

3.2 Experimental design

Human conditional immortalized podocytes were treated with PAN. Then autophagy was being investigated by immunofluorescence staining for LC3 puncta and Western blotting for LC3. Podocyte apoptosis was evaluated by flow cytometry (YO-PRO-1/PI assay and active caspase 3 assay). Molecules involved in the mTOR pathway were also being evaluated. Furthermore, for studying the mechanism of autophagy on podocyte apoptosis, 3-Methyladenine (3-MA) and Chloroquine (CQ) were used to inhibit autophagy. The disruption of podocyte cytoskeleton was analysed by immunofluorescence staining of F-actin. For the detailed materials and methods, please refer to Chapter 2.

3.3 Results

3.3.1 PAN induced autophagy prior to apoptosis in human podocytes

To investigate the relationship between autophagy and apoptosis in podocytes, conditionally immortalized human podocytes were used in the present study. The level of autophagy was evaluated by the expression of microtubule-associated protein 1A/1B-light chain 3 (LC3). LC3 is a soluble protein in mammalian cells including two forms (LC3-I and LC3-II). LC3-I is constitutively expressed in many cell types. It is less sensitive to be detected by certain anti-LC3 antibodies and it is more labile than LC3-II. The elongation of autophagosome requires LC3-II which is the conjugated product of LC3-I and phosphatidylethanolamine (PE). Thus, the increased LC3-II is regarded as the standard marker for autophagy activation (Mizushima, Yoshimori and Levine 2010). As shown in Figure 3.1, when podocytes were treated with different doses of PAN for 24 hours, the expression of LC3-II increased significantly at the dose of 30 and 50 μ g/ml. There was no significant difference between these two doses. Hence, the concentration of 30 μ g/ml was selected for the subsequent experiments.

We found that LC3-II increased after PAN treatment and peaked at 24h, but it decreased afterwards and returned nearly to the basal level at 48h (Figure 3.2). To confirm the PAN-induced autophagy detected above, we performed LC3 immunofluorescence staining in PAN treated podocytes. It is known that LC3-II binds to the autophagosomal membrane and forms puncta in the formation of autophagosome. Therefore, immunofluorescence staining can be used to analyse

LC3 distribution and monitor autophagy in cells. As shown in Figure 3.3, a large number of bright puncta were visualised in the cytoplasm of human podocytes at 24h after PAN treatment. On the contrary, only very small scattered immunofluorescent dots were detected in the 0h, 12h and 48h post PAN treatment. The statistical results from LC3 staining are consistent with the data generated from Western blotting.

Apoptosis is typically characterized by altered membrane permeability as determined by YO-PRO-1/PI assay in this study. Our data showed that after PAN (30 µg/ml) treatment, the percentage of apoptotic podocytes at 24h was similar to the control (Figure 3.4), but it increased significantly at the 48h time point. Moreover, active caspase-3 which is the cleaved product of caspase 3 indicates cell undergoing apoptosis. As shown in Figure 3.5, the percentage of podocytes with active caspase-3 increased significantly at 48h after PAN treatment. Taken the data of autophagy and apoptosis together, it was clearly shown that PAN induced autophagy prior to apoptosis in human podocytes.

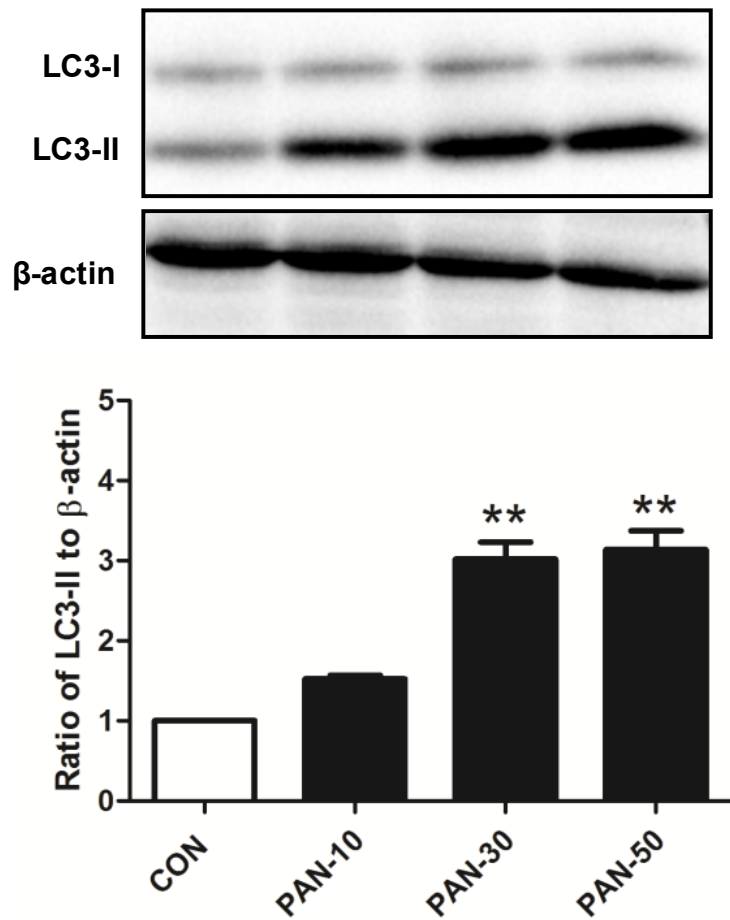


Figure 3.1 PAN induced podocyte autophagy in a dose-dependent manner

The LC3-II expression increased in a dose-dependent manner after PAN treatment. Conditionally immortalized human podocytes were treated with 10, 30 and 50 μ g/ml of PAN for 24 h. The LC3-II was measured by Western blotting. The data were expressed as the relative change compared with the control group (CON). A representative immunoblot is shown along with the quantitative data which represents the mean \pm SEM (n=5), ** p <0.01 versus CON.

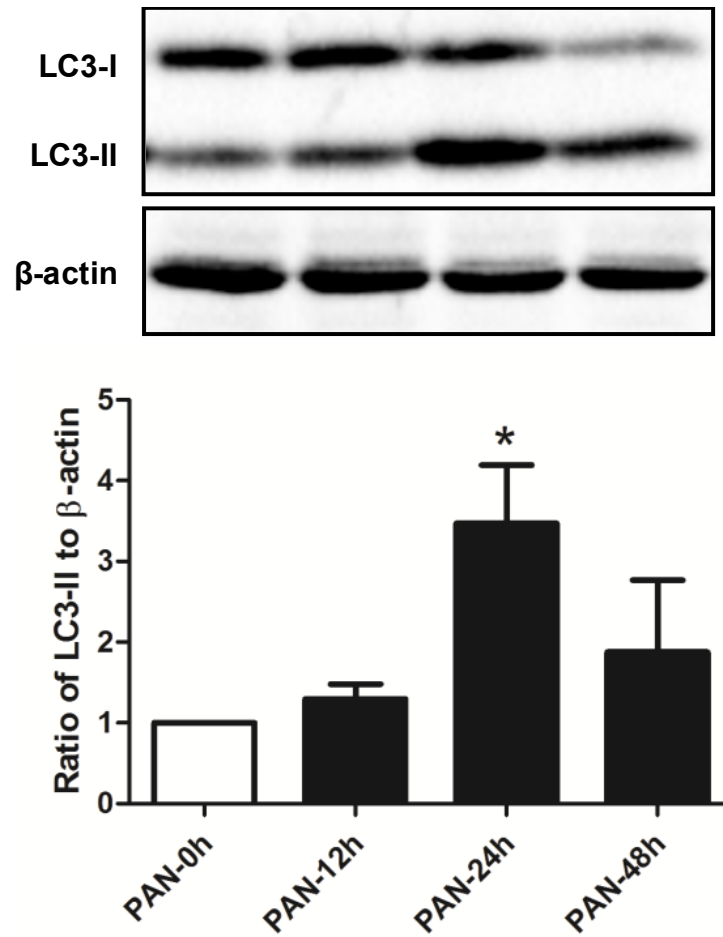


Figure 3.2 PAN induced podocyte autophagy in a time-dependent manner

The LC3-II expression in podocytes peaked at 24h after PAN treatment (30μg/ml).

The results represent the mean±SEM (n=4), * $p < 0.05$ versus PAN-0h.

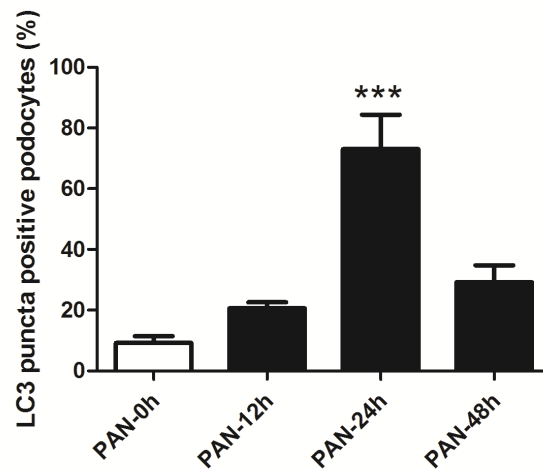
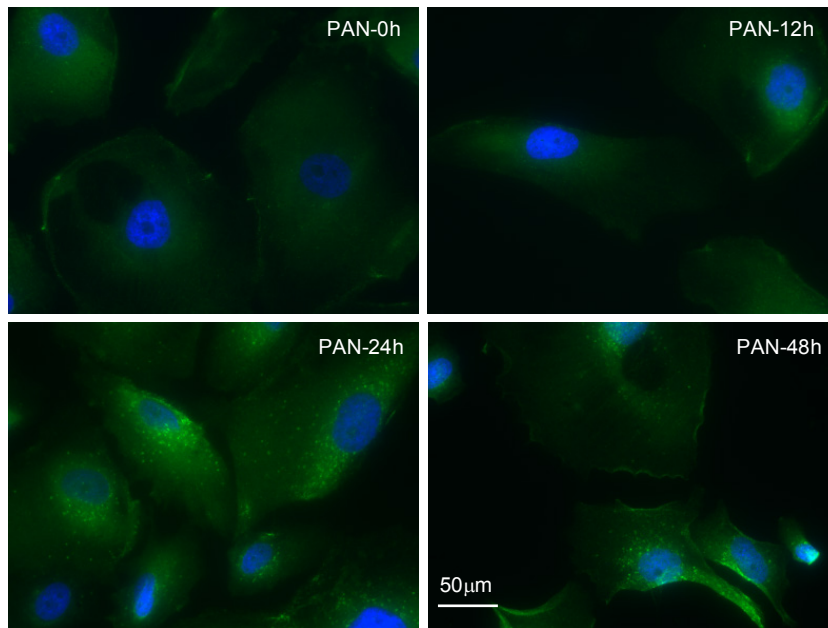


Figure 3.3 LC3 immunostaining in PAN-treated human podocytes

Large number of bright LC3 puncta (green) at 24h after PAN treatment (30 μ g/ml) were visualised by confocal microscopy. Representative LC3 immunostaining (green) and statistical results from 6 independent experiments were shown, *** p <0.001 versus PAN-0h. The nuclei of the podocytes were stained with DAPI (blue).

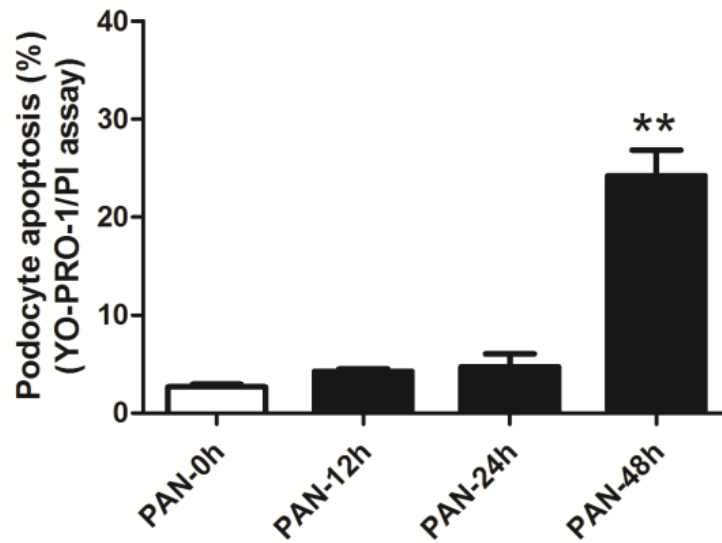


Figure 3.4 PAN induced apoptosis in human podocytes

Podocyte apoptosis peaked at 48h after PAN treatment (30 $\mu\text{g/ml}$). Apoptosis was measured by flow cytometry (YO-PRO-1/PI assay). The results represent the mean \pm SEM, n = 8, ** p <0.01 versus PAN-0h.

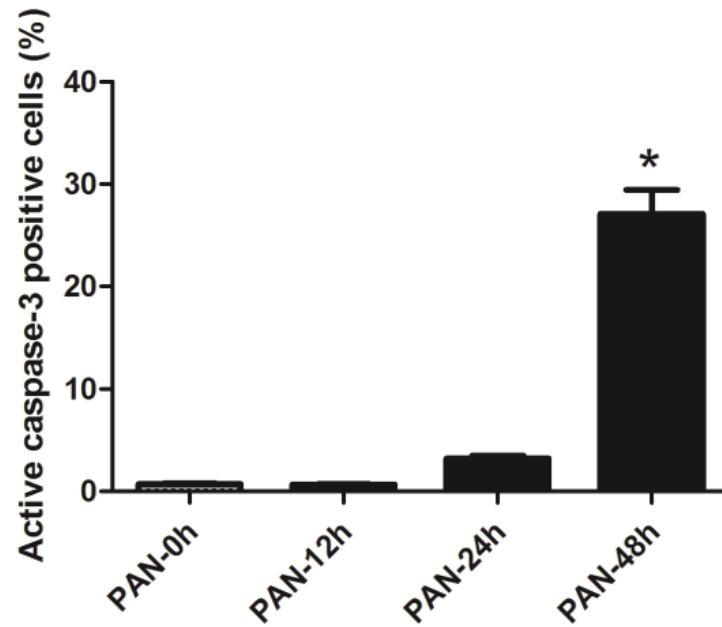


Figure 3.5 PAN increased active caspase-3 positive podocytes

Active caspase-3 positive podocytes increased at 48h after PAN treatment. Flow cytometry was used for the measurement. n=4, * $p < 0.05$ versus PAN-0h.

3.3.2 mTORC1 was activated in PAN-treated human podocytes

To examine the activity of mTORC1 in PAN treated podocytes, we measured the levels of phospho-mTOR (p-mTOR) and its downstream target marker, phospho-p70S6K (p-p70S6K). It was shown that the expression of p-mTOR was maintained at the basal level in the first 12 hours but increased gradually over time. Its expression level was significantly higher than the control at 24, 36 and 48h time points. Similarly, p-p70S6K was induced gradually over time and reached significantly high level after 24 h post PAN treatment (Figure 3.6).

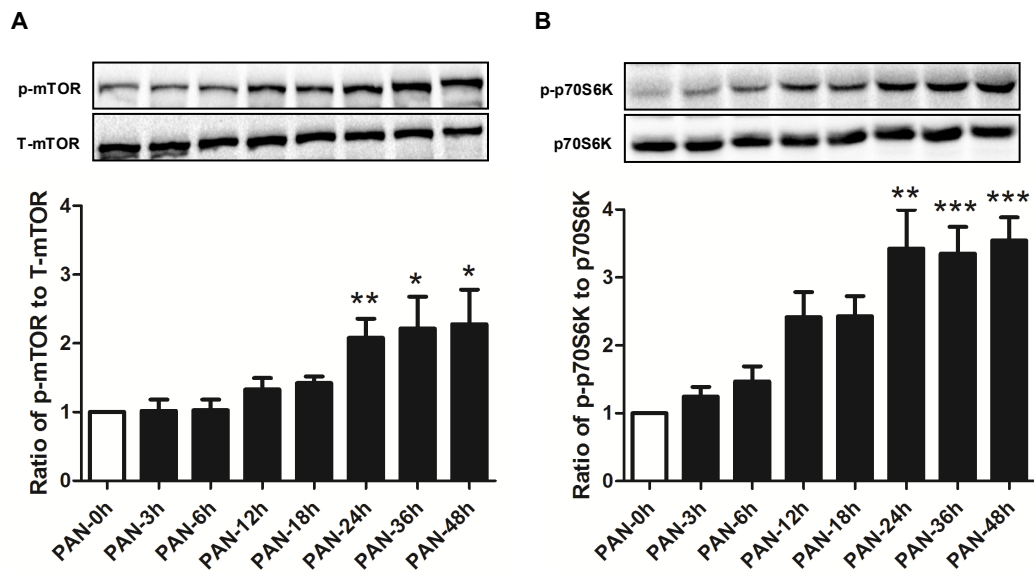


Figure 3.6 mTORC1 was activated in PAN-treated podocytes

(A) The expression level of p-mTOR (Ser2448) in PAN (30 μ g/ml)-treated podocytes increased significantly at 24, 36 and 48 h. The p-mTOR expression level was measured by Western blotting. The data was expressed as the relative change compared with PAN-0h. A representative immunoblot is shown along with the quantitative data which represent the mean \pm SEM (n=13), * p <0.05; ** p <0.01 versus PAN-0h.

(B) Similarly, the expression level of p-p70S6K (Thr389) increased significantly at the same time points. A representative immunoblot is shown along with the quantitative data which represent the mean \pm SEM (n=9), ** p <0.01; *** p <0.001 versus PAN-0h.

3.3.3 Inhibition of PAN-induced autophagy increased apoptosis in human podocytes

Based on our observation of low percentage of apoptotic podocytes but high autophagy at 24h after PAN treatment, we speculated that autophagy may play a cytoprotective role against podocyte apoptosis. To verify this hypothesis and investigate the potential mechanism, two inhibitors were used to suppress autophagy in PAN-treated human podocytes. 3-MA blocks autophagy at the initial stage by suppressing PI3K, whereas CQ increases lysosomal pH, thereby inhibits autolysosomal degradation, which is featured with accumulation of the two autophagy substrates LC3-II and p62/SQSTM1 (p62). Additionally, polyubiquitinated proteins and aggregates can be oligomerized by p62, and binds to LC3 on the autophagosome membrane, eventually damaged organelles or unfolded proteins will be degraded in the autophagy pathway (Bjorkoy et al. 2005). Hence, we also measured p62 to confirm the inhibition of autophagy by these inhibitors.

As shown in Figure 3.7, PAN-induced podocyte autophagy was indicated by the increased LC3-II and decreased p62 levels at 24h. The addition of 3-MA successfully suppressed the PAN-induced autophagy which was characterized by the low LC3-II and accumulation of p62. Concurrently, there was a significant increase in podocyte apoptosis (Figure 3.8-3.9), along with the percentage of active caspase-3 positive podocytes (Figure 3.10).

Similarly, CQ arrested autophagy which was presented with LC3-II and p62 accumulation (Figure 3.11). The blockage of autophagy by CQ also led to an increase in podocyte apoptosis and the percentage of active caspase-3 positive cells (Figures 3.12-3.14).

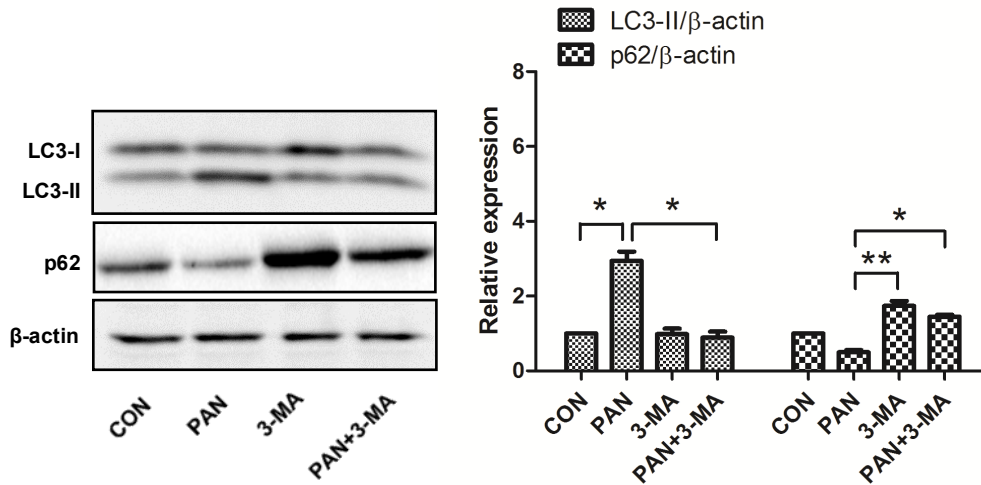


Figure 3.7 3-MA inhibited PAN-induced autophagy

PAN-induced autophagy was inhibited by 3-MA. The expression of LC3-II increased in podocytes which were treated with PAN (30 μ g/ml) for 24hours, it was decreased by 3-MA (5mM). The expression of p62 decreased in PAN-treated podocytes, but it increased significantly after the addition of 3-MA. The representative immunoblot is shown along with the quantitative data which represent the mean \pm SEM (n=5), * p <0.05, ** p <0.01.

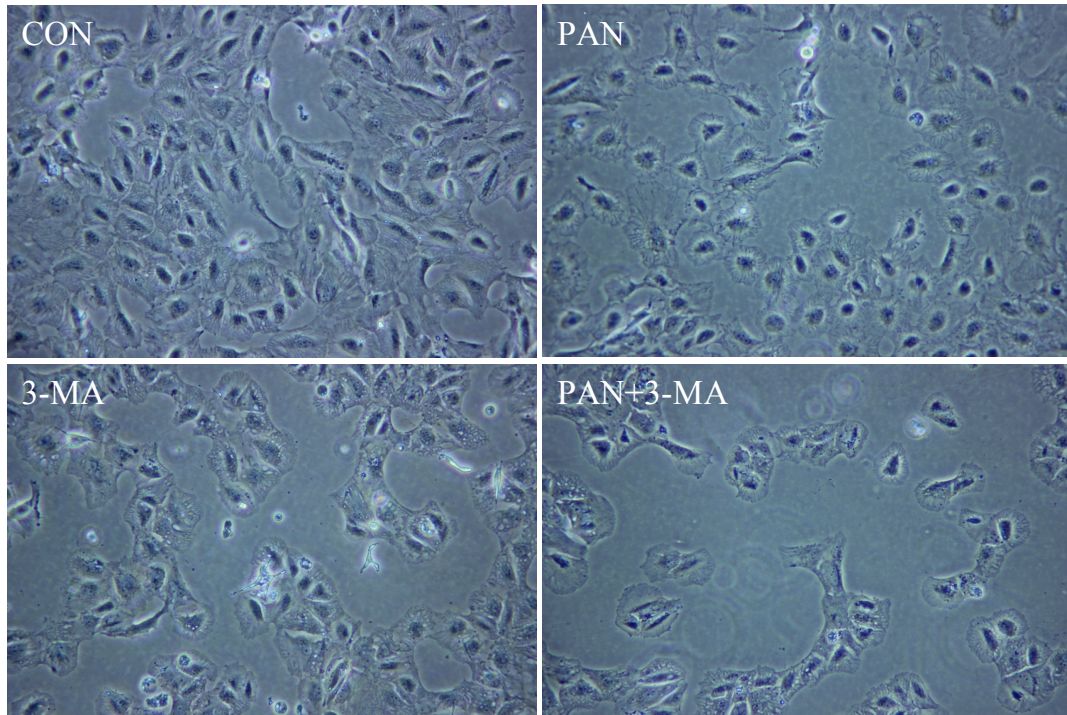


Figure 3.8 Morphology changes in human podocytes after 3-MA inhibited PAN-induced autophagy ($\times 200$)

There were no obvious morphological changes in podocytes after 24h PAN treatment ($30\mu\text{g/ml}$). 3-MA (5mM) decreased the cell density and shranked the cell size, and more severe damages have been found in PAN-treated human podocytes after autophagy inhibition by 3-MA.

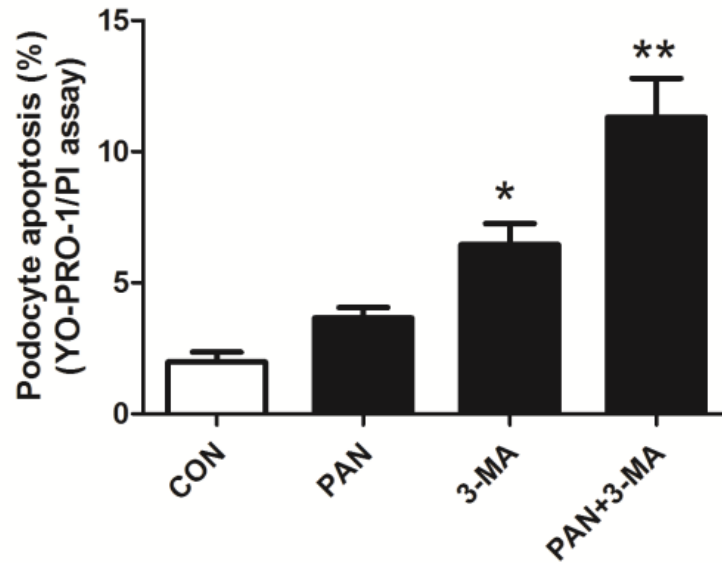


Figure 3.9 Podocyte apoptosis increased after 3-MA inhibited PAN-induced autophagy

Podocyte apoptosis increased significantly at 24h after autophagy inhibition. The results represent the mean \pm SEM (n=4), * p <0.05, ** p <0.01 versus CON.

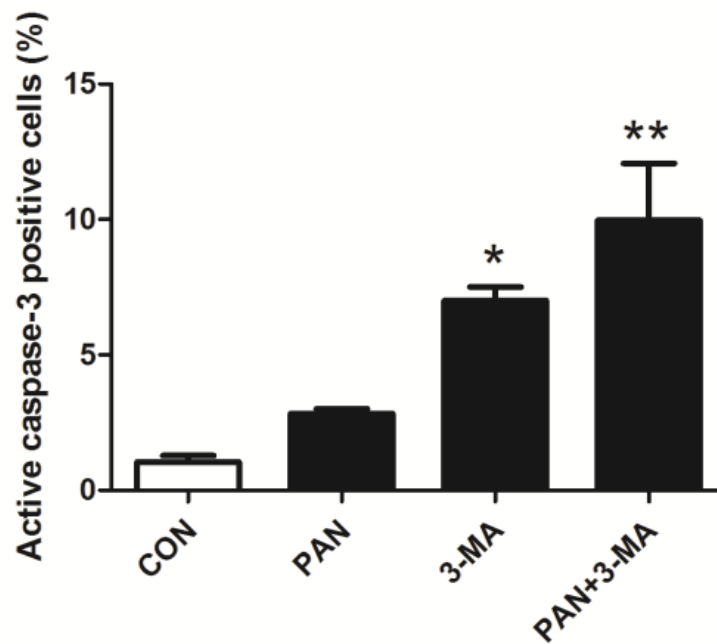


Figure 3.10 Active caspase-3 positive podocytes increased after autophagy inhibition by 3-MA

No apparent elevation was showed in the percentage of active caspase-3 positive podocytes after PAN treatment (30 μ g/ml) for 24hour. However, active caspase-3 positive podocytes increased significantly after 3-MA treatment, particularly in PAN+3-MA group. Flow cytometry was used for the measurement. The data represent the mean \pm SEM (n=4), * p <0.05, ** p <0.01 versus CON.

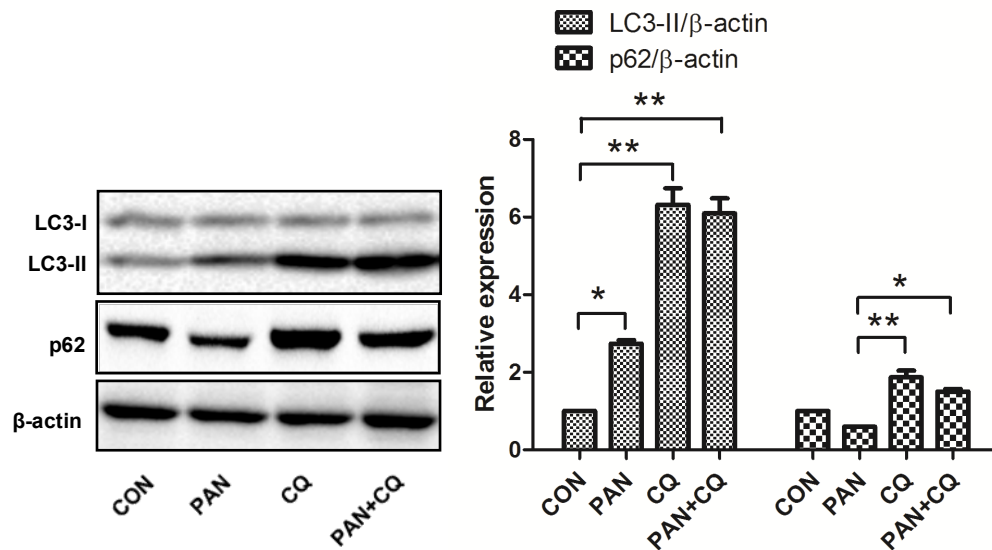


Figure 3.11 CQ inhibited PAN-induced autophagy

PAN-induced autophagy was inhibited by CQ (25 μ M) for 24h. The PAN-induced autophagy was blocked by CQ which resulted in the increased LC3-II expression. The expression of p62 decreased in PAN-treated podocytes, but it increased significantly after the addition of CQ. The representative immunoblot is shown along with the quantitative data which represent the mean \pm SEM (n=5), * p <0.05, ** p <0.01.

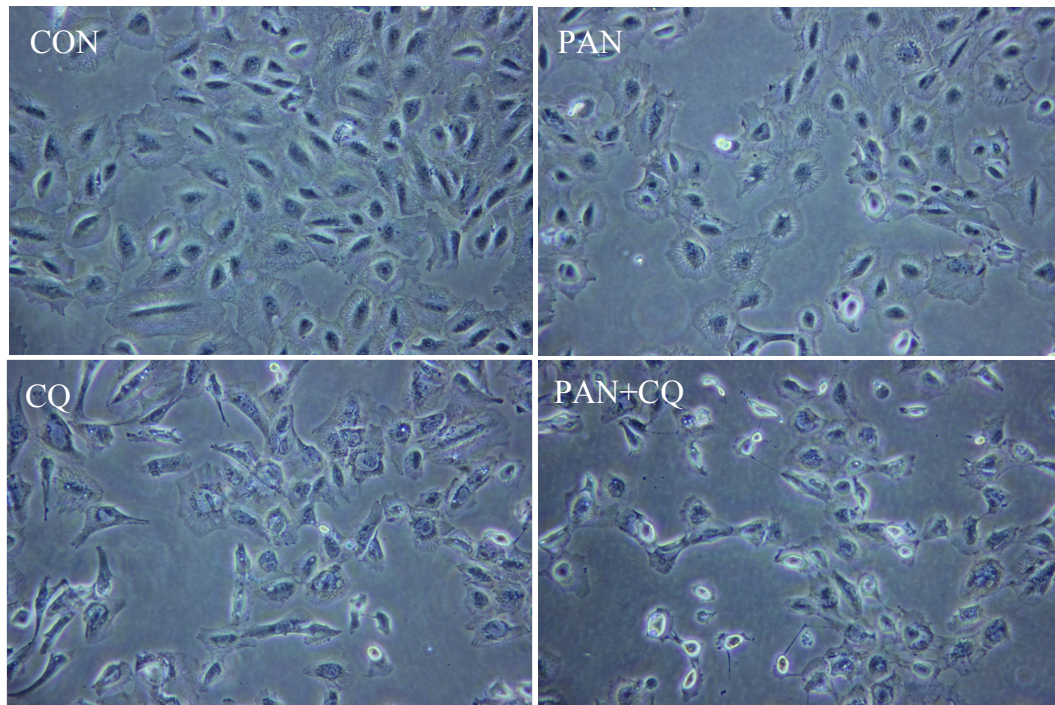


Figure 3.12 Morphology changes in human podocytes after CQ inhibited PAN-induced autophagy ($\times 200$)

CQ (25 μM , 24h) decreased podocyte density and shrunk cell size. More severe damages have been shown in PAN-treated human podocytes after autophagy inhibition by CQ.

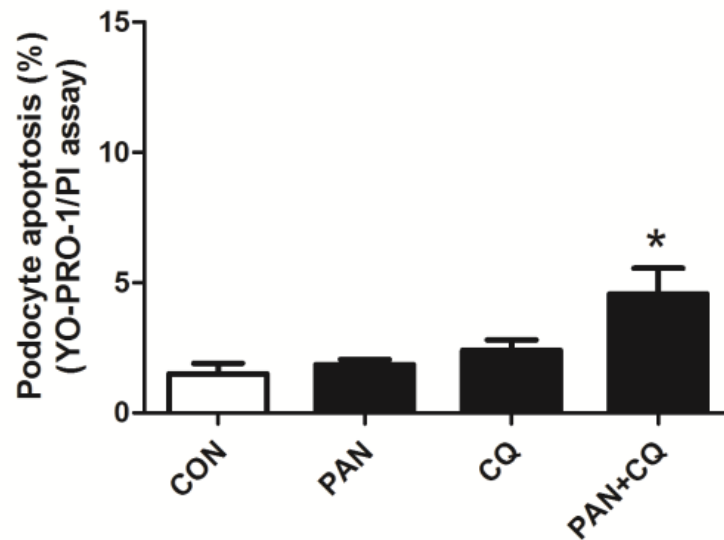


Figure 3.13 Podocyte apoptosis increased after CQ inhibited PAN-induced autophagy

Podocyte apoptosis significantly increased after autophagy inhibition by CQ (25 μ M, 24h). The results represent the mean \pm SEM (n=4), * p <0.05 versus CON.

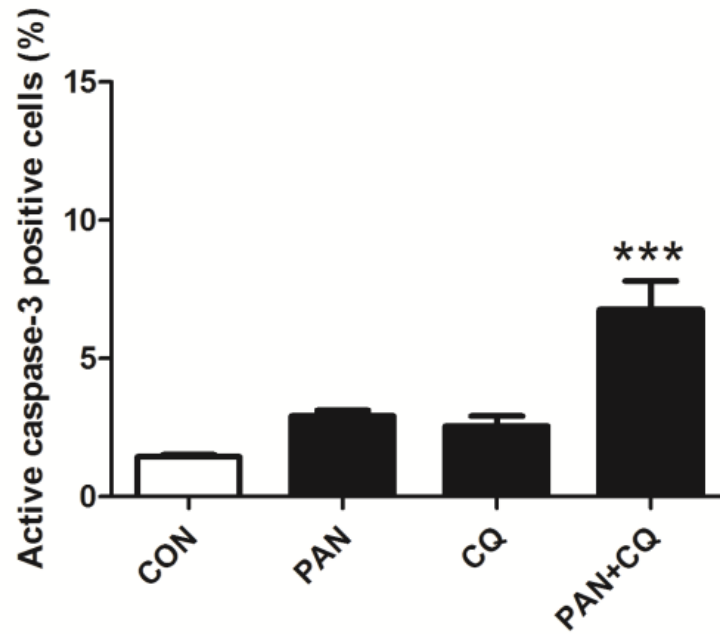


Figure 3.14 Active caspase-3 positive podocytes increased after autophagy inhibition by CQ

The percentage of active caspase-3 positive podocytes increased after autophagy inhibition by CQ (25 μ M) for 24h. The results represent the mean \pm SEM (n=4),

*** p <0.001 versus CON.

3.3.4 Inhibition of PAN-induced autophagy disrupted podocyte cytoskeleton

Disruption of cytoskeleton is the hallmark of many glomerular diseases and lead to the podocyte effacement resulting in proteinuria (Jeruschke et al. 2013). To test whether the inhibition of induced autophagy affects the stability of podocyte cytoskeleton, we checked the status of F-actin in human podocytes when the PAN-induced autophagy was inhibited by 3-MA or CQ at 24h. As shown in Figure 3.15-3.16, podocyte cytoskeleton damage was featured with cell retraction, the loss of actin-stress fibre organization and the formation of cortical cytoskeleton. The percentage of podocytes with disrupted cytoskeleton increased significantly after the inhibition of PAN-induced autophagy.

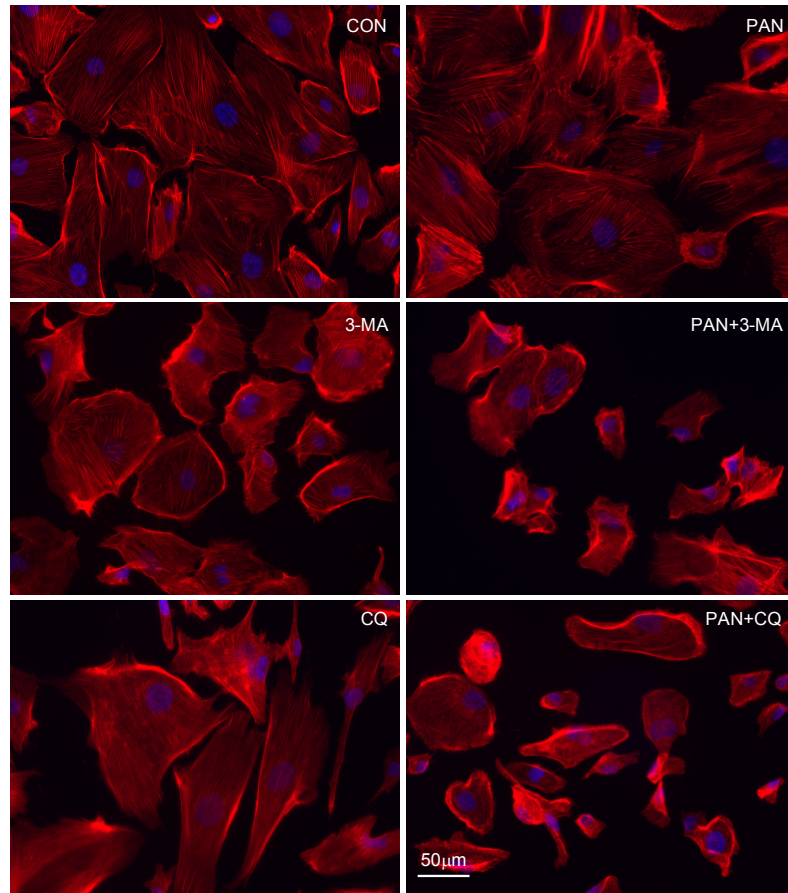


Figure 3.15 The inhibition of PAN-induced autophagy disrupted podocyte cytoskeleton

The podocytes with disrupted F-actin increased when PAN-induced autophagy was inhibited by 3-MA (5mM) or CQ (25µM) for 24 hours. Regular bundles of intracellular actin filaments (red) were observed in untreated cells (CON). The nuclei of the podocytes were stained with DAPI (blue). PAN, 3-MA and CQ alone slightly disrupted the actin filaments in podocytes at 24h. However, cell retraction, the loss of actin-stress fiber organization and the formation of cortical cytoskeleton were observed in the PAN+3-MA and PAN+CQ groups.

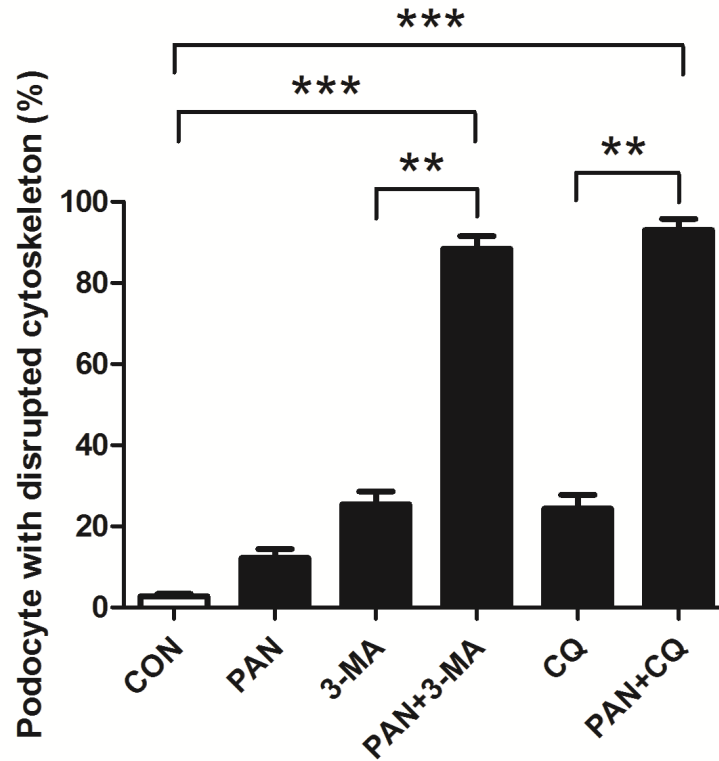


Figure 3.16 Podocytes with disrupted actin cytoskeleton increased after autophagy inhibition

The quantitative data of Figure 3.15 were expressed as mean±SEM from 6 independent experiments, ** $p < 0.01$, *** $p < 0.001$ versus CON.

3.4 Discussion

Autophagy is a conserved catabolic process for keeping cell homeostasis and serves as the quality control mechanism which is particularly important for the long lived cells such as neurons. Similarly, podocytes are terminally differentiated cells characterized by the high basal level of autophagy (Jeruschke et al. 2013), suggesting the significance of autophagy in keeping podocyte homeostasis. Previously PAN has been shown to induce autophagy in murine podocytes (Asanuma et al. 2003, Wu et al. 2013). Here we reveal the role of the induced autophagy in PAN-treated human podocytes.

In the present study, a relationship between autophagy and apoptosis was suggested in PAN-treated podocytes. We found that the expression of LC3-II peaked at 24h, the increased LC3 puncta were also observed in the cytoplasm at the same time point. Additionally, our study showed that the induction of autophagy was transient and the expression of LC3-II nearly dropped to the basal level at 48h. Combining with our observation of low percentage of apoptotic cells at 24h and peak apoptosis with the increased active caspase-3 positive podocytes at 48 h, we speculate that PAN induced cell stress in podocytes and triggered both autophagy and apoptosis. At the early time point, autophagy played a cytoprotective role to keep apoptosis at the low level. However, as cell stress persisted over time, autophagy was overridden by apoptosis at 48 h.

The changes of autophagy and apoptosis in PAN-treated podocytes described above may be associated with mTORC1. We observed a significant increase in the level of p-mTOR and p-p70S6K at 24, 36 and 48h, suggesting the activation of mTORC1 after PAN treatment. Recently it has been demonstrated that the mTORC1 activation in diabetic nephropathy leads to the misallocation of slit diaphragm proteins and an epithelial mesenchymal transition-like phenotypic switch (Inoki et al. 2011). Thus, we postulate that the activation of mTORC1 was responsible for the podocyte apoptosis. In addition, mTORC1 is also known to negatively regulate the autophagy. As expected, the increased activity of mTORC1 suppressed autophagy in the last 24 hours of PAN treatment (from the time point of 24h to 48h). However, it seems to be puzzling at the time point of 24h that the peaked autophagy was coupled with the activated mTORC1. Actually, similar phenomenon has also been described recently by Huber *et al* that high basal autophagy level was observed in podocytes despite the activation of mTOR (Huber et al. 2012). This interesting finding could also be explained by the newly identified TASCC which is located at the site of the Golgi apparatus (Narita et al. 2011). TASCC sequesters cellular mTORC1 with autolysosomes and leads to a low concentration of mTORC1 in the environment outside the TASCC in favour for autophagy induction. Therefore, TASCC enables the simultaneous existing of the activation of mTORC1 and autophagy. In addition, it also can be not excluded that an mTOR-independent pathway exists in PAN-treated podocytes.

Rapamycin, a mTOR inhibitor, has been shown to alleviate podocyte injury by inducing autophagy (Wu et al. 2013). To verify the potential cytoprotective role of PAN-induced autophagy, we used 3-MA and CQ to inhibit the autophagy at the early and late stage respectively. Our results showed that 3-MA decreased the expression of LC3-II, while CQ led to the accumulation of LC3-II, suggesting that both of them can efficiently suppress PAN-induced autophagy. Consistently, p62 decreased at 24h after PAN treatment but up-regulated with the addition of 3-MA and CQ, further revealing that PAN can induce podocyte autophagy and 3-MA or CQ blocked the PAN-induced autophagy flux. Thus, it suggested that the damaged cellular components caused by PAN treatment accumulated in podocytes and could not proceed for degradation. Furthermore, it has been reported that the accumulation of p62 promotes cellular stress that leads to diseases (Komatsu et al. 2010). As a consequence, podocyte apoptosis increased after 24h, along with the up-regulation of active caspase-3 positive podocytes, further showing the death pathway was activated. Therefore, the PAN-induced autophagy was essential for protecting podocyte against apoptosis in the first 24h after treatment.

The disruption of podocyte cytoskeleton is commonly recognized as the key pathological changes in glomerular diseases (Yu et al. 2013). It is also known that F-actin depolymerization occurs before the formation of apoptotic bodies and is an early step of apoptosis. In the present study, we showed that the percentage of podocytes with disrupted F-actin increased significantly when the PAN-induced autophagy was being inhibited. Therefore, it suggested that PAN-induced autophagy

may play a critical role in maintaining the stability of podocyte cytoskeleton and prevented podocytes from undergoing apoptosis.

In this study, we have provided direct evidence that inhibition of PAN-induced autophagy increased podocyte apoptosis. The induced autophagy may be an early adaptive protective mechanism for PAN-treated podocytes. Since both apoptosis and autophagy were triggered by PAN, there may be common signals that involve similar downstream signaling molecules. The crosstalk between the cell death pathways may contribute to the functional link between autophagy and apoptosis. We reason that by modulating the molecules involved in podocyte autophagy, the effect of apoptosis will be ameliorated and this cytoprotective role of autophagy may be harnessed for the treatment of glomerular diseases in the future.

Chapter 4

Trehalose, an mTOR independent autophagy inducer, alleviates human podocyte injury after PAN treatment

(This chapter has been submitted to PLOS One, manuscript number PONE-D-14-17769, under revision)

4.1 Introduction

Glomerular diseases are characterized by the disrupted renal filtration barrier which consists of endothelial cells, basement membrane and epithelial cells (also called podocytes). Podocytes have been regarded as the key target of harmful stimuli in renal diseases (Welsh and Saleem 2012). It is evident that podocyte effacement is commonly found in glomerular diseases such as MCNS and FSGS (Deegens et al. 2008). In addition, the gene mutation of podocyte cytoskeleton proteins is associated with congenital nephrotic syndrome (Akchurin and Reidy 2014). Thus, the ideal therapeutic strategies of glomerular diseases are aiming to ameliorate podocyte injury including apoptosis and actin cytoskeleton rearrangement.

Several studies revealed that cyclosporine A and dexamethasone show direct protective effects in podocytes (Faul et al. 2008, Liu et al. 2012). However, the multiple adverse effects of these agents cannot be ignored. Researchers continued to look for strategies to repair podocyte damage and autophagy has emerged as a

potential approach recently. Autophagy is a highly conserved catabolic mechanism of which the unwanted organelles and misfold proteins are delivered to lysosome for degradation (Hartleben, Wanner and Huber 2014). The final metabolic products can be recycled as nutrient for keeping cell homeostasis. Podocytes are postmitotic and long-lived cells. Therefore, strong self-protective mechanisms are required for counteracting different detrimental challenges. As expected, the higher basal autophagy has been demonstrated in podocytes than other renal cells (Asanuma et al. 2003, Hartleben et al. 2010). The autophagy deficient mice presents with accumulated dysfunction proteins, endoplasmic reticulum stress and proteinuria. Moreover, they are more susceptible to drug-induced models of glomerular diseases (Hartleben et al. 2010). Our previous study also showed that inhibition of autophagy increases apoptosis and actin cytoskeleton depolymerisation in PAN-treated human podocytes (Kang et al. 2014). Additionally, it was reported that autophagy may become as a new therapeutic approach for diabetic nephropathy (Kume et al. 2014). Collectively, it is suggested that autophagy can be harnessed for the treatment of glomerular diseases by attenuating podocyte injury (Hartleben et al. 2014, Takabatake et al. 2014).

Autophagy is precisely regulated by a network of proteins. For instance, mTOR which is a highly conserved serine/threonine kinase negatively regulates autophagy induction (Inoki 2014). Rapamycin is the representative agent for inducing autophagy via inhibition of mTOR activity. It was demonstrated that autophagy induced by rapamycin alleviates podocyte injury *in vitro* (Wu et al. 2013). However,

proteinuria was observed in patients with organ transplantation after rapamycin treatment (Inoki and Huber 2012), while the underlying reasons of proteinuria remains unclear. Thus, it is essential to find alternative safe autophagy inducers for the treatment of renal diseases.

Trehalose is a natural disaccharide found in many organisms (Ohtake and Wang 2011). It induces autophagy in an mTOR-independent manner and shows protective effects in various cells against harmful stimuli such as heat, dehydration, cold, desiccation, and oxidation (Elbein et al. 2003). The protective effect of trehalose has been demonstrated in neurodegenerative diseases, such as Alzheimer's disease, frontotemporal dementia, progressive supranuclear palsy and corticobasal degeneration (Sarkar et al. 2007, Kruger et al. 2012). Meanwhile, no mutagenicity, carcinogenicity, acute toxicity, embryotoxicology and teratology have been reported. Despite the effects of trehalose was recognized in the brain, it remains unclear whether trehalose induces autophagy and shows cytoprotective effects in podocytes.

In the present study, we are the first to show that trehalose induced autophagy in an mTOR independent manner in human podocytes. Moreover, podocyte apoptosis and actin cytoskeleton depolymerisation can be alleviated by trehalose. Therefore, this study confirmed that autophagy can be utilized for protecting podocytes and trehalose may be a potential candidate for the treatment of glomerular diseases.

4.2 Experimental design

Human conditional immortalized podocytes were treated with trehalose. Then autophagy was being investigated by immunofluorescence staining for LC3 puncta and Western blotting for LC3 and Atg5. To elucidate the signalling pathway in trehalose-induced podocyte autophagy, p-AMPK, ROS, mTOR and its substrates were measured. In attempting to test the efficacy of trehalose in PAN-treated human podocytes, apoptosis and necrosis were evaluated by flow cytometry and by measuring LDH activity respectively. We also performed the podocyte migration assay to evaluate podocyte recovery. Furthermore, for studying the role of trehalose-induced autophagy, CQ and WT were used to inhibit autophagy. For the detailed materials and methods, please refer to Chapter 2.

4.3 Results

4.3.1 Trehalose induced autophagy in human podocytes

To test whether trehalose induces autophagy in human podocytes, we investigated the expression of LC3 and Atg5 in treated cells. Briefly, LC3 consists of LC3-I and LC3-II, LC3-I converts into LC3-II which adheres to the membrane of phagophore for the formation of autophagosome. LC3-II presents with bright puncta in immunofluorescence staining (Mizushima et al. 2010). Atg5 is essential for the elongation of autophagosome (Pyo et al. 2013). As shown in Figures 4.1-4.2, the expression of LC3-II increased in a dosage and time dependent manner, the immunofluorescence staining results were consistent with these findings. The LC3-II puncta positive podocytes significantly increased in the cytoplasm after 36h-trehalose treatment (Figures 4.3-4.4). In addition, similar expression profile was found in Atg5 (Figure 4.5).

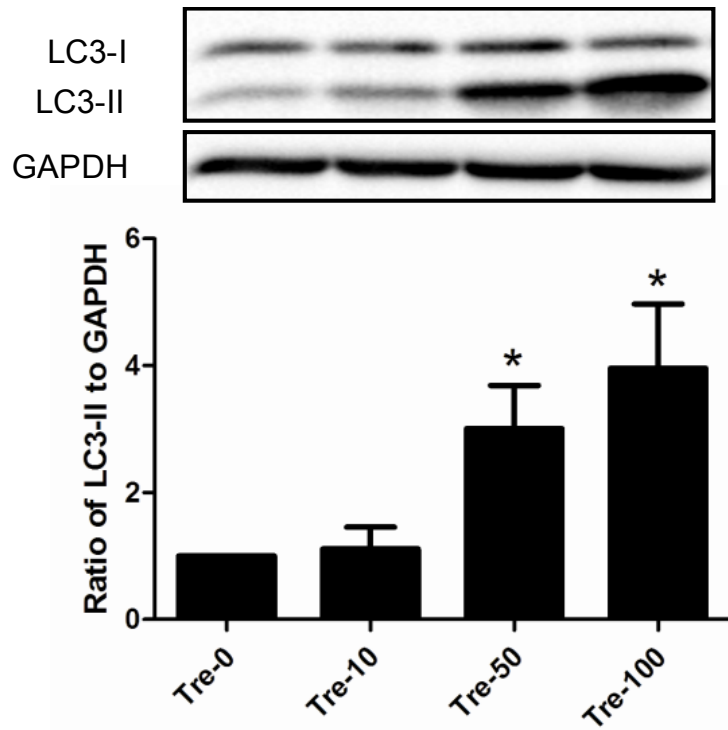


Figure 4.1 Trehalose induced autophagy in a dose dependent manner

The expression of LC3-II increased in a dose dependent manner. Conditionally immortalized human podocytes were treated with 0, 10, 50 and 100 mM of trehalose (Tre) for 48h. LC3-II was measured by Western blotting. The data (mean±SEM) were expressed as the relative changes compared with Tre-0mM group. Representative immunoblot images were shown along with the statistical results.

* $p < 0.05$ versus Tre-0mM, $n = 5$.

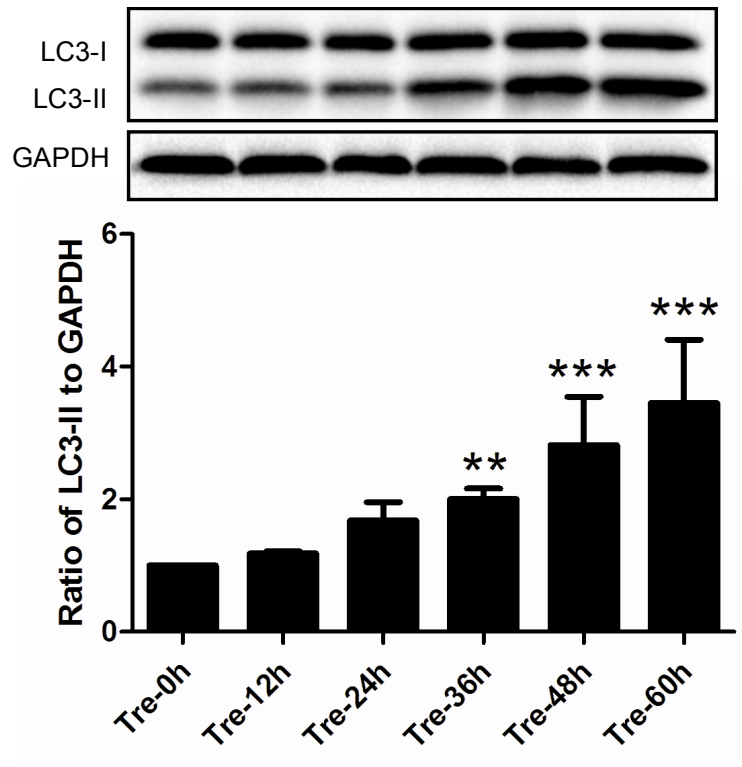


Figure 4.2 Trehalose induced autophagy in a time dependent manner

LC3-II increased in a time dependent manner. Podocytes were treated with 50mM trehalose for 0, 12, 24, 36, 48 and 60h. The results represent the mean±SEM (n=7), ** p <0.01, *** p <0.001 versus Tre-0h.

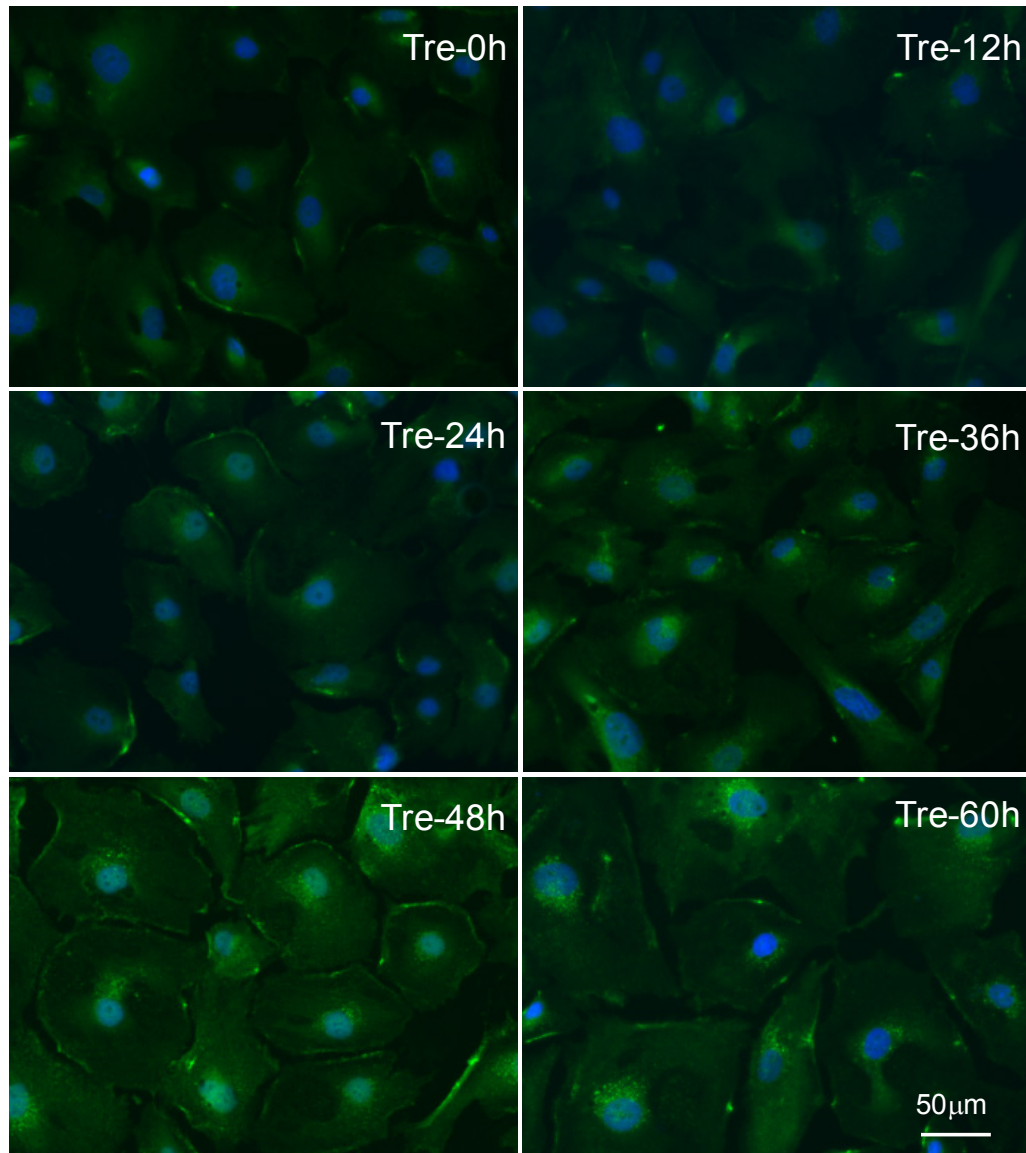


Figure 4.3 LC3 immunostaining in trehalose-treated human podocytes

LC3-II puncta increased after trehalose treatment. LC3 immunostaining in podocytes was performed at 0, 12, 24, 36, 48 and 60h after trehalose treatment (50mM). Significant increased bright puncta (green) can be observed in cytoplasm after 48h-trehalose treatment. Podocyte nuclei were stained with DAPI (blue).

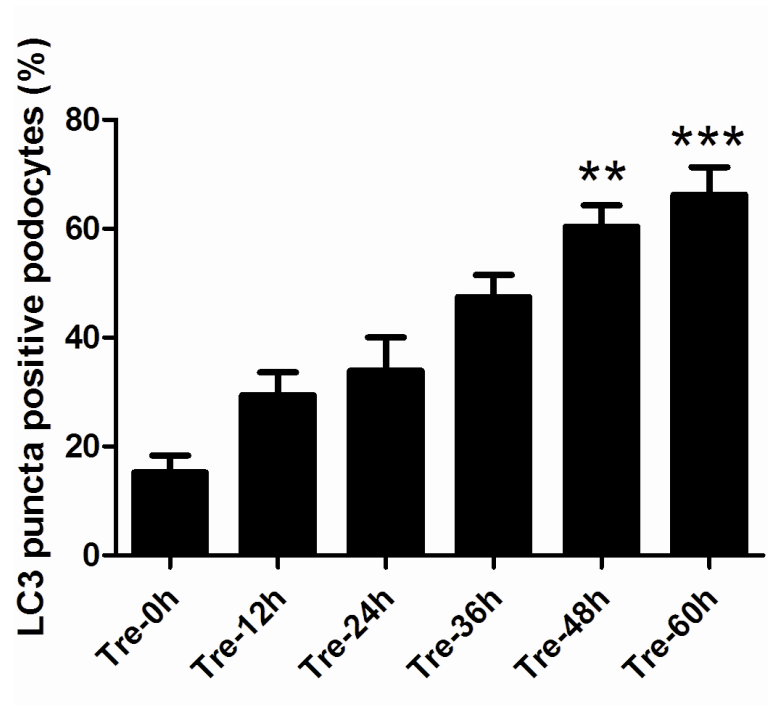


Figure 4.4 LC3 puncta positive podocytes increased after trehalose treatment

The statistical result of Figure 4.3 was derived from 6 independent experiments. The results represent the mean \pm SEM, ** p <0.01, *** p <0.001 versus Tre-0h.

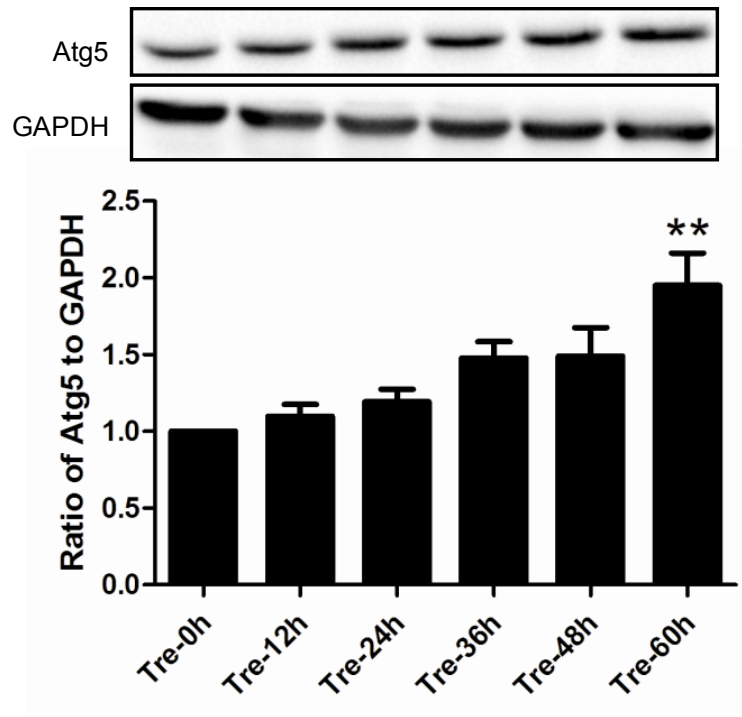


Figure 4.5 Trehalose increased the expression of Atg5

The expression of Atg5 was up-regulated in trehalose-treated podocytes (50mM). Podocytes were treated with 50mM trehalose for 0, 12, 24, 36, 48 and 60h. The expression of Atg5 significantly increased at the time point of 60h. The results represent the mean \pm SEM (n=5), ** p <0.01 versus Tre-0h.

4.3.2 Trehalose induced podocyte autophagy in an mTOR independent manner

mTOR negatively regulates autophagy induction, whereas trehalose triggers autophagic flux in other cell types such as neuron without altering the level of phospho-mTOR (p-mTOR) (Sarkar et al. 2007). It remains unknown whether the same pathway occurs in trehalose-treated podocytes. We measured the level of p-mTOR and its substrates p-p70S6K, p-4E-BP1. As shown in Figures 4.6, these three markers did not change significantly over the 60h trehalose treatment.

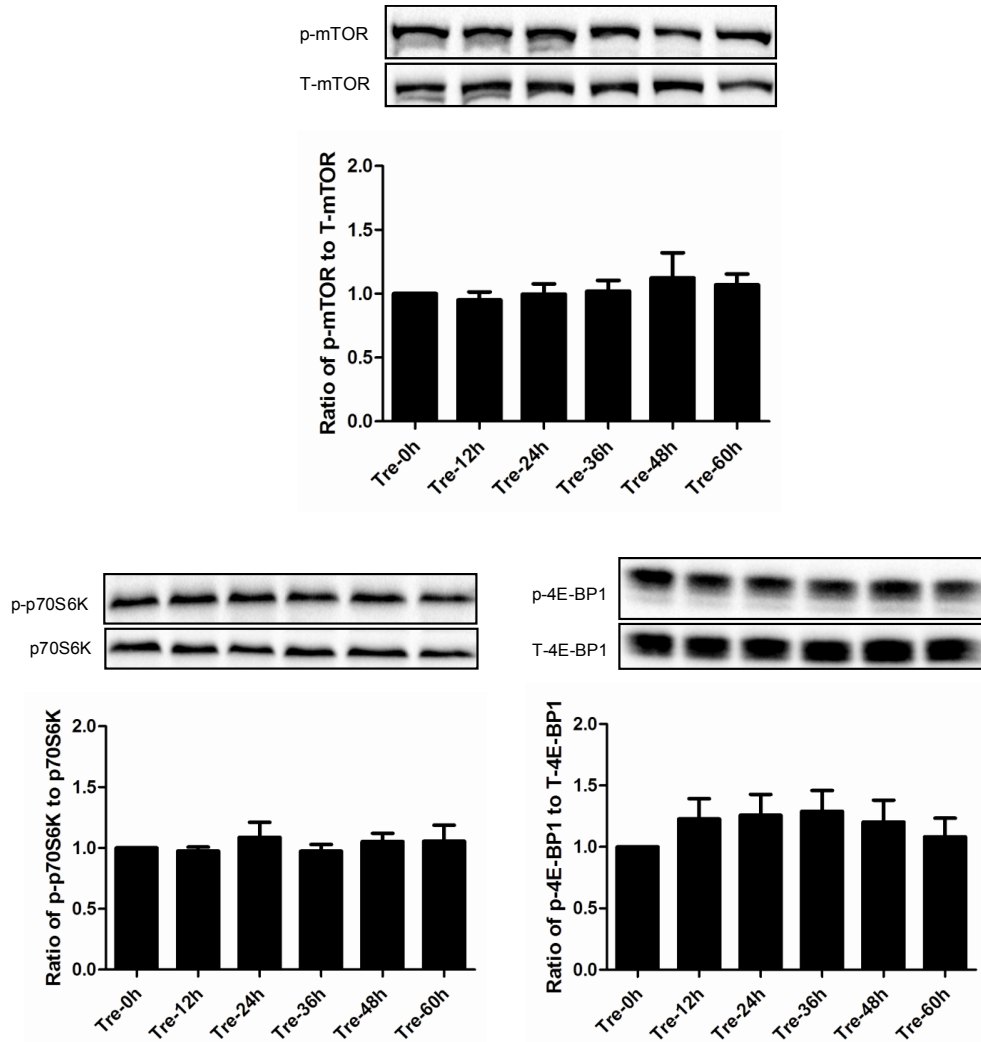


Figure 4.6 Trehalose induced podocyte autophagy in an mTOR independent manner

mTOR activity was not altered in trehalose-treated podocytes. Podocytes were treated with trehalose (50mM) for 0, 12, 24, 36, 48 and 60h. The levels of p-mTOR and its substrates p-p70S6K, p-4E-BP1 were measured by Western blotting. However, no significant changes were observed, n=5, 5 and 6 respectively. The representative immunoblot was shown along with the statistical results.

4.3.3 Trehalose-induced autophagy was independent of ROS

Starvation is the most common stimulus for inducing autophagy. To verify whether trehalose-induced autophagy attributes to calorie limitation, we examined the expression level of AMPK which is an energy sensor in mammalian cells. After the ratio of AMP to ATP decreases, p-AMPK responsively up-regulates and subsequently leads to autophagy induction by inhibiting the activity of mTOR (Kim et al. 2011, Salminen and Kaarniranta 2012). As shown in Figure 4.7, there was a slight decrease in the level of p-AMPK from the time point of 36h to 60h. However, the changes were not statistically significant.

The underlying mechanism of starvation-induced autophagy is the generation of ROS which is essential for the initiation of autophagic flux (Azad, Chen and Gibson 2009). Therefore, to confirm whether ROS involves in the trehalose-induced autophagy, we monitored the ROS production. Consistently, ROS did not change significantly when compared with control group (Figure 4.8).

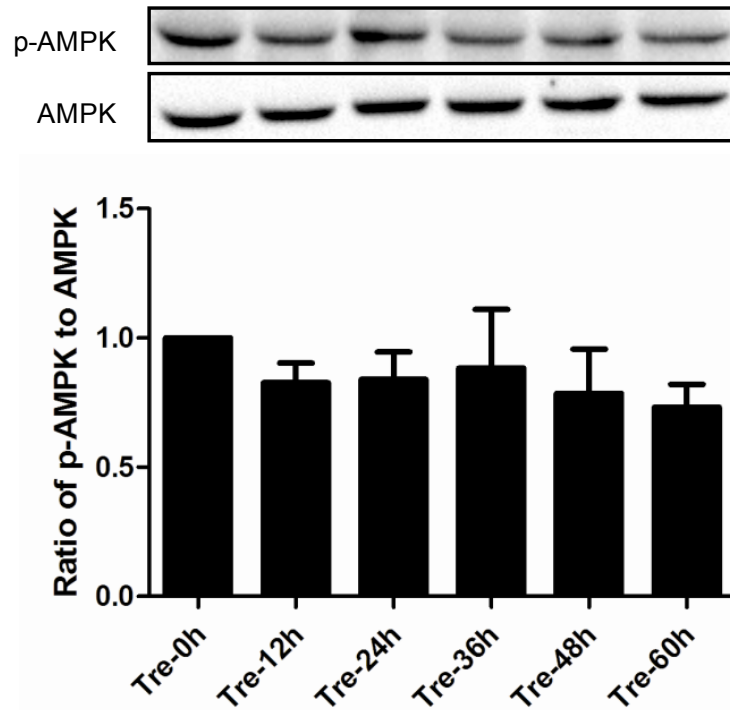


Figure 4.7 Trehalose-induced podocyte autophagy was not associated with energy restriction

Trehalose-treated podocytes (50mM) were harvested for p-AMPK measurement at the time points of 0, 12, 24, 36, 48 and 60h. The expression level of p-AMPK did not change significantly, n=6.

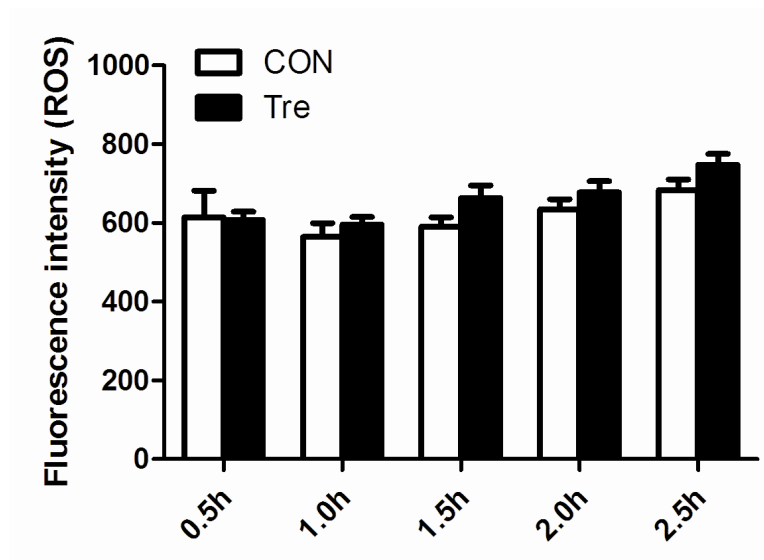


Figure 4.8 Trehalose-induced podocyte autophagy was independent of ROS

ROS level was recorded every half an hour after trehalose treatment (50mM), the data representing immunofluorescence intensity (mean±SEM) within 2.5h were shown (n=6). No significant changes were noted.

4.3.4 Trehalose decreased PAN-induced apoptosis in human podocytes via the induction of autophagy

Interplay exists between autophagy and apoptosis. It has been reported that autophagy suppresses cell apoptosis by inhibiting apoptotic proteins (Mukhopadhyay et al. 2014). Since trehalose can induce autophagy in podocytes without increasing ROS, we hypothesized that trehalose decreases podocyte apoptosis. Thus, PAN was used to induce podocyte apoptosis *in vitro*. We found that trehalose up-regulated the expression of LC3-II in PAN-treated human podocytes (Figure 4.9). The data of LC3 immunostaining confirmed this finding as LC3-II bright puncta were obviously presented in trehalose alone and Tre+PAN groups (Figures 4.10). To confirm the protective effects of trehalose, LDH was measured to evaluate podocyte necrosis. As shown in Figure 4.11, the changes in LDH level were negligible. However, PAN-induced apoptosis was significantly down-regulated after trehalose treatment, accompanying with the decrease in active caspase-3 positive cells (Figures 4.12-4.13).

To verify whether the cytoprotective effects of trehalose are attributed to autophagy induction, CQ and WT were used to inhibit autophagy. CQ blocks the fusion between autophagosome and lysosome, resulting in an accumulation of LC3-II. WT, a potent and specific PI3K inhibitor, inhibits autophagy at the initial stage with the decreased LC3-II (Klionsky et al. 2012). As shown in Figures 4.14, CQ increased the expression of LC3-II in trehalose-treated groups. Meanwhile, WT showed the opposite pattern. The inhibitory effects were further confirmed by the elevated p62,

even though the expression of p62 in Tre+PAN+CQ and Tre+PAN+WT groups was lower than Tre+CQ and Tre+WT groups. LDH increased significantly when trehalose-induced autophagy was being inhibited (Figure 4.15). Correspondingly, podocyte apoptosis increased after CQ or WT treatment as well as the percentage of active caspase-3 positive podocytes (Figures 4.16-4.17).

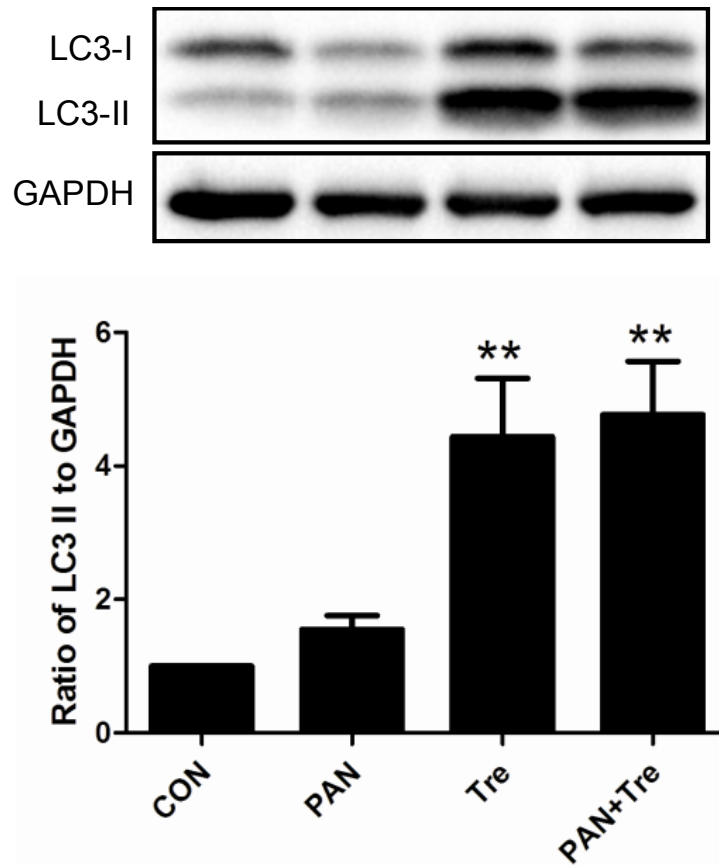


Figure 4.9 Trehalose induced autophagy in PAN-treated human podocytes

The expression of LC3-II slightly increased after 48h PAN treatment (30 μ g/ml), while trehalose (50mM) strongly up-regulated LC3-II. Representative immunoblot images were shown along with the statistical results. ** p <0.01 versus CON, n=6.

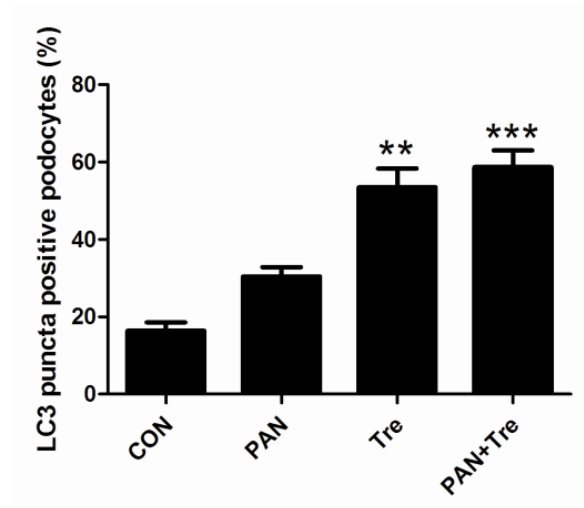
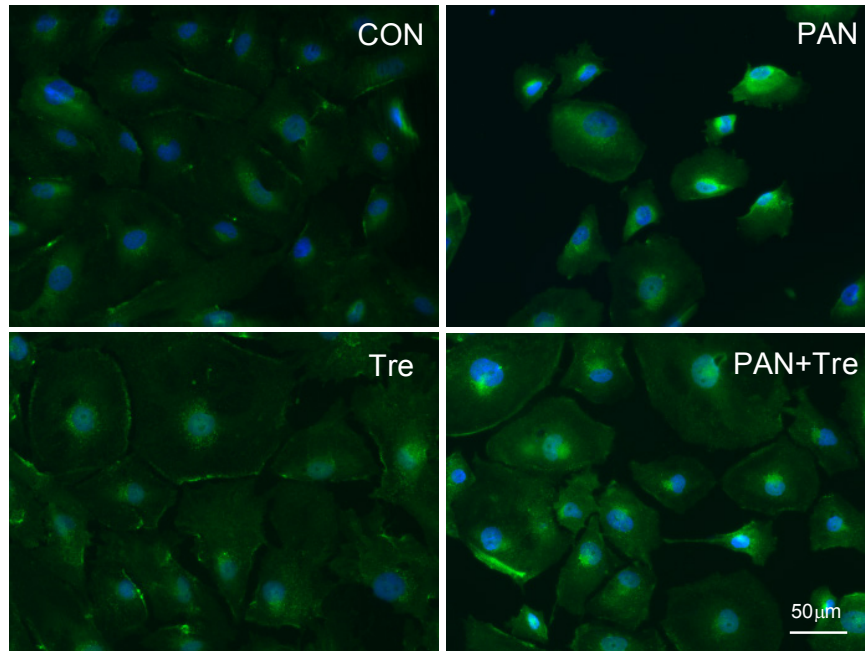


Figure 4.10 LC3 immunostaining in PAN or (and) trehalose-treated human podocytes

The findings of Figure 4.9 were confirmed by LC3 immunostaining. Obvious elevated LC3-II bright green puncta were visualized in trehalose-treated groups, the representative images and statistical results were shown. Nuclei were stained in blue.

** $p < 0.01$, *** $p < 0.001$ versus CON, $n = 6$.

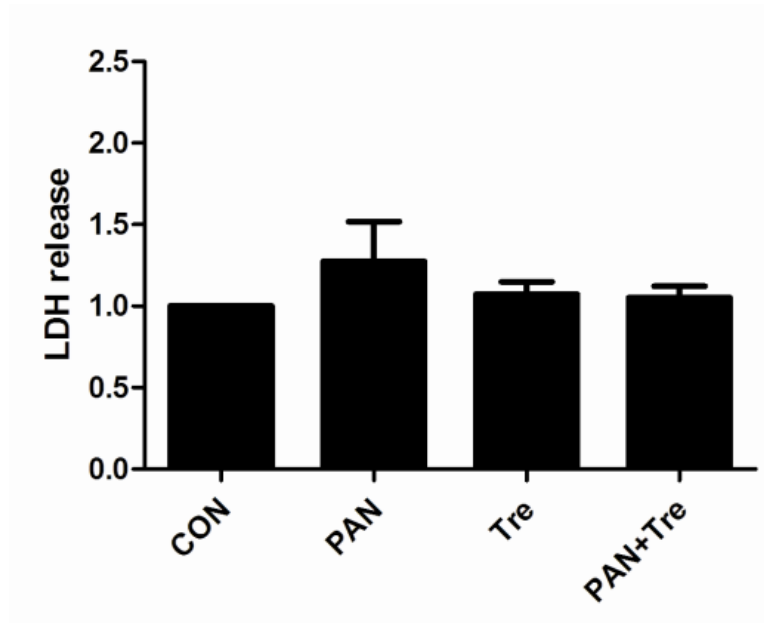


Figure 4.11 No elevated necrosis in PAN or (and) trehalose-treated human podocytes

LDH in culture medium was measured, and no significant changes were observed in podocyte necrosis. The results represent the mean \pm SEM (n=4).

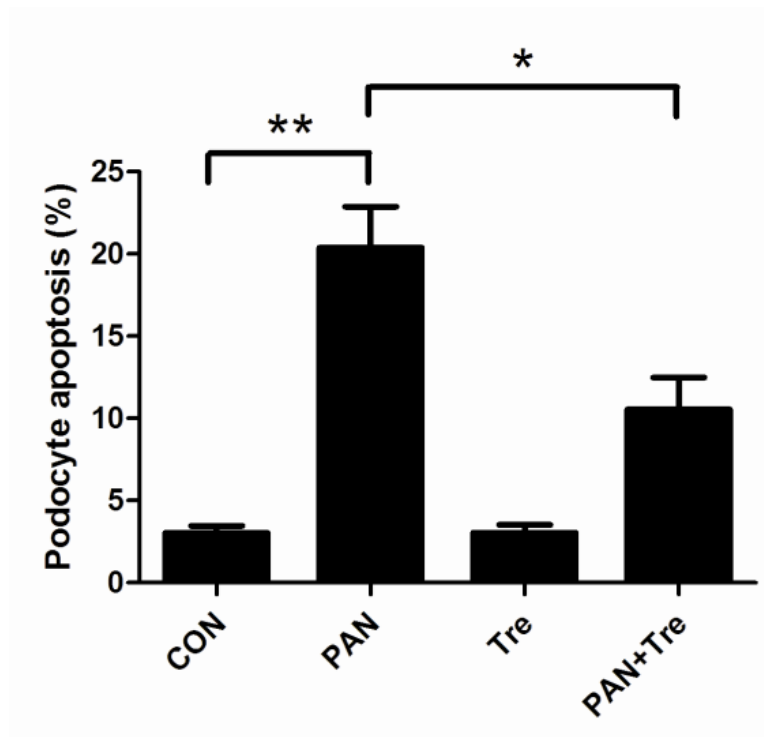


Figure 4.12 Trehalose decreased PAN-induced podocyte apoptosis

Podocyte apoptosis was induced by PAN (30 μ g/ml) and decreased significantly by trehalose (50mM, 48h). Apoptosis was measured by flow cytometry with YO-PRO-1/PI assay. The results represent the mean \pm SEM (n=6), * p <0.05, ** p <0.01 versus CON.

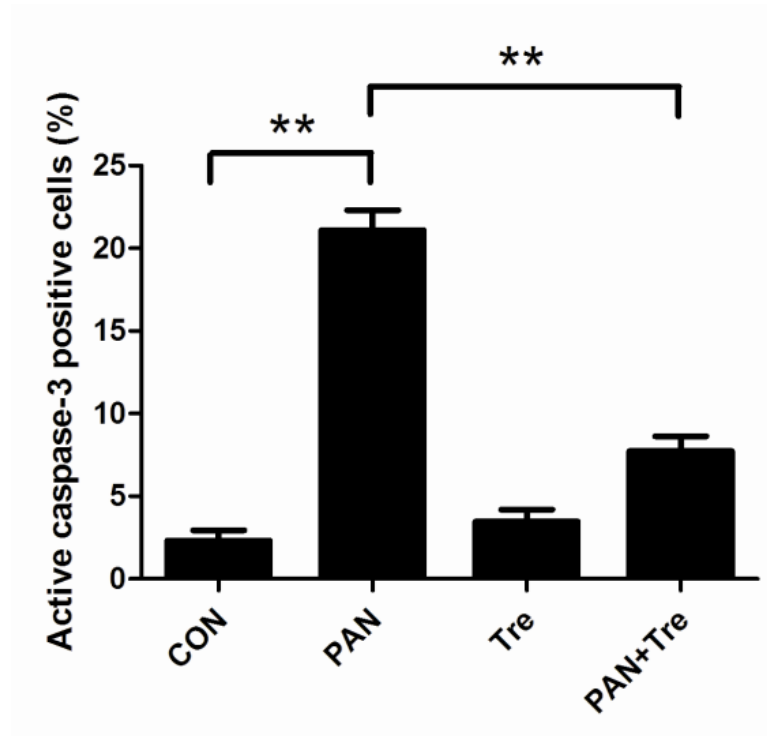


Figure 4.13 Trehalose decreased the percentage of active caspase-3 positive podocytes

The active caspase-3 positive podocytes were measured by flow cytometry. The changes pattern was similar to podocyte apoptosis measured by YO-PRO-1/PI assay.

The results represent the mean±SEM (n=6), ** $p < 0.01$ versus CON.

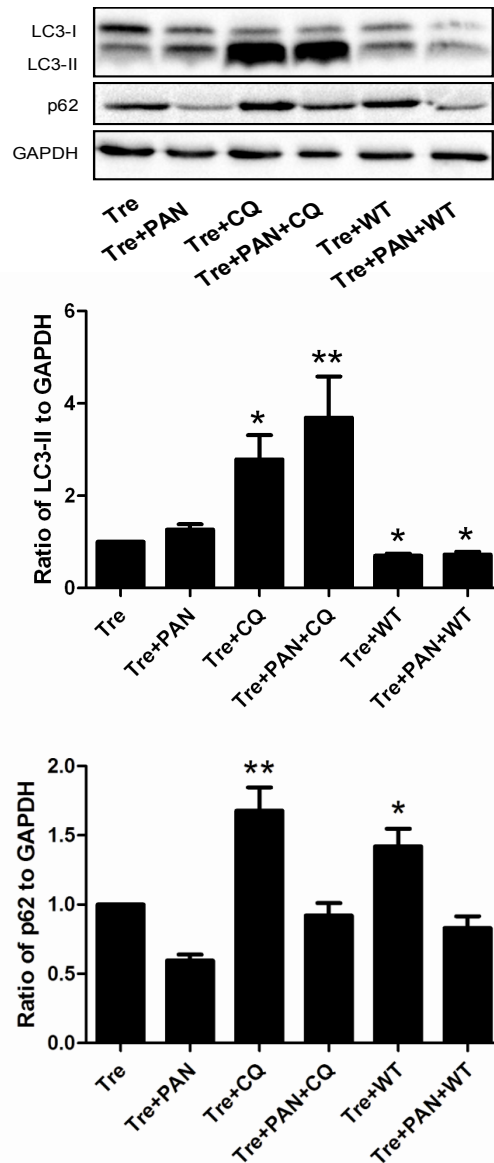


Figure 4.14 CQ and WT inhibited trehalose-induced autophagy

The expression of LC3-II dramatically increased after CQ treatment (25 μ M), while it was decreased significantly by WT (0.2 μ M). p62 slightly decreased in PAN+Tre group, whereas it was significantly increased in Tre+CQ and Tre+WT groups. The immunoblot images were shown along with statistical data (mean \pm SEM). * p <0.05, ** p <0.01 versus Tre group, n=7.

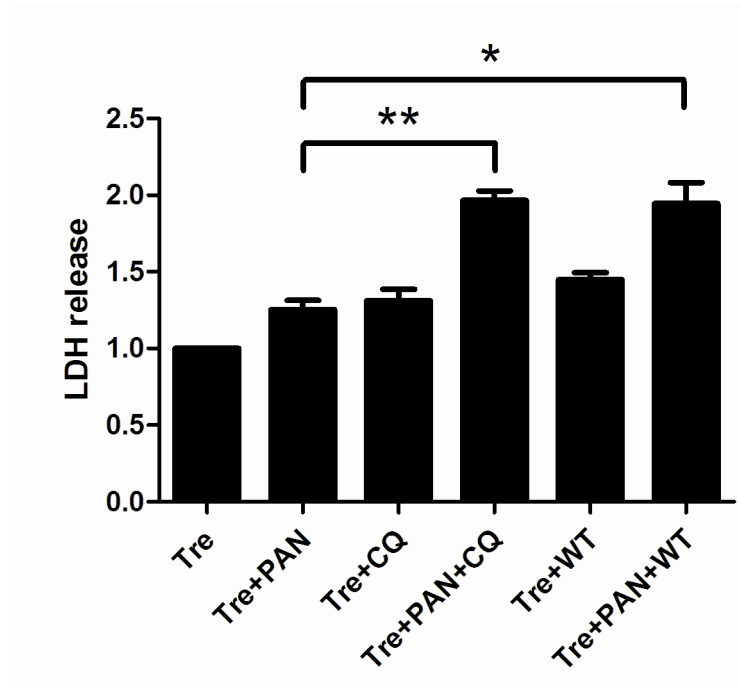


Figure 4.15 Necrosis increased after the inhibition of trehalose-induced autophagy

LDH was much higher in Tre+PAN+CQ and Tre+PAN+WT groups than the PAN+Tre group. The results represent the mean±SEM (n=6). * p <0.05, ** p <0.01 versus Tre+PAN group.

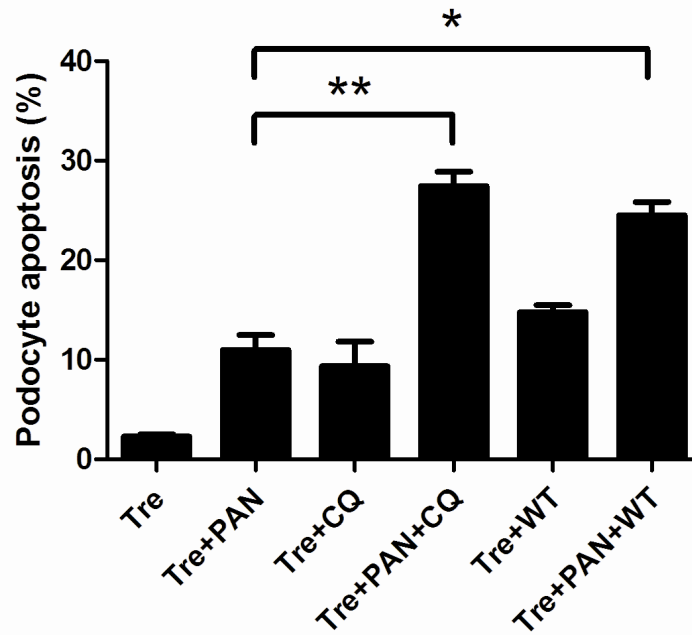


Figure 4.16 Podocyte apoptosis increased after the inhibition of trehalose-induced autophagy

The percentage of apoptotic podocytes was much higher in Tre+PAN+CQ and Tre+PAN+WT groups than the PAN+Tre group. The results represent the mean±SEM (n=7). * $p < 0.05$, ** $p < 0.01$ versus Tre +PAN group.

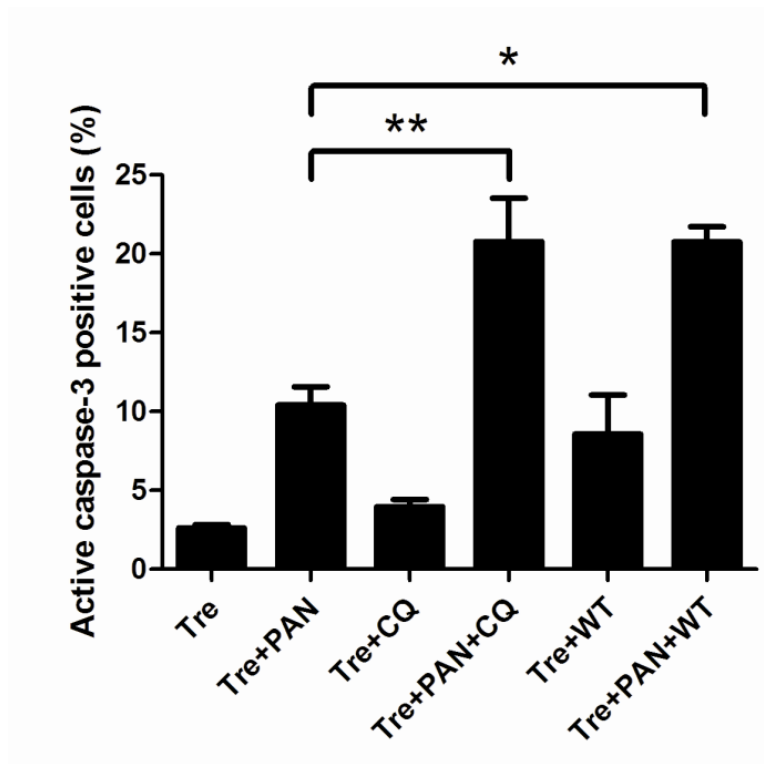


Figure 4.17 Inhibition of trehalose-induced autophagy increased the percentage of active caspase-3 positive podocytes

The percentage of active caspase-3 positive podocytes increased after inhibition of trehalose-induced autophagy. The percentage of active caspase-3 positive podocytes was much higher in Tre+PAN+CQ and Tre+PAN+WT groups than the PAN+Tre group. The results represent the mean±SEM (n=8). * p <0.05, ** p <0.01 versus Tre+PAN group.

4.3.5 Trehalose alleviated PAN-induced actin cytoskeleton injury in human podocytes

The actin cytoskeleton is the major mechanical support for maintaining the integrity and contractility of podocytes (Welsh and Saleem 2012). PAN-treated podocytes are characterized by the disrupted actin cytoskeleton and generation of lamellipodia. After trehalose treatment, the percentage of podocytes with disrupted actin cytoskeleton decreased as well as the number of lamellipodias (Figure 4.18-4.19).

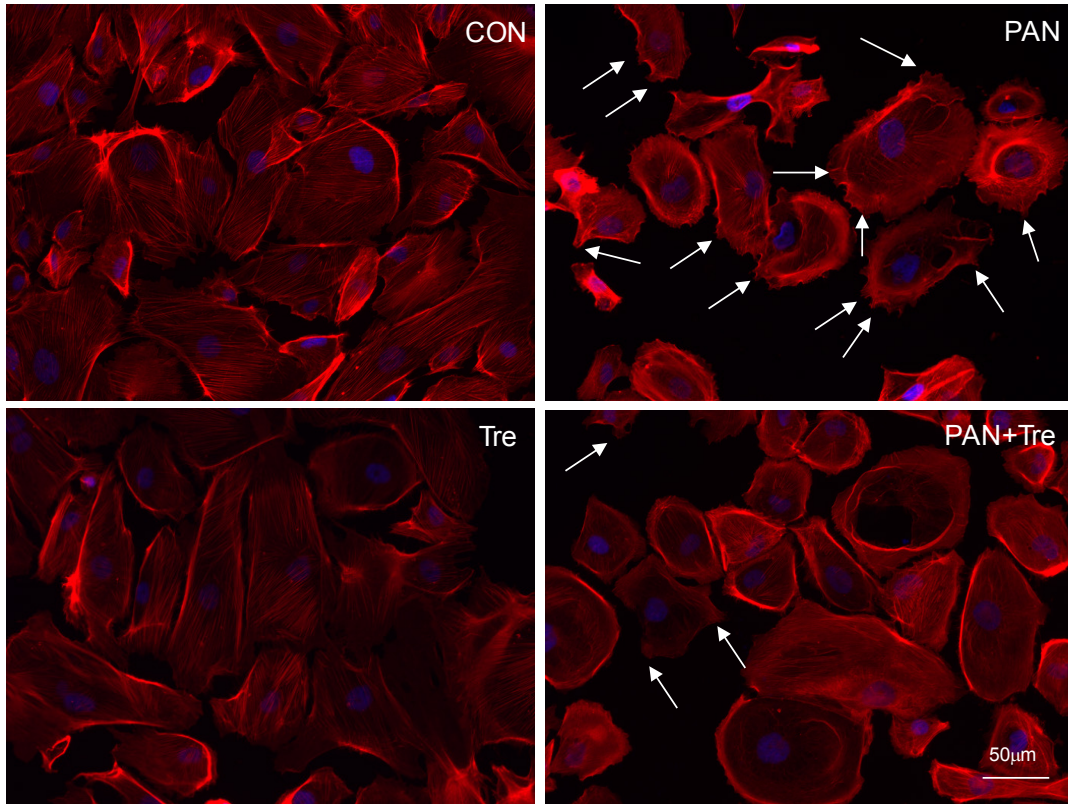


Figure 4.18 Trehalose alleviated PAN-induced actin cytoskeleton injury in human podocytes

F-actin was stained for evaluating the integrity of actin cytoskeleton. PAN (30µg/ml) induced actin cytoskeleton depolymerisation which was characterized by irregular distribution of F-actin. Meanwhile, plenty of lamellipodias were formed (indicated by white arrows). The actin cytoskeleton damages were partially reversed by 48h-trehalose treatment (50mM). The representative F-actin staining images were shown.

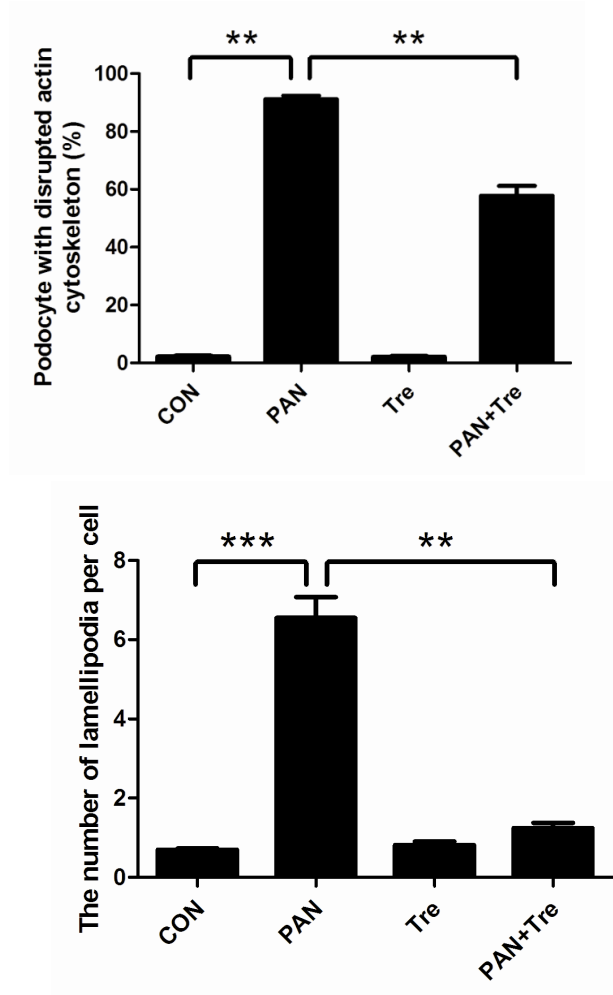


Figure 4.19 PAN-induced actin cytoskeleton damage in podocytes was alleviated by trehalose

The PAN-treated podocytes with disrupted actin cytoskeleton were down-regulated by trehalose, accompanying with decreased lamellipodias. The results represent the mean±SEM (n=6, 6). ** p <0.01, *** p <0.001 versus CON.

4.3.6 Trehalose diminished cell motility in PAN-treated human podocytes

The limited physiological motility is essential for keeping podocytes in normal function. Either enhanced motility or low level motility of podocytes is detrimental and considered to be the cause of proteinuria (Welsh and Saleem 2012). As shown in Figures 4.20-4.21, PAN-treated podocytes migrated faster than control, whereas the enhanced motility was decreased to the normal level after trehalose treatment.

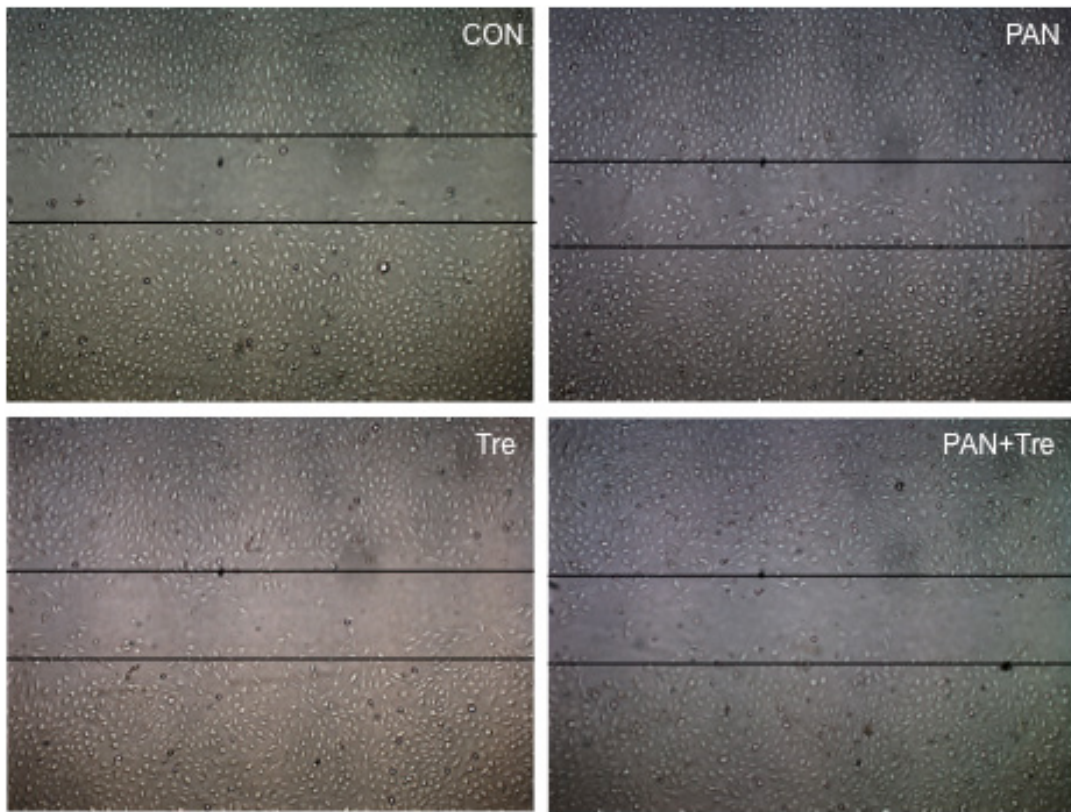


Figure 4.20 Trehalose diminished cell motility in PAN-treated human podocytes

The number of cells migrating into the gap increased after PAN treatment, whereas trehalose diminished podocyte motility. The representative images were taken under inverted microscope (50 \times).

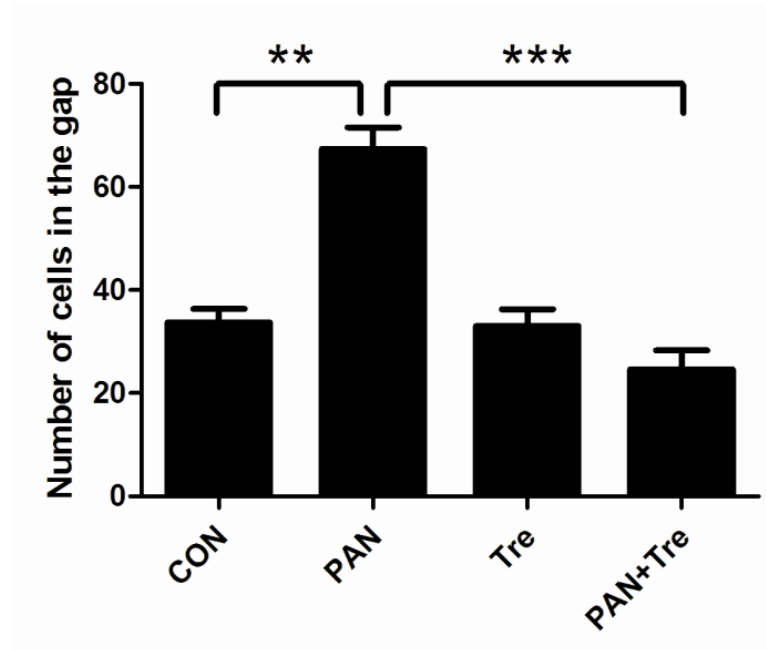


Figure 4.21 PAN-increased motility was suppressed by trehalose

The statistical result of Figure 4.20 was shown. The number of cells migrating into the gap was calculated for evaluating podocyte motility. The migrated podocytes after 12h-PAN treatment (30µg/ml) increased significantly, whereas trehalose (50mM) suppressed this enhanced motility. The results represent the mean±SEM (n=6). ** p <0.01, *** p <0.001 versus CON.

4.4 Discussion

Glomerular capillary is encircled by foot processes withstanding high filtration pressure. Podocyte damage is regarded as the determining factor of glomerular diseases (Mathieson 2012). Thus, alleviating podocyte injury becomes the therapeutic aim. High basal level of autophagy has been demonstrated in podocytes *in vitro* and *in vivo*, suggesting that autophagy plays a vital role in promoting podocyte survival (Asanuma et al. 2003, Hartleben et al. 2010). Theoretically, autophagy induction may ameliorate podocyte damage and autophagy inducers may be developed as new therapeutic agents for renal diseases. Here, we showed that PAN-induced podocyte injury was alleviated by trehalose.

Trehalose is regarded as the autophagy inducer in neurological studies. Moreover, the safety of trehalose is well recognized. Therefore, we investigated whether trehalose provided benefits to the damaged podocytes. Firstly, we revealed that trehalose induced autophagy in human podocytes. The expression of LC3-II and Atg5 in podocytes increased after trehalose treatment in a dose and time dependent manner. The results of LC3 immunostaining also demonstrated that elevated LC3-II puncta were formed in cytoplasm. Hence, trehalose is an autophagy inducer in human podocytes as well and a potential agent for the treatment of glomerular diseases.

mTOR is one of the most important cellular negative regulators of autophagy (Huber et al. 2011). Our data showed that trehalose did not significantly alter the

level of p-mTOR and its substrates including p-p70S6K and p-4E-BP1. Therefore, in accordance with the results of trehalose studies in other disciplines such as neurology (Zhang et al. 2014a), our data elucidated that trehalose induced autophagy in an mTOR independent manner in human podocytes. In addition, ROS has been regarded as the common signaling molecular for autophagy induction. For instance, starvation induces autophagy via the production of ROS which specially regulates the activity of Atg4 (Scherz-Shouval, Shvets and Elazar 2007a). In our study, the level of p-AMPK did not change significantly, and no sign of the activation of AMPK was detected. Therefore, it suggested that trehalose induced autophagy without changing the energy status. Meanwhile, trehalose did not promote the generation of ROS, suggesting no induction of cell stress in podocytes. Similarly, it has been reported that ROS does not change after trehalose treatment in HeLa cells (Underwood et al. 2010). Thus, ROS was not the signaling messenger for trehalose to induce autophagy, also hinting that trehalose is a safe agent.

PAN-treated podocytes are characterized by the increased apoptosis and actin cytoskeleton rearrangement (Srivastava et al. 2013). This classical model was used in the present study to test the efficacy of trehalose. We found PAN slightly increased the expression of LC3-II at 48h. It was consistent with our previous publication demonstrating that PAN induces autophagy and peaks at 24h, while autophagy drops down at 48h. It is suggested that autophagy triggered by PAN was kept at a low level at this time point. Additionally, trehalose enhanced autophagy in PAN-treated podocytes. Necrosis slightly increased after PAN treatment but without

any statistical significance. PAN-induced apoptosis was down-regulated by trehalose. Similarly, the percentage of active caspase-3 positive podocytes increased after PAN treatment and was decreased by trehalose. Taken together, it was demonstrated that trehalose played a role in preventing podocyte against apoptosis.

To answer the question of whether trehalose protected podocytes via inducing autophagy, two autophagy inhibitors (CQ and WT) based on different principle were used to block trehalose-induced autophagy. The expression pattern of LC3-II in podocytes after CQ and WT treatment revealed that autophagy has been successfully suppressed. Meanwhile, these inhibitory results were confirmed by the expression of p62, it increased after CQ or WT treatment, but it may be puzzling that p62 was not elevated in Tre+PAN+CQ and Tre+PAN+WT groups. The possible reason is that p62 was partially degraded in advance by PAN which also induced a low level of autophagy in podocytes at 48h. Consequently, necrosis increased after autophagic inhibition. Meanwhile, the decreased apoptosis by trehalose rebounded after administration of inhibitors suggesting that trehalose decreased podocyte apoptosis via autophagy induction.

Actin cytoskeleton depolymerisation was another important feature of glomerular diseases (Srivastava et al. 2013). Trehalose partially reversed actin cytoskeleton reorganization and suppressed the formation of lamellipodia which was associated with cell motility. In addition, it is well known that podocytes are motile cells, but the motility is kept at an optimal level. Thus, the enhanced motility is detrimental to

podocytes and is responsible for podocyte effacement *in vivo*. The results of migration assay showed that PAN accelerated podocyte migration, whereas trehalose decreased this enhanced motility to the normal level. Taken together, it is suggested that trehalose also protected podocytes by maintaining the stability and normal motility of actin cytoskeleton.

In conclusion, trehalose induced autophagy and alleviated podocyte injury including apoptosis and actin cytoskeleton depolymerisation. Notably, trehalose is safer than other autophagy inducers, not only because it is a natural disaccharide widespread throughout the biological world, but also it induced autophagy in an mTOR independent manner in human podocytes. As mTOR is also involved in diverse cell functions such as protein synthesis, ribosome biogenesis and cell cycle, trehalose theoretically produces much less side effects. On the contrary, rapamycin is a strong autophagy inducer due to the inhibition of mTOR, but it engages in regulating multiple cellular processes. It may partially explain why rapamycin achieves remission in podocyte injury *in vitro* but it lead to proteinuria in patients with renal transplantation . Moreover, trehalose activated autophagic flux without causing cell stress in human podocytes. Therefore, we proposed that autophagy induction is a novel strategy for the treatment of glomerular diseases and trehalose is a good candidate for inducing autophagy in podocytes. However, autophagy is a double edged sword. Over-activation of autophagy or prolonged autophagy induction may lead to cell death as it may over-digest cellular components. In future studies, the

questions of how to minimize this risk and how to precisely regulate autophagy induction need to be addressed for autophagic therapy.

Chapter 5

Trehalose induced autophagy but failed to alleviate podocyte injury in PAN nephrosis rat model

5.1 Introduction

Glomerular diseases have become a global health challenge, as its relapse rate remains high and a large population of these patients progress to end stage renal diseases (ESRD) (Jolly et al. 2014). A huge amount of expenses are spent on the treatment of patients with ESRD annually. In the past several decades, the advances in underlying glomerular diseases revealed that podocyte effacement results in proteinuria and is the key pathological change (Kalluri 2006). Enough evidence showed that podocytes undergo apoptosis, actin cytoskeleton reorganizations and detachment in some primary and secondary glomerular diseases (Ziyadeh and Wolf 2008, Logar et al. 2007). The current treatment approaches include anti-inflammation by steroid and immunosuppressive therapy by immunosuppressants (Wang and Xu 2013). The off-targets of current therapies promote researchers to develop new strategies to alleviate podocyte injury.

As described before, we found that autophagy plays a cytoprotective role in protecting podocytes against damage. Our *in vitro* data also suggested that podocyte apoptosis and actin cytoskeleton depolymerisation can be alleviated by trehalose. Moreover, trehalose induced podocyte autophagy in an mTOR independent manner

and without increasing ROS production. In neurodegenerative diseases, the efficacy of trehalose has been confirmed as it helps to degrade mutant proteins (Zhang et al. 2014b). Therefore, we hypothesize that trehalose induces autophagy and decreases proteinuria by alleviating podocyte injury in glomerular diseases.

Currently, the commonly used podocyte injury models can be established by injection of PAN, adriamycin, LPS and overload of albumin (Pippin et al. 2009). PAN nephrosis rat model is characterized by foot process effacement which is similar to MCNS in human (Kanellis et al. 2004, Kim et al. 2005). Thus, PAN nephrosis rat model is widely applied for revealing molecular mechanism of nephrotic syndrome and developing new therapeutic approaches. Urinary proteins including total proteins and albumin are used for evaluating the outcomes of PAN nephrosis rat as well as renal pathology.

In this study, we are the first to test the efficacy of trehalose in PAN nephrosis rat model. We found that trehalose induces autophagy in rat glomerulus. However, total urinary proteins and albumin did not decrease significantly after trehalose treatment. PAN-damaged renal ultrastructure was also not attenuated by trehalose. Therefore, it may suggest that podocyte injury after PAN treatment *in vivo* can not be alleviated by trehalose.

5.2 Experimental design

Male Sprague–Dawley rats were divided into 4 groups: (1) Control, (2) PAN alone in a single intraperitoneal injection of 15mg/100g body weight, (3) 2% trehalose alone, and (4) 2% Trehalose + PAN (see Chapter 2.9). The rat urine protein, serum albumin and urinary creatinine levels were determined by automated analyzer. On Day 10 after PAN injection, animals were sacrificed and the kidneys were taken for Western blotting, PAS staining and transmission electron microscopy. We also determined the expression of the autophagy marker, LC3 II. For the detailed materials and methods, please refer to Chapter 2.

5.3 Results

5.3.1 Trehalose induced autophagy in glomerulus

To evaluate whether autophagy has been induced in rats, we measured the expression level of LC3. As depicted in Figure 5.1, the expression of LC3-II increased significantly after trehalose treatment.

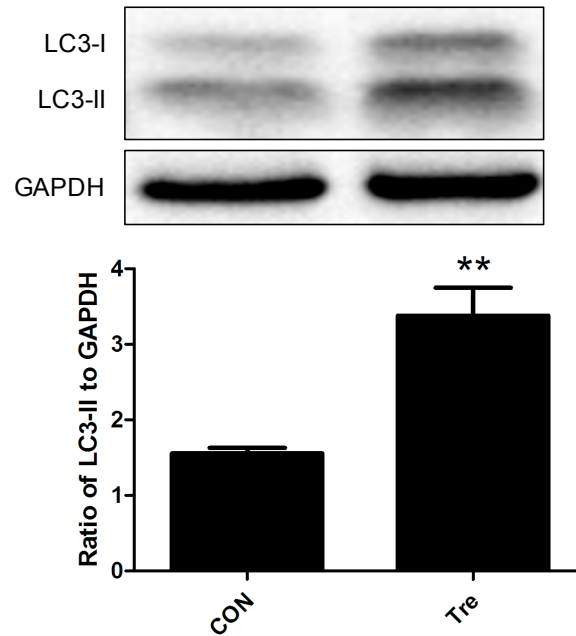


Figure 5.1 Trehalose induced autophagy in glomerulus

The expression level of LC3-II was increased after 4 weeks trehalose treatment (2%). LC3-II was measured by Western blotting. The data (mean±SEM) were expressed as the relative changes compared with control group (CON).

Representative immunoblot images were shown along with the statistical results.

** $p < 0.01$ versus CON, $n = 6$.

5.3.2 Proteinuria was not decreased by trehalose in PAN nephrosis rat model

To test whether trehalose alleviates renal injury in PAN nephrosis rat model, total urinary protein was normalized by urinary creatinine. As shown in Figure 5.2, proteinuria was not down-regulated significantly by trehalose.

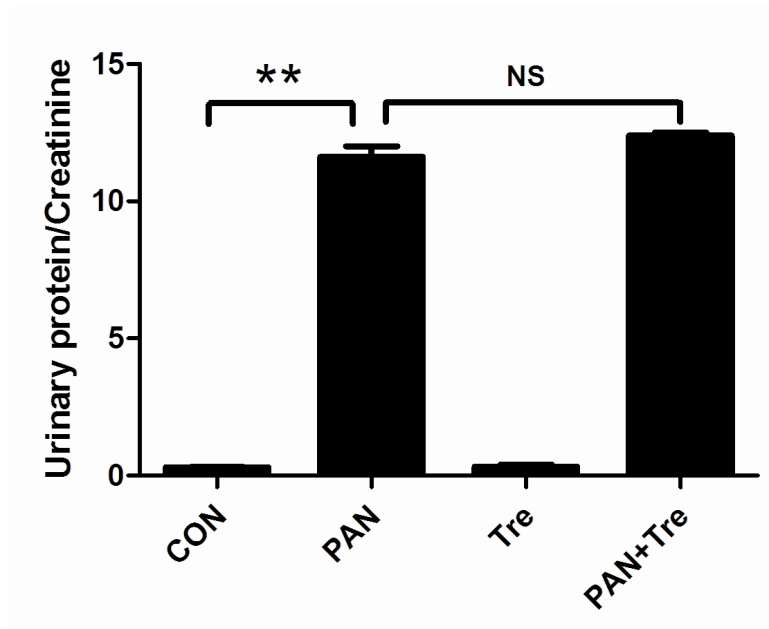


Figure 5.2 Trehalose failed to decrease proteinuria in PAN nephrosis rat model

Heavy proteinuria was presented on day 10 after PAN injection. However, proteinuria was not decreased after trehalose treatment. The results represent the mean±SEM (n=6). ** $p < 0.01$ versus CON. NS= not significant. Urinary Protein in g/l and Urinary Creatinine in $\mu\text{M/l}$.

5.3.3 Hypoalbuminemia was not alleviated after trehalose treatment in PAN nephrosis rat model

Hypoalbuminemia is the key clinical feature in PAN nephrosis rat model. We measured serum albumin to confirm the efficacy of trehalose. As shown in Figure 5.3, the decreased serum albumin was not up-regulated significantly by trehalose.

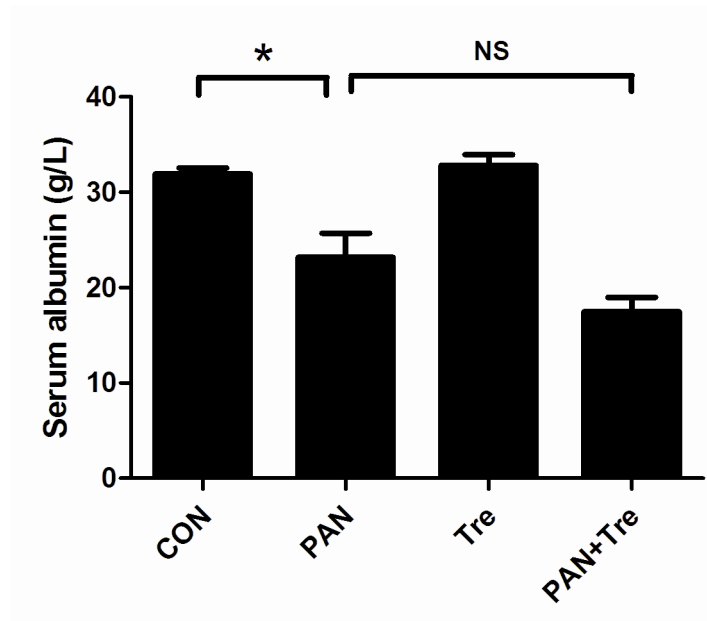


Figure 5.3 Trehalose failed to alleviate hypoalbuminemia in PAN nephrosis rat model

Hypoalbuminemia was presented on day 10 after PAN injection. However, serum albumin was not increased after trehalose treatment. The results represent the mean \pm SEM (n=6). * p <0.05 versus CON. NS= not significant

5.3.4 Renal pathological changes in PAN nephrosis rat model was not alleviated after trehalose treatment

To evaluate whether trehalose alleviates renal injury in PAN nephrosis rat model, we examined renal pathology using PAS staining and electronic microscopy. As shown in Figure 5.4, no obvious pathological changes were observed in PAS staining images. Moreover, PAN-induced podocyte effacement was not attenuated by trehalose (Figure 5.5).

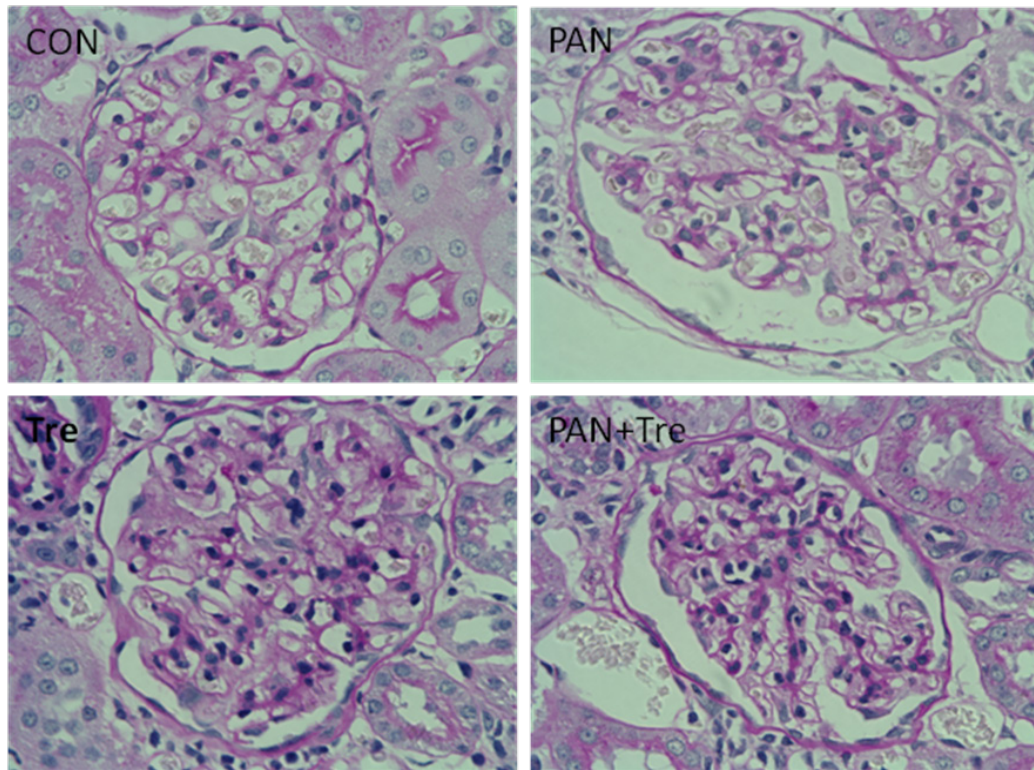


Figure 5.4 No obvious glomerular lesions were observed in PAN nephrosis rat under PAS staining

The renal structure after PAN injection or (and) trehalose treatment were similar (PAS staining, 400×).

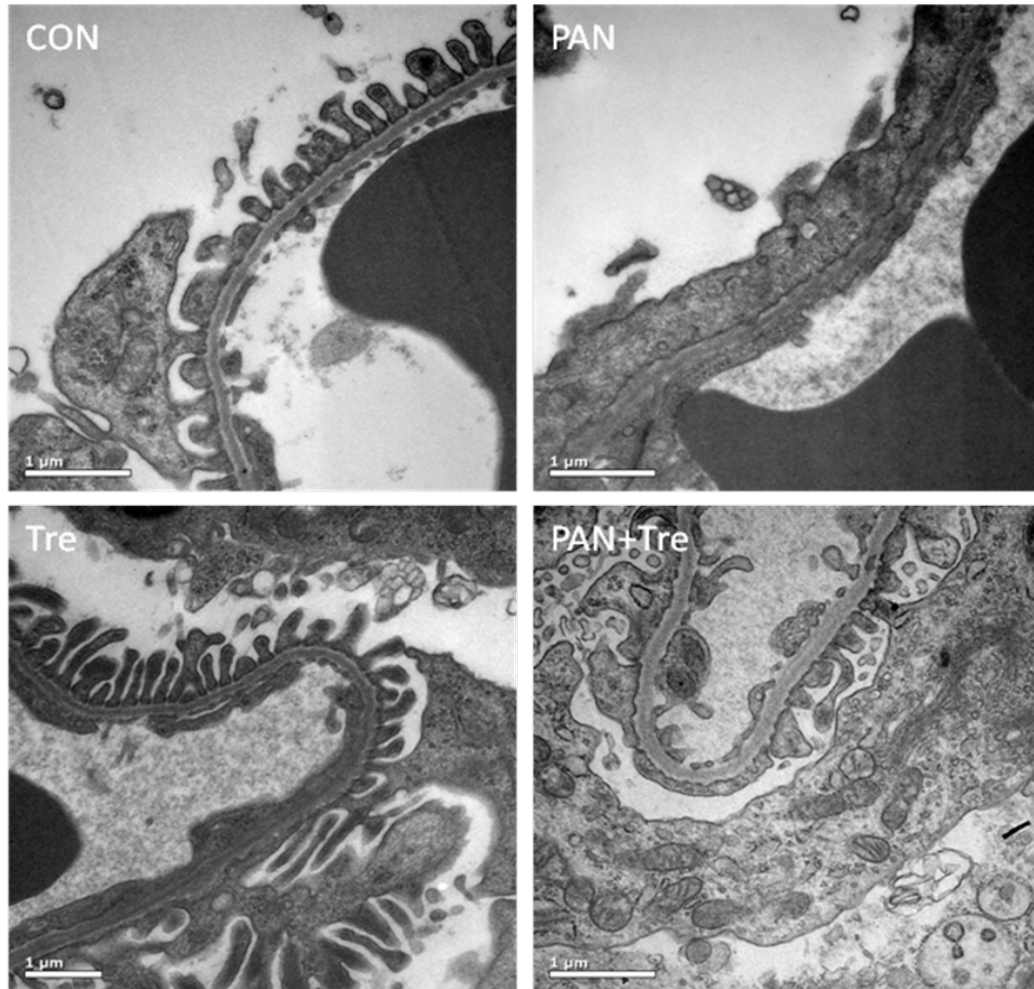


Figure 5.5 Trehalose failed to attenuate renal pathological changes in PAN nephrosis rat model

Podocyte effacement was presented after PAN treatment (Day 10). However, renal injury was not alleviated after trehalose treatment.

5.4 Discussion

Autophagy is a highly conserved catabolic process in which the unwanted organelles and proteins are degraded and recycled as nutrition (Weide and Huber 2011). Basal level of autophagy is kept in cells to maintain cellular homeostasis and autophagic flux can be induced to resist harmful stimuli (Akers et al. 2012). Over-activation of autophagy may lead to cell death, but optimal level of autophagy is beneficial to cell survival (Takacs-Vellai, Bayci and Vellai 2006). Thus, it is reasonable to harness autophagy for protecting podocytes against injury. We investigated the efficacy of trehalose in PAN nephrosis rat model which is characterized by podocyte injury. It revealed that trehalose induced autophagy in glomerulus, but proteinuria can not be decreased in PAN nephrosis rat model.

In our previous studies, we are the first showing that trehalose induced autophagy in podocytes *in vitro* and alleviated PAN-induced podocyte injury including apoptosis and actin cytoskeleton rearrangement. In attempting to verify whether trehalose alleviates podocyte injury *in vivo*, PAN nephrosis rat model was established and treated with trehalose. The dosage of trehalose is 2% which was verified in other studies and its effects of autophagy induction have been confirmed (Tanaka et al. 2004). As expected, autophagy in glomerulus has been induced by trehalose. However, proteinuria and hypoalbuminemia were not attenuated as well as the renal pathological changes, suggesting that no beneficial effects were obtained in PAN nephrosis rat model.

The inconsistent data between *in vitro* and *in vivo* studies may be involved in several factors. Firstly, PAN nephrosis rat model was established by PAN with the dosage of 15mg/100g, heavy proteinuria is presented on day 3-4 and peaked on day 9. Until day 28, proteinuria automatically decreases to the normal level (Pippin et al. 2009). In other words, podocyte injury in PAN nephrosis rat model created by this commonly used dosage is too severe to be reversed, as podocyte effacement last for nearly one month. Secondly, the cytoprotective effects of autophagy are limited, so it may be overcome by the severe podocyte injury. Higher basal autophagy exists in podocytes comparing other cell types (Hartleben et al. 2010), not only suggesting that autophagy is critical for podocyte survival, but may also hinting that it is limited capacity to further elevate autophagy for protecting podocytes against injury. Thirdly, it is also possible that trehalose may act on other cell types of the kidney which interact with podocytes. Further experiment is needed to dissect the complex relationship between different kidney cells in the trehalose treated rat.

In addition, it has been known that over-activation of autophagy may lead to cell death, suggesting that the role of autophagy depends on the increased levels. However, it remains unknown whether persistent induced autophagy shows cytoprotective effects. It is possible that autophagy induced by trehalose did not play a cytoprotective role as PAN nephrosis rats were persistently administered with trehalose, as it may consume more cellular energy for induction of autophagy. Furthermore, it has been well known that PAN induces podocyte apoptosis *in vitro* and *in vivo* due to the activation of mitochondrial pathway (Hagiwara et al. 2006, Li

et al. 2014). Hence, persistent induced autophagy may excessively remove mitochondrial and lead to the failure of trehalose treatment. At last, it also can not be excluded that over-activation of autophagy may have been induced at the late stage of treatment which counteracts the benefits.

Even though the dosage optimization has been carried out in this PAN nephrosis rat model, we also admit that there are also some limitations of this animal study. For instance, only PAN nephrosis rat model was used to test the efficacy of trehalose and this model may not be suitable. Trehalose may benefit other relative mild podocyte injury model such as LPS nephritis model and secondary glomerular injury model. In addition, multiple concentration of trehalose may be set up to compare its benefits. The therapeutic approach may also change from persistent treatment to tide therapy for allowing podocytes to restore cellular homeostasis.

In conclusion, even though the beneficial effects of trehalose have been demonstrated in our *in vitro* studies, its cytoprotective role can not be confirmed in PAN nephrosis rat model. It suggested that autophagy is a sophisticated mechanism, autophagy induced by reagents needed to be optimized and precisely regulated for achieving remission in glomerulus diseases. In future studies, more podocyte injury model are needed to be employed, and the treatment period is required to optimize. Since autophagy is the key self-protective mechanism in cells, more safe and efficient autophagy inducer can be developed for alleviating podocyte injury.

Chapter 6

General discussion and Conclusion

6.1 General discussion

In the present study, we investigated the role of autophagy in human podocytes under cell stress induced by PAN, revealing that autophagy was essential for podocyte survival in response to harmful stimuli. Furthermore, trehalose, an mTOR autophagy inducer, alleviated PAN-induced podocyte injury. In attempt to confirm these findings of *in vitro* studies, the efficacy of trehalose has been tested in the PAN nephrosis rat model. Autophagy has been induced in glomerulus. However, proteinuria and hypoalbuminemia was not improved by trehalose treatment. The major findings are discussed as follows:

Autophagy was induced prior to apoptosis in human podocytes under cell stress

The crosstalk between autophagy and apoptosis has been well recognized in some cell types (B'Chir et al. 2014, Martyniszyn et al. 2013). Autophagy is a cell survival mechanism which degrades dysfunction long lived proteins and organelles, while apoptosis is a programmed cell death. Autophagy helps to decrease cell apoptosis by removing pro-apoptotic stimuli. However, autophagy induced beyond a threshold may lead to cell death (Nishida, Yamaguchi and Otsu 2008). In our studies, we found that high level of autophagy has been induced in podocytes before the peak

level of apoptosis after PAN treatment. When autophagy was decreased to the basal level, PAN-induced apoptosis dramatically increased, suggesting that autophagy and apoptosis were induced after PAN treatment. The same phenomenon is also reported in angiotensin II and high glucose (Yadav et al. 2010, Ma et al. 2013). In other words, the factors which lead to cellular stress have the capacity of inducing autophagy in cells. The order of both cellular processes suggested that autophagy appears to be protective mechanism at the early stage of cellular insults. However, the persistent existence of harmful stimuli diminished the cytoprotective effect of autophagy and led to cell apoptosis. Thus, it suggested that autophagy is an adaptive protective mechanism for monitoring and resisting any detrimental stimuli, but has a limited capacity of coping with insults.

The cytoprotective role of PAN-induced autophagy in human podocytes

Podocyte apoptosis dramatically increased after 3-MA or CQ inhibits PAN-induced autophagy. This finding suggested that autophagy decreased podocyte apoptosis. It has been reported that autophagic degradation of active caspase-8 attributed to the inhibition of apoptosis (Hou et al. 2010). Additionally, the activation of Bid which is a pro-apoptotic protein can be prevented by autophagic protein-Beclin 1, resulting in a decreased apoptosis (Kang et al. 2011). As autophagy and apoptosis share some common signalling molecules, the crosstalk between them has been recognized. On the contrary, apoptosis is also able to inhibit autophagy via the degradation or inactivation of autophagic proteins such as Beclin 1, Atg 4 and Atg 5 (Kang et al. 2011). That could explain that in our present study, podocyte apoptosis was kept at a

low level at the beginning of PAN treatment (24h) and peaked at 48h as well as the increased apoptosis after inhibiting PAN-induced autophagy.

The inhibition of PAN-induced autophagy by 3-MA or CQ also increased the percentage of cells with disrupted actin cytoskeleton. The damage actin cytoskeleton and changed cell morphology are the early features of cell apoptosis. Nonetheless, it is well known that proteinuria in patients with MCNS is attributed to podocyte effacement or detachment which is mainly caused by actin cytoskeleton injury (Patrikka et al. 2002). Thus, our results suggested that the interaction may also exist between autophagy and actin cytoskeleton.

In autophagy deficient embryonic fibroblast cells (MEFs) (Atg 7 knockout), F-actin was also disrupted (Zhuo et al. 2013). However, it remains unknown how autophagy affects the stability of actin cytoskeleton. The blockage of autophagic flux may sensitize podocytes to PAN treatment as the cellular adaptive self-protective mechanism was abolished. It may be associated with, especially RhoA, Rac1 and Cdc42 which are involved in regulating cytoskeleton dynamics (Mouawad et al. 2013). In addition, it cannot be excluded that the inhibition of autophagy may alter the expression level of some adaptive proteins in podocytes such as α -actinin-4 and synaptopodin. Meanwhile, it is still possible that autophagy inhibition may disrupt calcium reflux which is required for regulating cytoskeleton dynamic in podocytes.

Since autophagy decreases apoptosis and actin cytoskeleton rearrangement, it is reasonable to speculate that autophagy can be utilized to promote cell survival. It also suggested that autophagy deficiency or impairment should be considered in some glomerular diseases such as FSGS which presented with severe podocyte effacement, as it is absolutely possible that some glomerular diseases are secondary to autophagic gene mutation or single nucleotide polymorphism (SNP). Therefore, in the aspect of renal aetiology, autophagy abnormality need to be evaluated in the diagnosis of renal diseases. Meanwhile, autophagy may become a potential therapeutic approach for alleviating kidney injury.

mTORC1 was activated in PAN-treated human podocytes

Our data showed that mTORC1 was activated after PAN treatment. It seems to be confusing that the activated mTORC1 was accompanying with the induction of autophagy by PAN, as only mTOR inhibition induces autophagy. This paradox can be reconciled by TASC. Recently an elegant study also demonstrated that TASC exists in trans site of Golgi apparatus in podocytes, this compartment enriches autolysosomes and mTOR (Narita et al. 2011). As a result, environment with low mTOR was created in cytoplasm for inducing autophagy. TASC may be evolved for cells to survive in tough situation, and it would be particular important to podocytes which stand with pulse hydrostatic pressure. TASC may be an important mechanism to help podocytes resisting insults by facilitating the induction of autophagy.

mTORC1 is an important regulator involving multiple cellular biological processes, such as protein synthesis and ribosome biogenesis (Huber et al. 2011). In diabetic nephropathy animal model, the activation of mTORC1 changes the distribution of SD proteins (Godel et al. 2011). Therefore, PAN-induced podocyte apoptosis and actin cytoskeleton rearrangement may be associated with mTORC1. Our study highlights the importance of mTORC1 inhibition in alleviating podocyte injury, as it not only induces autophagy to degrade unwanted proteins and organelles, but also may stabilize SD structure. Additionally, it has been shown that mTORC1 inhibition may be associated with the longevity of animals (Drake et al. 2013). Currently, rapamycin is widely used to inhibit mTORC1, and its benefits have been reported in podocytes. Thus, mTORC1 could be a vital therapeutic target in glomerular diseases.

Trehalose induced autophagy in human podocytes

In attempting to harness autophagy for alleviating podocyte injury, trehalose has been investigated in the present study. The results demonstrated that trehalose induces autophagy in podocytes. Different from rapamycin, trehalose did not alter the level of p-mTOR, p-p70S6K and p-4E-BP-1, suggesting that it induces autophagy in an mTOR independent manner. To date, several mTOR independent pathways have been discovered. For instance, lithium, carbamazepine or valproic acid induce autophagy by decreasing inositol via the inositol signaling pathway (Sarkar et al. 2005). L-type Ca^{2+} channel antagonists such as verapamil, loperamide, amiodarone, nimodipine and nitrendipine enhance autophagy by activating the Ca^{2+} /Calpain pathway (Williams et al. 2008). In addition, the cAMP/Epac/Ins (1, 4,

5) P₃ pathway and JNK1/Beclin-1/PI3KC3 pathway are also reported (Meijer et al. 2014). To the best of our knowledge, it is still unknown which pathway is involved in trehalose-induced autophagy. Notably, the additive effects are presented in combination of autophagy inducers which go through different pathways. For example, trehalose together with rapamycin significantly elevates the LC3-II expression than either of them does (Sarkar et al. 2007). Thus, more researches could be conducted to explore the underlying mechanisms of trehalose, as it may help to develop multiple targets autophagic therapy in combination of mTOR dependent inducer.

Trehalose-induced autophagy was independent of ROS

It has been known that ROS is a common messenger for inducing autophagy by stimuli such as starvation, angiotensin II and high glucose (Yadav et al. 2010, Ma et al. 2013). Our data revealed that ROS is not involved in trehalose-induced autophagy, suggesting that no cell stress was generated by trehalose. In other words, trehalose is a safe autophagy enhancer as cellular stress is also pro-apoptotic factor. Additionally, the safety of trehalose is supported by the fact that it has no mutagenicity, carcinogenicity, acute toxicity, embrotoxicology and teratology. Thus, it has been using as food additive (Richards et al. 2002).

Trehalose decreased PAN-induced apoptosis in human podocytes via the induction of autophagy *in vitro*

Since trehalose induces autophagy in podocytes without the involvement of mTOR and ROS, we hypothesized that trehalose decreases podocyte apoptosis after PAN treatment. As expected, podocyte apoptosis was decreased by trehalose. The inhibition of autophagy by CQ or WT revealed that the cytoprotective effects of trehalose are due to the induction of autophagy. In Chapter 3, we demonstrated that PAN leads to the activation of mTOR which may be the cause of podocyte injury. However, in Chapter 4, we showed that trehalose alleviated podocyte injury without inhibition of mTOR. These results suggested that trehalose reached the same goal as mTOR dependent autophagy inducer does. Furthermore, the combination of autophagy inducers which are mTOR dependent and independent may be a more beneficial therapy to the severe podocyte injury.

Trehalose alleviated PAN-induced actin cytoskeleton damage in human podocytes

In Chapter 3, it has been revealed that the inhibition of autophagy lead to the disruption of actin cytoskeleton in podocytes. Consistently, we found that the induction of autophagy alleviated PAN-induced actin cytoskeleton injury. It suggests that autophagy not only decreases apoptosis, but also participates in the regulating the stability of podocytes. This finding may shed new lights on the development of therapeutic strategies for glomerular diseases, especially in MCNS.

Trehalose decreases cell motility of PAN-treated human podocytes

Either elevated or decreased podocyte motility leads to the damage of renal filtration barrier (Welsh and Saleem 2012). Hence, it is critical to alter the abnormal podocyte dynamics and maintain cell motility at an optimal level which is essential for removing deposits in sub-podocyte space. Trehalose has the capability of diminishing the enhanced motility by PAN in human podocytes. These results are consistent with our previous findings that trehalose decreases the number of PAN-induced lamellipodia which is vital to increase podocyte motility. However, it is unknown whether the diminished cell motility is attributed to autophagy induced by trehalose. Pharmacologically or genetically inhibiting autophagy leads to the rearrangement of podocyte actin cytoskeleton per se. Therefore, it is difficult to verify whether trehalose diminished cell motility via inducing autophagy. However, it clearly suggests that trehalose may be a therapeutic candidate for decreasing proteinuria.

Trehalose induced autophagy in rat glomerulus but fail to alleviate renal injury

It has been known that oral administration of 2% trehalose induces autophagy in mouse (Tanaka et al. 2004). We are the first to find that autophagy also can be induced in rat glomerulus by trehalose. However, trehalose did not alleviate PAN-induced renal injury including proteinuria and hypoalbuminemia. Podocyte effacement after PAN treatment was also not recovered. The inconsistency between *in vitro* and *in vivo* study may suggest that autophagy has the limited capacity to cope with severe podocyte injury.

Future studies

We have investigated the role of autophagy in human podocytes and also have tested the efficacy of trehalose *in vitro* and *in vivo*. Based on the results of the present study, future studies will focus on the following topics:

- **The mechanism of autophagy decreasing podocyte apoptosis**

Our data showed that autophagy decreased podocyte apoptosis, but the mechanism is still unclear. As PAN increases the generation of ROS and leads to podocyte apoptosis via the mitochondrial pathway (Vega-Warner et al. 2004, Hagiwara et al. 2006), we need to explore whether autophagy cleaves or inhibits apoptotic proteins such as Bid, Bax or Cytochrome C. It would also be interesting to test whether autophagy decreases apoptosis via extrinsic pathways such as the Fas/FasL pathway. Autophagy is a cellular catabolic mechanism sharing some molecules with apoptosis. Therefore, future studies can investigate the function of these proteins such as the role of Bcl-2/Beclin 1 complex in regulating autophagy and apoptosis.

- **The role of mTORC2 in regulating actin cytoskeleton**

mTORC1 was activated after PAN treatment and play a vital role in podocyte apoptosis and autophagy. However, little is known about the role of mTORC2 in podocytes. Future studies may reveal the role of mTORC2 in podocyte dynamics, and the links between mTORC2 and Rho GTPase may be explored. It may help to develop new therapeutic strategies to target

mTORC1 and mTORC2 simultaneously for decreasing apoptosis and maintaining the stability of actin cytoskeleton in podocytes.

- **The role of ROS in autophagy induction**

Since many stimulators induce autophagy with the involvement of ROS which regulating the activity of Atg4 (Scherz-Shouval et al. 2007b). Thus, it would be helpful to define which level of ROS is sufficient to induce autophagy and minimise its pro-apoptotic effects in podocytes. Additionally, ROS may also regulate the dissociation of Bcl-2/Beclin 1 complex to initiate the formation of phagophore.

- **The interaction between autophagy and actin cytoskeleton**

Our studies showed that the inhibition disrupted the actin cytoskeleton, so it would be interesting to investigate the underlying mechanism, including screening the related autophagic proteins and cytoskeleton proteins. Meanwhile, as autophagy consists of several steps which occur in different locations of cytoplasm, it would be practical to investigate whether actin cytoskeleton is needed to transport these necessary items for the formation of autophagosome or autolysosome.

- **The role of toll like receptors (TLR) in autophagy induction**

B7-1 is considered as the key regulator of actin cytoskeleton in podocytes and regulated by TLR4 which can be activated by LPS (Reiser et al. 2004, Chang et al. 2013). Furthermore, it has been reported that the crosstalk exists between TLRs and autophagy. Thus, TLRs may link immunology and autophagy with podocyte injury. TLRs may become new therapeutic targets for renal diseases.

- **The management of autophagy for the treatment of glomerular diseases**

In our *in vitro* studies, trehalose alleviated podocyte injury. However, it failed to achieve remission in PAN nephrosis rat model. Therefore, other proteinuria rodent models of podocytopahty, such as adriamycin nephrosis or overload proteinuria, may be employed to test the efficacy of trehalose. Careful optimisation of dosage and time points for inducing an optimal level of autophagy is necessary, as over-activation may lead to the detrimental effects. Additionally, new autophagy inducers are needed to be explored and applied to the treatment of glomerular diseases.

6.2 Conclusion

The cytoprotective role of autophagy has been shown in PAN-treated human podocytes. Trehalose alleviated podocyte injury via inducing autophagy *in vitro*. Further investigation is warranted to determine the application of autophagy in the treatment of podocyte related renal diseases.

References

- Aguib, Y., A. Heiseke, S. Gilch, C. Riemer, M. Baier, H. M. Schatzl & A. Ertmer (2009) Autophagy induction by trehalose counteracts cellular prion infection. *Autophagy*, 5, 361-9.
- Akchurin, O. & K. J. Reidy (2014) Genetic causes of proteinuria and nephrotic syndrome: Impact on podocyte pathobiology. *Pediatr Nephrol*.
- Alers, S., A. S. Loffler, S. Wesselborg & B. Stork (2012) Role of AMPK-mTOR-Ulk1/2 in the regulation of autophagy: cross talk, shortcuts, and feedbacks. *Mol Cell Biol*, 32, 2-11.
- Anderson, M., H. Roshanravan, J. Khine & S. E. Dryer (2014) Angiotensin II activation of TRPC6 channels in rat podocytes requires generation of reactive oxygen species. *J Cell Physiol*, 229, 434-42.
- Angliker, N. & M. A. Ruegg (2013) In vivo evidence for mTORC2-mediated actin cytoskeleton rearrangement in neurons. *Bioarchitecture*, 3, 113-118.
- Asanuma, K., I. Tanida, I. Shirato, T. Ueno, H. Takahara, T. Nishitani, E. Kominami & Y. Tomino (2003) MAP-LC3, a promising autophagosomal marker, is processed during the differentiation and recovery of podocytes from PAN nephrosis. *FASEB J*, 17, 1165-7.
- Asanuma, K., E. Yanagida-Asanuma, C. Faul, Y. Tomino, K. Kim & P. Mundel (2006) Synaptopodin orchestrates actin organization and cell motility via regulation of RhoA signalling. *Nat Cell Biol*, 8, 485-91.

- Azad, M. B., Y. Chen & S. B. Gibson (2009) Regulation of autophagy by reactive oxygen species (ROS): implications for cancer progression and treatment. *Antioxid Redox Signal*, 11, 777-90.
- B'Chir, W., C. Chaveroux, V. Carraro, J. Averous, A. C. Maurin, C. Jousse, Y. Muranishi, L. Parry, P. Fafournoux & A. Bruhat (2014) Dual role for CHOP in the crosstalk between autophagy and apoptosis to determine cell fate in response to amino acid deprivation. *Cell Signal*, 26, 1385-91.
- Bjorkoy, G., T. Lamark, A. Brech, H. Outzen, M. Perander, A. Overvatn, H. Stenmark & T. Johansen (2005) p62/SQSTM1 forms protein aggregates degraded by autophagy and has a protective effect on huntingtin-induced cell death. *J Cell Biol*, 171, 603-14.
- Blasutig, I. M., L. A. New, A. Thanabalasuriar, T. K. Dayarathna, M. Goudreault, S. E. Quaggin, S. S. Li, S. Gruenheid, N. Jones & T. Pawson (2008) Phosphorylated YDXV motifs and Nck SH2/SH3 adaptors act cooperatively to induce actin reorganization. *Mol Cell Biol*, 28, 2035-46.
- Bolignano, D., S. C. Palmer, S. D. Navaneethan & G. F. Strippoli (2014) Aldosterone antagonists for preventing the progression of chronic kidney disease. *Cochrane Database Syst Rev*, 4, CD007004.
- Boute, N., O. Gribouval, S. Roselli, F. Benessy, H. Lee, A. Fuchshuber, K. Dahan, M. C. Gubler, P. Niaudet & C. Antignac (2000) NPHS2, encoding the glomerular protein podocin, is mutated in autosomal recessive steroid-resistant nephrotic syndrome. *Nat Genet*, 24, 349-54.

- Brandt, D. T. & R. Grosse (2007) Get to grips: steering local actin dynamics with IQGAPs. *EMBO Rep*, 8, 1019-23.
- Brinkkoetter, P. T., P. Olivier, J. S. Wu, S. Henderson, R. D. Krofft, J. W. Pippin, D. Hockenbery, J. M. Roberts & S. J. Shankland (2009) Cyclin I activates Cdk5 and regulates expression of Bcl-2 and Bcl-XL in postmitotic mouse cells. *J Clin Invest*, 119, 3089-101.
- Chang, J. M., D. Y. Hwang, S. C. Chen, M. C. Kuo, C. C. Hung, S. J. Hwang, J. C. Tsai & H. C. Chen (2013) B7-1 expression regulates the hypoxia-driven cytoskeleton rearrangement in glomerular podocytes. *Am J Physiol Renal Physiol*, 304, F127-36.
- Chevrier, M., N. Brakch, L. Celine, D. Genty, Y. Ramdani, S. Moll, M. Djavaheri-Mergny, C. Brasse-Lagnel, A. L. Annie Laquerriere, F. Barbey & S. Bekri (2010) Autophagosome maturation is impaired in Fabry disease. *Autophagy*, 6, 589-99.
- Chuang, P. Y., Y. Dai, R. Liu, H. He, M. Kretzler, B. Jim, C. D. Cohen & J. C. He (2011) Alteration of forkhead box O (foxo4) acetylation mediates apoptosis of podocytes in diabetes mellitus. *PLoS One*, 6, e23566.
- Cina, D. P., T. Onay, A. Paltoo, C. Li, Y. Maezawa, J. De Arteaga, A. Jurisicova & S. E. Quaggin (2012a) Inhibition of MTOR disrupts autophagic flux in podocytes. *J Am Soc Nephrol*, 23, 412-20.
- (2012b) MTOR regulates autophagic flux in the glomerulus. *Autophagy*, 8, 696-8.
- Coers, W., J. T. Vos, P. H. Van der Meide, M. L. Van der Horst, S. Huitema & J. J. Weening (1995) Interferon-gamma (IFN-gamma) and IL-4 expressed during

- mercury-induced membranous nephropathy are toxic for cultured podocytes. *Clin Exp Immunol*, 102, 297-307.
- Cormack-Aboud, F. C., P. T. Brinkkoetter, J. W. Pippin, S. J. Shankland & R. V. Durvasula (2009) Rosuvastatin protects against podocyte apoptosis in vitro. *Nephrol Dial Transplant*, 24, 404-12.
- Crowe, J. H. (2007) Trehalose as a "chemical chaperone": fact and fantasy. *Adv Exp Med Biol*, 594, 143-58.
- D'Agati, V. D. (2008) Podocyte injury in focal segmental glomerulosclerosis: Lessons from animal models (a play in five acts). *Kidney Int*, 73, 399-406.
- Dai, C., M. A. Saleem, L. B. Holzman, P. Mathieson & Y. Liu (2010) Hepatocyte growth factor signaling ameliorates podocyte injury and proteinuria. *Kidney Int*, 77, 962-73.
- Dandapani, S. V., H. Sugimoto, B. D. Matthews, R. J. Kolb, S. Sinha, R. E. Gerszten, J. Zhou, D. E. Ingber, R. Kalluri & M. R. Pollak (2007) Alpha-actinin-4 is required for normal podocyte adhesion. *J Biol Chem*, 282, 467-77.
- Deegens, J. K., H. B. Dijkman, G. F. Borm, E. J. Steenbergen, J. G. van den Berg, J. J. Weening & J. F. Wetzels (2008) Podocyte foot process effacement as a diagnostic tool in focal segmental glomerulosclerosis. *Kidney Int*, 74, 1568-76.
- Dessapt, C., M. O. Baradez, A. Hayward, A. Dei Cas, S. M. Thomas, G. Viberti & L. Gnudi (2009) Mechanical forces and TGFbeta1 reduce podocyte adhesion

- through alpha3beta1 integrin downregulation. *Nephrol Dial Transplant*, 24, 2645-55.
- Djavaheri-Mergny, M., M. Amelotti, J. Mathieu, F. Besancon, C. Bauvy & P. Codogno (2007) Regulation of autophagy by NFkappaB transcription factor and reactive oxygen species. *Autophagy*, 3, 390-2.
- Djavaheri-Mergny, M., M. C. Maiuri & G. Kroemer (2010) Cross talk between apoptosis and autophagy by caspase-mediated cleavage of Beclin 1. *Oncogene*, 29, 1717-9.
- Drake, J. C., F. F. Peelor, 3rd, L. M. Biela, M. K. Watkins, R. A. Miller, K. L. Hamilton & B. F. Miller (2013) Assessment of mitochondrial biogenesis and mTORC1 signaling during chronic rapamycin feeding in male and female mice. *J Gerontol A Biol Sci Med Sci*, 68, 1493-501.
- Elbein, A. D., Y. T. Pan, I. Pastuszak & D. Carroll (2003) New insights on trehalose: a multifunctional molecule. *Glycobiology*, 13, 17R-27R.
- Elmore, S. (2007) Apoptosis: a review of programmed cell death. *Toxicol Pathol*, 35, 495-516.
- Emanuele, E. (2014) Can trehalose prevent neurodegeneration? Insights from experimental studies. *Curr Drug Targets*, 15, 551-7.
- Endlich, N. & K. Endlich (2012) The challenge and response of podocytes to glomerular hypertension. *Semin Nephrol*, 32, 327-41.
- Erdag, G., A. Eroglu, J. Morgan & M. Toner (2002) Cryopreservation of fetal skin is improved by extracellular trehalose. *Cryobiology*, 44, 218-28.

- Faul, C., K. Asanuma, E. Yanagida-Asanuma, K. Kim & P. Mundel (2007) Actin up: regulation of podocyte structure and function by components of the actin cytoskeleton. *Trends Cell Biol*, 17, 428-37.
- Faul, C., M. Donnelly, S. Merscher-Gomez, Y. H. Chang, S. Franz, J. Delfgaauw, J. M. Chang, H. Y. Choi, K. N. Campbell, K. Kim, J. Reiser & P. Mundel (2008) The actin cytoskeleton of kidney podocytes is a direct target of the antiproteinuric effect of cyclosporine A. *Nat Med*, 14, 931-8.
- Fernandez-Estevez, M. A., M. J. Casarejos, J. Lopez Sendon, J. Garcia Caldentey, C. Ruiz, A. Gomez, J. Perucho, J. G. de Yebenes & M. A. Mena (2014) Trehalose reverses cell malfunction in fibroblasts from normal and Huntington's disease patients caused by proteasome inhibition. *PLoS One*, 9, e90202.
- Fornoni, A., H. Li, A. Foschi, G. E. Striker & L. J. Striker (2001) Hepatocyte growth factor, but not insulin-like growth factor I, protects podocytes against cyclosporin A-induced apoptosis. *Am J Pathol*, 158, 275-80.
- Foster, R. R., M. A. Saleem, P. W. Mathieson, D. O. Bates & S. J. Harper (2005) Vascular endothelial growth factor and nephrin interact and reduce apoptosis in human podocytes. *Am J Physiol Renal Physiol*, 288, F48-57.
- Friedrich, C., N. Endlich, W. Kriz & K. Endlich (2006) Podocytes are sensitive to fluid shear stress in vitro. *Am J Physiol Renal Physiol*, 291, F856-65.
- Fukasawa, H., S. Bornheimer, K. Kudlicka & M. G. Farquhar (2009) Slit diaphragms contain tight junction proteins. *J Am Soc Nephrol*, 20, 1491-503.

- Gagliardini, E., N. Perico, P. Rizzo, S. Buelli, L. Longaretti, L. Perico, S. Tomasoni, C. Zoja, D. Macconi, M. Morigi, G. Remuzzi & A. Benigni (2013) Angiotensin II contributes to diabetic renal dysfunction in rodents and humans via Notch1/Snail pathway. *Am J Pathol*, 183, 119-30.
- Gao, S. Y., C. Y. Li, T. Shimokawa, T. Terashita, S. Matsuda, E. Yaoita & N. Kobayashi (2007) Rho-family small GTPases are involved in forskolin-induced cell-cell contact formation of renal glomerular podocytes in vitro. *Cell Tissue Res*, 328, 391-400.
- Garg, P., R. Verma, L. Cook, A. Soofi, M. Venkatareddy, B. George, K. Mizuno, C. Gurniak, W. Witke & L. B. Holzman (2010) Actin-depolymerizing factor cofilin-1 is necessary in maintaining mature podocyte architecture. *J Biol Chem*, 285, 22676-88.
- Godel, M., B. Hartleben, N. Herbach, S. Liu, S. Zschiedrich, S. Lu, A. Debreczeni-Mor, M. T. Lindenmeyer, M. P. Rastaldi, G. Hartleben, T. Wiech, A. Fornoni, R. G. Nelson, M. Kretzler, R. Wanke, H. Pavenstadt, D. Kerjaschki, C. D. Cohen, M. N. Hall, M. A. Ruegg, K. Inoki, G. Walz & T. B. Huber (2011) Role of mTOR in podocyte function and diabetic nephropathy in humans and mice. *J Clin Invest*, 121, 2197-209.
- Grahammer, F., C. Schell & T. B. Huber (2013) Molecular understanding of the slit diaphragm. *Pediatr Nephrol*, 28, 1957-62.
- Greka, A. & P. Mundel (2012) Cell biology and pathology of podocytes. *Annu Rev Physiol*, 74, 299-323.

- Gwinn, D. M., D. B. Shackelford, D. F. Egan, M. M. Mihaylova, A. Mery, D. S. Vasquez, B. E. Turk & R. J. Shaw (2008) AMPK phosphorylation of raptor mediates a metabolic checkpoint. *Mol Cell*, 30, 214-26.
- Hagiwara, M., K. Yamagata, R. A. Capaldi & A. Koyama (2006) Mitochondrial dysfunction in focal segmental glomerulosclerosis of puromycin aminonucleoside nephrosis. *Kidney Int*, 69, 1146-52.
- Hartleben, B., M. Godel, C. Meyer-Schwesinger, S. Liu, T. Ulrich, S. Kobler, T. Wiech, F. Grahammer, S. J. Arnold, M. T. Lindenmeyer, C. D. Cohen, H. Pavenstadt, D. Kerjaschki, N. Mizushima, A. S. Shaw, G. Walz & T. B. Huber (2010) Autophagy influences glomerular disease susceptibility and maintains podocyte homeostasis in aging mice. *J Clin Invest*, 120, 1084-96.
- Hartleben, B., N. Wanner & T. B. Huber (2014) Autophagy in glomerular health and disease. *Semin Nephrol*, 34, 42-52.
- He, F. F., S. Chen, H. Su, X. F. Meng & C. Zhang (2013) Actin-associated Proteins in the Pathogenesis of Podocyte Injury. *Curr Genomics*, 14, 477-84.
- Heikkila, E., M. Ristola, M. Havana, N. Jones, H. Holthofer & S. Lehtonen (2011) Trans-interaction of nephrin and Neph1/Neph3 induces cell adhesion that associates with decreased tyrosine phosphorylation of nephrin. *Biochem J*, 435, 619-28.
- Hohenstein, B., M. Colin, C. Foellmer, K. U. Amann, R. A. Brekken, C. Daniel & C. P. Hugo (2010) Autocrine VEGF-VEGF-R loop on podocytes during glomerulonephritis in humans. *Nephrol Dial Transplant*, 25, 3170-80.

- Holthofer, H., H. Ahola, M. L. Solin, S. Wang, T. Palmén, P. Luimula, A. Miettinen & D. Kerjaschki (1999) Nephrin localizes at the podocyte filtration slit area and is characteristically spliced in the human kidney. *Am J Pathol*, 155, 1681-7.
- Hou, W., J. Han, C. Lu, L. A. Goldstein & H. Rabinowich (2010) Autophagic degradation of active caspase-8: a crosstalk mechanism between autophagy and apoptosis. *Autophagy*, 6, 891-900.
- Hsieh, Y. C., M. Athar & I. H. Chaudry (2009) When apoptosis meets autophagy: deciding cell fate after trauma and sepsis. *Trends Mol Med*, 15, 129-38.
- Hsu, H. H., S. Hoffmann, N. Endlich, A. Velic, A. Schwab, T. Weide, E. Schlatter & H. Pavenstadt (2008) Mechanisms of angiotensin II signaling on cytoskeleton of podocytes. *J Mol Med (Berl)*, 86, 1379-94.
- Huang, C., L. A. Bruggeman, L. M. Hydo & R. T. Miller (2012) Shear stress induces cell apoptosis via a c-Src-phospholipase D-mTOR signaling pathway in cultured podocytes. *Exp Cell Res*, 318, 1075-85.
- Huber, T. B., C. L. Edelstein, B. Hartleben, K. Inoki, M. Jiang, D. Koya, S. Kume, W. Lieberthal, N. Pallet, A. Quiroga, K. Ravichandran, K. Susztak, S. Yoshida & Z. Dong (2012) Emerging role of autophagy in kidney function, diseases and aging. *Autophagy*, 8, 1009-31.
- Huber, T. B., H. C. Reinhardt, M. Exner, J. A. Burger, D. Kerjaschki, M. A. Saleem & H. Pavenstadt (2002) Expression of functional CCR and CXCR chemokine receptors in podocytes. *J Immunol*, 168, 6244-52.

- Huber, T. B., G. Walz & E. W. Kuehn (2011) mTOR and rapamycin in the kidney: signaling and therapeutic implications beyond immunosuppression. *Kidney Int*, 79, 502-11.
- Inoki, K. (2014) mTOR signaling in autophagy regulation in the kidney. *Semin Nephrol*, 34, 2-8.
- Inoki, K. & T. B. Huber (2012) Mammalian target of rapamycin signaling in the podocyte. *Curr Opin Nephrol Hypertens*, 21, 251-7.
- Inoki, K., H. Mori, J. Wang, T. Suzuki, S. Hong, S. Yoshida, S. M. Blattner, T. Ikenoue, M. A. Ruegg, M. N. Hall, D. J. Kwiatkowski, M. P. Rastaldi, T. B. Huber, M. Kretzler, L. B. Holzman, R. C. Wiggins & K. L. Guan (2011) mTORC1 activation in podocytes is a critical step in the development of diabetic nephropathy in mice. *J Clin Invest*, 121, 2181-96.
- Inoki, K., H. Ouyang, T. Zhu, C. Lindvall, Y. Wang, X. Zhang, Q. Yang, C. Bennett, Y. Harada, K. Stankunas, C. Y. Wang, X. He, O. A. MacDougald, M. You, B. O. Williams & K. L. Guan (2006) TSC2 integrates Wnt and energy signals via a coordinated phosphorylation by AMPK and GSK3 to regulate cell growth. *Cell*, 126, 955-68.
- Ishikawa, Y. & M. Kitamura (1999) Inhibition of glomerular cell apoptosis by heparin. *Kidney Int*, 56, 954-63.
- Jaffer, A. T., W. U. Ahmed, D. S. Raju & P. Jahan (2011) Foothold of NPHS2 mutations in primary nephrotic syndrome. *J Postgrad Med*, 57, 314-20.
- Jalanko, H., J. Patrakka, K. Tryggvason & C. Holmberg (2001) Genetic kidney diseases disclose the pathogenesis of proteinuria. *Ann Med*, 33, 526-33.

- Jeruschke, S., A. K. Buscher, J. Oh, M. A. Saleem, P. F. Hoyer, S. Weber & P. Nalbant (2013) Protective effects of the mTOR inhibitor everolimus on cytoskeletal injury in human podocytes are mediated by RhoA signaling. *PLoS One*, 8, e55980.
- Jiang, M., K. Liu, J. Luo & Z. Dong (2010) Autophagy is a renoprotective mechanism during in vitro hypoxia and in vivo ischemia-reperfusion injury. *Am J Pathol*, 176, 1181-92.
- Jolly, S. E., S. D. Navaneethan, J. D. Schold, S. Arrigain, J. W. Sharp, A. K. Jain, M. J. Schreiber, J. F. Simon & J. V. Nally (2014) Chronic kidney disease in an electronic health record problem list: quality of care, ESRD, and mortality. *Am J Nephrol*, 39, 288-96.
- Jones, N., I. M. Blasutig, V. Eremina, J. M. Ruston, F. Bladt, H. Li, H. Huang, L. Larose, S. S. Li, T. Takano, S. E. Quaggin & T. Pawson (2006) Nck adaptor proteins link nephrin to the actin cytoskeleton of kidney podocytes. *Nature*, 440, 818-23.
- Josselyn, S. A. & P. W. Frankland (2013) mTORC2: actin on your memory. *Nat Neurosci*, 16, 379-80.
- Jung, C. H., S. H. Ro, J. Cao, N. M. Otto & D. H. Kim (2010) mTOR regulation of autophagy. *FEBS Lett*, 584, 1287-95.
- Kalluri, R. (2006) Proteinuria with and without renal glomerular podocyte effacement. *J Am Soc Nephrol*, 17, 2383-9.

- Kanellis, J., V. Levidiotis, T. Khong, A. J. Cox, S. A. Stacker, R. E. Gilbert, M. E. Cooper & D. A. Power (2004) A study of VEGF and its receptors in two rat models of proteinuria. *Nephron Physiol*, 96, P26-36.
- Kang, R., H. J. Zeh, M. T. Lotze & D. Tang (2011) The Beclin 1 network regulates autophagy and apoptosis. *Cell Death Differ*, 18, 571-80.
- Kang, Y. L., M. A. Saleem, K. W. Chan, B. Y. Yung & H. K. Law (2014) The cytoprotective role of autophagy in puromycin aminonucleoside treated human podocytes. *Biochem Biophys Res Commun*, 443, 628-34.
- Kaplan, J. M., S. H. Kim, K. N. North, H. Rennke, L. A. Correia, H. Q. Tong, B. J. Mathis, J. C. Rodriguez-Perez, P. G. Allen, A. H. Beggs & M. R. Pollak (2000) Mutations in ACTN4, encoding alpha-actinin-4, cause familial focal segmental glomerulosclerosis. *Nat Genet*, 24, 251-6.
- Kaushik, J. K. & R. Bhat (2003) Why is trehalose an exceptional protein stabilizer? An analysis of the thermal stability of proteins in the presence of the compatible osmolyte trehalose. *J Biol Chem*, 278, 26458-65.
- Kim, B. S., H. C. Park, S. W. Kang, K. H. Choi, S. K. Ha, D. S. Han & H. Y. Lee (2005) Impact of cyclosporin on podocyte ZO-1 expression in puromycin aminonucleoside nephrosis rats. *Yonsei Med J*, 46, 141-8.
- Kim, J., M. Kundu, B. Viollet & K. L. Guan (2011) AMPK and mTOR regulate autophagy through direct phosphorylation of Ulk1. *Nat Cell Biol*, 13, 132-41.
- Kim, J. M., H. Wu, G. Green, C. A. Winkler, J. B. Kopp, J. H. Miner, E. R. Unanue & A. S. Shaw (2003) CD2-associated protein haploinsufficiency is linked to glomerular disease susceptibility. *Science*, 300, 1298-300.

- Klionsky, D. J., F. C. Abdalla, H. Abeliovich, R. T. et al. (2012) Guidelines for the use and interpretation of assays for monitoring autophagy. *Autophagy*, 8, 445-544.
- Komatsu, M., H. Kurokawa, S. Waguri, K. Taguchi, A. Kobayashi, Y. Ichimura, Y. S. Sou, I. Ueno, A. Sakamoto, K. I. Tong, M. Kim, Y. Nishito, S. Iemura, T. Natsume, T. Ueno, E. Kominami, H. Motohashi, K. Tanaka & M. Yamamoto (2010) The selective autophagy substrate p62 activates the stress responsive transcription factor Nrf2 through inactivation of Keap1. *Nat Cell Biol*, 12, 213-23.
- Kruger, U., Y. Wang, S. Kumar & E. M. Mandelkow (2012) Autophagic degradation of tau in primary neurons and its enhancement by trehalose. *Neurobiol Aging*, 33, 2291-305.
- Kume, S., K. Yamahara, M. Yasuda, H. Maegawa & D. Koya (2014) Autophagy: emerging therapeutic target for diabetic nephropathy. *Semin Nephrol*, 34, 9-16.
- Kummer, S., S. Jeruschke, L. V. Wegerich, A. Peters, P. Lehmann, A. Seibt, F. Mueller, N. Koleganova, E. Halbenz, C. P. Schmitt, M. Bettendorf, E. Mayatepek, M. L. Gross-Weissmann & J. Oh (2011) Estrogen receptor alpha expression in podocytes mediates protection against apoptosis in-vitro and in-vivo. *PLoS One*, 6, e27457.
- Lai, K. W., C. L. Wei, L. K. Tan, P. H. Tan, G. S. Chiang, C. G. Lee, S. C. Jordan & H. K. Yap (2007) Overexpression of interleukin-13 induces minimal-change-like nephropathy in rats. *J Am Soc Nephrol*, 18, 1476-85.

- Lee, J. W., S. Park, Y. Takahashi & H. G. Wang (2010) The association of AMPK with ULK1 regulates autophagy. *PLoS One*, 5, e15394.
- Li, C., V. Ruotsalainen, K. Tryggvason, A. S. Shaw & J. H. Miner (2000) CD2AP is expressed with nephrin in developing podocytes and is found widely in mature kidney and elsewhere. *Am J Physiol Renal Physiol*, 279, F785-92.
- Li, D. D., L. L. Wang, R. Deng, J. Tang, Y. Shen, J. F. Guo, Y. Wang, L. P. Xia, G. K. Feng, Q. Q. Liu, W. L. Huang, Y. X. Zeng & X. F. Zhu (2009) The pivotal role of c-Jun NH2-terminal kinase-mediated Beclin 1 expression during anticancer agents-induced autophagy in cancer cells. *Oncogene*, 28, 886-98.
- Li, X., H. Tao, K. Xie, Z. Ni, Y. Yan, K. Wei, P. Y. Chuang, J. C. He & L. Gu (2014) cAMP signaling prevents podocyte apoptosis via activation of protein kinase A and mitochondrial fusion. *PLoS One*, 9, e92003.
- Liebau, M. C., F. Braun, K. Hopker, C. Weitbrecht, V. Bartels, R. U. Muller, S. Brodesser, M. A. Saleem, T. Benzing, B. Schermer, M. Cybulla & C. E. Kurschat (2013) Dysregulated autophagy contributes to podocyte damage in Fabry's disease. *PLoS One*, 8, e63506.
- Lin, Y., J. Rao, X. L. Zha & H. Xu (2013) Angiopoietin-like 3 induces podocyte F-actin rearrangement through integrin alpha(V)beta(3)/FAK/PI3K pathway-mediated Rac1 activation. *Biomed Res Int*, 2013, 135608.
- Liu, B. C., X. Song, X. Y. Lu, D. T. Li, D. C. Eaton, B. Z. Shen, X. Q. Li & H. P. Ma (2013) High glucose induces podocyte apoptosis by stimulating TRPC6

- via elevation of reactive oxygen species. *Biochim Biophys Acta*, 1833, 1434-42.
- Liu, H., X. Gao, H. Xu, C. Feng, X. Kuang, Z. Li & X. Zha (2012) alpha-Actinin-4 is involved in the process by which dexamethasone protects actin cytoskeleton stabilization from adriamycin-induced podocyte injury. *Nephrology (Carlton)*, 17, 669-75.
- Loeffler, I. & G. Wolf (2014) Transforming growth factor-beta and the progression of renal disease. *Nephrol Dial Transplant*, 29 Suppl 1, i37-i45.
- Logar, C. M., P. T. Brinkkoetter, R. D. Kroffft, J. W. Pippin & S. J. Shankland (2007) Darbepoetin alfa protects podocytes from apoptosis in vitro and in vivo. *Kidney Int*, 72, 489-98.
- Lopez-Hernandez, F. J. & J. M. Lopez-Novoa (2012) Role of TGF-beta in chronic kidney disease: an integration of tubular, glomerular and vascular effects. *Cell Tissue Res*, 347, 141-54.
- Lowenborg, E. K., G. Jaremko & U. B. Berg (2000) Glomerular function and morphology in puromycin aminonucleoside nephropathy in rats. *Nephrol Dial Transplant*, 15, 1547-55.
- Luo, S. & D. C. Rubinsztein (2010) Apoptosis blocks Beclin 1-dependent autophagosome synthesis: an effect rescued by Bcl-xL. *Cell Death Differ*, 17, 268-77.
- Ma, T., J. Zhu, X. Chen, D. Zha, P. C. Singhal & G. Ding (2013) High glucose induces autophagy in podocytes. *Exp Cell Res*, 319, 779-89.

- Mao, C., R. Liu, L. Bo, N. Chen, S. Li, S. Xia, J. Chen, D. Li, L. Zhang & Z. Xu (2013) High-salt diets during pregnancy affected fetal and offspring renal renin-angiotensin system. *J Endocrinol*, 218, 61-73.
- Markowitz, G. S., S. H. Nasr, M. B. Stokes & V. D. D'Agati (2010) Treatment with IFN- α , - β , or - γ is associated with collapsing focal segmental glomerulosclerosis. *Clin J Am Soc Nephrol*, 5, 607-15.
- Martyniszyn, L., L. Szulc-Dabrowska, A. Boratynska-Jasinska, J. Struzik, A. Winnicka & M. Niemialtowski (2013) Crosstalk between autophagy and apoptosis in RAW 264.7 macrophages infected with ectromelia orthopoxvirus. *Viral Immunol*, 26, 322-35.
- Mathieson, P. W. (2012) The podocyte as a target for therapies--new and old. *Nat Rev Nephrol*, 8, 52-6.
- Meijer, A. J., S. Lorin, E. F. Blommaart & P. Codogno (2014) Regulation of autophagy by amino acids and MTOR-dependent signal transduction. *Amino Acids*.
- Merline, R., S. Lazaroski, A. Babelova, W. Tsalastra-Greul, J. Pfeilschifter, K. D. Schluter, A. Gunther, R. V. Iozzo, R. M. Schaefer & L. Schaefer (2009) Decorin deficiency in diabetic mice: aggravation of nephropathy due to overexpression of profibrotic factors, enhanced apoptosis and mononuclear cell infiltration. *J Physiol Pharmacol*, 60 Suppl 4, 5-13.
- Miceli, I., D. Burt, E. Tarabra, G. Camussi, P. C. Perin & G. Gruden (2010) Stretch reduces nephrin expression via an angiotensin II-AT(1)-dependent

- mechanism in human podocytes: effect of rosiglitazone. *Am J Physiol Renal Physiol*, 298, F381-90.
- Michaud, J. L., M. Hosseini-Abardeh, K. Farah & C. R. Kennedy (2009) Modulating alpha-actinin-4 dynamics in podocytes. *Cell Motil Cytoskeleton*, 66, 166-78.
- Mizushima, N., B. Levine, A. M. Cuervo & D. J. Klionsky (2008) Autophagy fights disease through cellular self-digestion. *Nature*, 451, 1069-75.
- Mizushima, N., T. Yoshimori & B. Levine (2010) Methods in mammalian autophagy research. *Cell*, 140, 313-26.
- Mouawad, F., H. Tsui & T. Takano (2013) Role of Rho-GTPases and their regulatory proteins in glomerular podocyte function. *Can J Physiol Pharmacol*, 91, 773-82.
- Mukerji, N., T. V. Damodaran & M. P. Winn (2007) TRPC6 and FSGS: the latest TRP channelopathy. *Biochim Biophys Acta*, 1772, 859-68.
- Mukhopadhyay, S., P. K. Panda, N. Sinha, D. N. Das & S. K. Bhutia (2014) Autophagy and apoptosis: where do they meet? *Apoptosis*, 19, 555-66.
- Mundel, P. & J. Reiser (2010) Proteinuria: an enzymatic disease of the podocyte? *Kidney Int*, 77, 571-80.
- Nakamura, T., C. Ushiyama, S. Suzuki, M. Hara, N. Shimada, K. Sekizuka, I. Ebihara & H. Koide (2000) Effects of angiotensin-converting enzyme inhibitor, angiotensin II receptor antagonist and calcium antagonist on urinary podocytes in patients with IgA nephropathy. *Am J Nephrol*, 20, 373-9.

- Narita, M., A. R. Young, S. Arakawa, S. A. Samarajiwa, T. Nakashima, S. Yoshida, S. Hong, L. S. Berry, S. Reichelt, M. Ferreira, S. Tavaré, K. Inoki & S. Shimizu (2011) Spatial coupling of mTOR and autophagy augments secretory phenotypes. *Science*, 332, 966-70.
- Neal, C. R., H. Crook, E. Bell, S. J. Harper & D. O. Bates (2005) Three-dimensional reconstruction of glomeruli by electron microscopy reveals a distinct restrictive urinary subpodocyte space. *J Am Soc Nephrol*, 16, 1223-35.
- Neal, C. R., P. R. Muston, D. Njegovan, R. Verrill, S. J. Harper, W. M. Deen & D. O. Bates (2007) Glomerular filtration into the subpodocyte space is highly restricted under physiological perfusion conditions. *Am J Physiol Renal Physiol*, 293, F1787-98.
- Nishida, K., O. Yamaguchi & K. Otsu (2008) Crosstalk between autophagy and apoptosis in heart disease. *Circ Res*, 103, 343-51.
- Oba, S., M. Hino & T. Fujita (2008) Adrenomedullin protects against oxidative stress-induced podocyte injury as an endogenous antioxidant. *Nephrol Dial Transplant*, 23, 510-7.
- Oh, J., J. Reiser & P. Mundel (2004) Dynamic (re)organization of the podocyte actin cytoskeleton in the nephrotic syndrome. *Pediatr Nephrol*, 19, 130-7.
- Ohtake, S. & Y. J. Wang (2011) Trehalose: current use and future applications. *J Pharm Sci*, 100, 2020-53.
- Otukesh, H., B. Ghazanfari, S. M. Fereshtehnejad, M. Bakhshayesh, M. Hashemi, R. Hoseini, M. Chalian, A. Salami, L. Mehdipor & A. Rahiminia (2009)

- NPHS2 mutations in children with steroid-resistant nephrotic syndrome. *Iran J Kidney Dis*, 3, 99-102.
- Patrakka, J., A. T. Lahdenkari, O. Koskimies, C. Holmberg, J. Wartiovaara & H. Jalanko (2002) The number of podocyte slit diaphragms is decreased in minimal change nephrotic syndrome. *Pediatr Res*, 52, 349-55.
- Patrakka, J. & K. Tryggvason (2007) Nephrin--a unique structural and signaling protein of the kidney filter. *Trends Mol Med*, 13, 396-403.
- Pavenstadt, H., W. Kriz & M. Kretzler (2003) Cell biology of the glomerular podocyte. *Physiol Rev*, 83, 253-307.
- Pawluczyk, I. Z., B. Yang, S. R. Patel, M. A. Saleem & P. S. Topham (2011) Low-level C-reactive protein levels exert cytoprotective actions on human podocytes. *Nephrol Dial Transplant*, 26, 2465-75.
- Periyasamy-Thandavan, S., M. Jiang, P. Schoenlein & Z. Dong (2009) Autophagy: molecular machinery, regulation, and implications for renal pathophysiology. *Am J Physiol Renal Physiol*, 297, F244-56.
- Petermann, A. T., J. Pippin, R. Krofft, M. Blonski, S. Griffin, R. Durvasula & S. J. Shankland (2004) Viable podocytes detach in experimental diabetic nephropathy: potential mechanism underlying glomerulosclerosis. *Nephron Exp Nephrol*, 98, e114-23.
- Pippin, J. W., P. T. Brinkkoetter, F. C. Cormack-Aboud, R. V. Durvasula, P. V. Hauser, J. Kowalewska, R. D. Krofft, C. M. Logar, C. B. Marshall, T. Ohse & S. J. Shankland (2009) Inducible rodent models of acquired podocyte diseases. *Am J Physiol Renal Physiol*, 296, F213-29.

- Pohlers, D., J. Brenmoehl, I. Loffler, C. K. Muller, C. Leipner, S. Schultze-Mosgau, A. Stallmach, R. W. Kinne & G. Wolf (2009) TGF-beta and fibrosis in different organs - molecular pathway imprints. *Biochim Biophys Acta*, 1792, 746-56.
- Pollak, M. R. (2008) Focal segmental glomerulosclerosis: recent advances. *Curr Opin Nephrol Hypertens*, 17, 138-42.
- Pradhan, S. A., M. I. Rather, A. Tiwari, V. K. Bhat & A. Kumar (2014) Evidence that TSC2 acts as a transcription factor and binds to and represses the promoter of Epiregulin. *Nucleic Acids Res*, 42, 6243-55.
- Pyo, J. O., S. M. Yoo, H. H. Ahn, J. Nah, S. H. Hong, T. I. Kam, S. Jung & Y. K. Jung (2013) Overexpression of Atg5 in mice activates autophagy and extends lifespan. *Nat Commun*, 4, 2300.
- Quaggin, S. E. & J. A. Kreidberg (2008) Development of the renal glomerulus: good neighbors and good fences. *Development*, 135, 609-20.
- Reiser, J., K. R. Polu, C. C. Moller, P. Kenlan, M. M. Altintas, C. Wei, C. Faul, S. Herbert, I. Villegas, C. Avila-Casado, M. McGee, H. Sugimoto, D. Brown, R. Kalluri, P. Mundel, P. L. Smith, D. E. Clapham & M. R. Pollak (2005) TRPC6 is a glomerular slit diaphragm-associated channel required for normal renal function. *Nat Genet*, 37, 739-44.
- Reiser, J. & S. Sever (2013) Podocyte biology and pathogenesis of kidney disease. *Annu Rev Med*, 64, 357-66.
- Reiser, J., G. von Gersdorff, M. Loos, J. Oh, K. Asanuma, L. Giardino, M. P. Rastaldi, N. Calvaresi, H. Watanabe, K. Schwarz, C. Faul, M. Kretzler, A.

- Davidson, H. Sugimoto, R. Kalluri, A. H. Sharpe, J. A. Kreidberg & P. Mundel (2004) Induction of B7-1 in podocytes is associated with nephrotic syndrome. *J Clin Invest*, 113, 1390-7.
- Ren, Z., W. Liang, C. Chen, H. Yang, P. C. Singhal & G. Ding (2012) Angiotensin II induces nephrin dephosphorylation and podocyte injury: role of caveolin-1. *Cell Signal*, 24, 443-50.
- Richards, A. B., S. Krakowka, L. B. Dexter, H. Schmid, A. P. Wolterbeek, D. H. Waalkens-Berendsen, A. Shigoyuki & M. Kurimoto (2002) Trehalose: a review of properties, history of use and human tolerance, and results of multiple safety studies. *Food Chem Toxicol*, 40, 871-98.
- Rinta-Valkama, J., T. Palmen, M. Lassila & H. Holthofer (2007) Podocyte-associated proteins FAT, alpha-actinin-4 and filtrin are expressed in Langerhans islets of the pancreas. *Mol Cell Biochem*, 294, 117-25.
- Rosa, A. C., L. Rattazzi, G. Miglio, M. Collino & R. Fantozzi (2012) Angiotensin II induces tumor necrosis factor-alpha expression and release from cultured human podocytes. *Inflamm Res*, 61, 311-7.
- Ruotsalainen, V., P. Ljungberg, J. Wartiovaara, U. Lenkkeri, M. Kestila, H. Jalanko, C. Holmberg & K. Tryggvason (1999) Nephrin is specifically located at the slit diaphragm of glomerular podocytes. *Proc Natl Acad Sci U S A*, 96, 7962-7.
- Sakai, N., T. Wada, K. Furuichi, Y. Iwata, K. Yoshimoto, K. Kitagawa, S. Kokubo, M. Kobayashi, A. Hara, J. Yamahana, T. Okumura, K. Takasawa, S. Takeda, M. Yoshimura, H. Kida & H. Yokoyama (2005) Involvement of

- extracellular signal-regulated kinase and p38 in human diabetic nephropathy. *Am J Kidney Dis*, 45, 54-65.
- Saleem, M. A. (2003) Biology of the human podocyte. *Nephron Exp Nephrol*, 95, e87-92.
- Saleem, M. A., M. J. O'Hare, J. Reiser, R. J. Coward, C. D. Inward, T. Farren, C. Y. Xing, L. Ni, P. W. Mathieson & P. Mundel (2002) A conditionally immortalized human podocyte cell line demonstrating nephrin and podocin expression. *J Am Soc Nephrol*, 13, 630-8.
- Salminen, A. & K. Kaarniranta (2012) AMP-activated protein kinase (AMPK) controls the aging process via an integrated signaling network. *Ageing Res Rev*, 11, 230-41.
- Salomon, R., M. C. Gubler & P. Niaudet (2000) Genetics of the nephrotic syndrome. *Curr Opin Pediatr*, 12, 129-34.
- Sancak, Y., T. R. Peterson, Y. D. Shaul, R. A. Lindquist, C. C. Thoreen, L. Bar-Peled & D. M. Sabatini (2008) The Rag GTPases bind raptor and mediate amino acid signaling to mTORC1. *Science*, 320, 1496-501.
- Sancak, Y., C. C. Thoreen, T. R. Peterson, R. A. Lindquist, S. A. Kang, E. Spooner, S. A. Carr & D. M. Sabatini (2007) PRAS40 is an insulin-regulated inhibitor of the mTORC1 protein kinase. *Mol Cell*, 25, 903-15.
- Sanchez-Nino, M. D., A. B. Sanz, E. Sanchez-Lopez, M. Ruiz-Ortega, A. Benito-Martin, M. A. Saleem, P. W. Mathieson, S. Mezzano, J. Egido & A. Ortiz (2012) HSP27/HSPB1 as an adaptive podocyte antiapoptotic protein activated by high glucose and angiotensin II. *Lab Invest*, 92, 32-45.

- Sarkar, S., J. E. Davies, Z. Huang, A. Tunnacliffe & D. C. Rubinsztein (2007) Trehalose, a novel mTOR-independent autophagy enhancer, accelerates the clearance of mutant huntingtin and alpha-synuclein. *J Biol Chem*, 282, 5641-52.
- Sarkar, S., R. A. Floto, Z. Berger, S. Imarisio, A. Cordenier, M. Pasco, L. J. Cook & D. C. Rubinsztein (2005) Lithium induces autophagy by inhibiting inositol monophosphatase. *J Cell Biol*, 170, 1101-11.
- Sarkar, S. & D. C. Rubinsztein (2008) Small molecule enhancers of autophagy for neurodegenerative diseases. *Mol Biosyst*, 4, 895-901.
- Sasai-Takedatsu, M., S. Taketani, N. Nagata, T. Furukawa, R. Tokunaga, T. Kojima & Y. Kobayashi (1996) Human trehalase: characterization, localization, and its increase in urine by renal proximal tubular damage. *Nephron*, 73, 179-85.
- Sato, S., H. Kitamura, A. Adachi, Y. Sasaki & M. Ghazizadeh (2006) Two types of autophagy in the podocytes in renal biopsy specimens: ultrastructural study. *J Submicrosc Cytol Pathol*, 38, 167-74.
- Sato, S., T. Yanagihara, M. Ghazizadeh, M. Ishizaki, A. Adachi, Y. Sasaki, T. Igarashi & Y. Fukunaga (2009) Correlation of autophagy type in podocytes with histopathological diagnosis of IgA nephropathy. *Pathobiology*, 76, 221-6.
- Scharpe, J., B. Maes & B. Van Damme (2005) The podocyte: from bench to bedside. *Acta Clin Belg*, 60, 86-93.
- Scherz-Shouval, R., E. Shvets & Z. Elazar (2007a) Oxidation as a post-translational modification that regulates autophagy. *Autophagy*, 3, 371-3.

- Scherz-Shouval, R., E. Shvets, E. Fass, H. Shorer, L. Gil & Z. Elazar (2007b) Reactive oxygen species are essential for autophagy and specifically regulate the activity of Atg4. *EMBO J*, 26, 1749-60.
- Schiffer, M., M. Bitzer, I. S. Roberts, J. B. Kopp, P. ten Dijke, P. Mundel & E. P. Bottinger (2001) Apoptosis in podocytes induced by TGF-beta and Smad7. *J Clin Invest*, 108, 807-16.
- Shao, H., J. H. Wang, M. R. Pollak & A. Wells (2010) alpha-actinin-4 is essential for maintaining the spreading, motility and contractility of fibroblasts. *PLoS One*, 5, e13921.
- Shi, C. S. & J. H. Kehrl (2010) TRAF6 and A20 regulate lysine 63-linked ubiquitination of Beclin-1 to control TLR4-induced autophagy. *Sci Signal*, 3, ra42.
- Shih, N. Y., J. Li, R. Cotran, P. Mundel, J. H. Miner & A. S. Shaw (2001) CD2AP localizes to the slit diaphragm and binds to nephrin via a novel C-terminal domain. *Am J Pathol*, 159, 2303-8.
- Sieber, J., M. T. Lindenmeyer, K. Kampe, K. N. Campbell, C. D. Cohen, H. Hopfer, P. Mundel & A. W. Jehle (2010) Regulation of podocyte survival and endoplasmic reticulum stress by fatty acids. *Am J Physiol Renal Physiol*, 299, F821-9.
- Sinha, S. & B. Levine (2008) The autophagy effector Beclin 1: a novel BH3-only protein. *Oncogene*, 27 Suppl 1, S137-48.

- Skoczynska, A., H. Martynowicz, R. Poreba, J. Antonowicz-Juchniewicz, A. Sieradzki & R. Andrzejak (2001) [Urinary trehalase activity as an indicator of renal dysfunction in lead smelters]. *Med Pr*, 52, 247-52.
- Srivastava, T., M. Sharma, K. H. Yew, R. Sharma, R. S. Duncan, M. A. Saleem, E. T. McCarthy, A. Kats, P. A. Cudmore, U. S. Alon & C. J. Harrison (2013) LPS and PAN-induced podocyte injury in an in vitro model of minimal change disease: changes in TLR profile. *J Cell Commun Signal*, 7, 49-60.
- Stitt-Cavanagh, E., L. MacLeod & C. Kennedy (2009) The podocyte in diabetic kidney disease. *ScientificWorldJournal*, 9, 1127-39.
- Tain, Y. L., T. Y. Chen & K. D. Yang (2003) Implications of serum TNF-beta and IL-13 in the treatment response of childhood nephrotic syndrome. *Cytokine*, 21, 155-9.
- Takabatake, Y., T. Kimura, A. Takahashi & Y. Isaka (2014) Autophagy and the kidney: health and disease. *Nephrol Dial Transplant*.
- Takacs-Vellai, K., A. Bayci & T. Vellai (2006) Autophagy in neuronal cell loss: a road to death. *Bioessays*, 28, 1126-31.
- Tanaka, M., Y. Machida, S. Niu, T. Ikeda, N. R. Jana, H. Doi, M. Kurosawa, M. Nekooki & N. Nukina (2004) Trehalose alleviates polyglutamine-mediated pathology in a mouse model of Huntington disease. *Nat Med*, 10, 148-54.
- Tang, D., R. Kang, K. M. Livesey, C. W. Cheh, A. Farkas, P. Loughran, G. Hoppe, M. E. Bianchi, K. J. Tracey, H. J. Zeh, 3rd & M. T. Lotze (2010) Endogenous HMGB1 regulates autophagy. *J Cell Biol*, 190, 881-92.

- Teng, B., A. Lukasz & M. Schiffer (2012) The ADF/Cofilin-Pathway and Actin Dynamics in Podocyte Injury. *Int J Cell Biol*, 2012, 320531.
- Thorburn, A. (2008) Apoptosis and autophagy: regulatory connections between two supposedly different processes. *Apoptosis*, 13, 1-9.
- Tian, D., S. M. Jacobo, D. Billing, A. Rozkalne, S. D. Gage, T. Anagnostou, H. Pavenstadt, H. H. Hsu, J. Schlondorff, A. Ramos & A. Greka (2010) Antagonistic regulation of actin dynamics and cell motility by TRPC5 and TRPC6 channels. *Sci Signal*, 3, ra77.
- Tuncdemir, M. & M. Ozturk (2011) The effects of angiotensin-II receptor blockers on podocyte damage and glomerular apoptosis in a rat model of experimental streptozotocin-induced diabetic nephropathy. *Acta Histochem*, 113, 826-32.
- Underwood, B. R., S. Imarisio, A. Fleming, C. Rose, G. Krishna, P. Heard, M. Quick, V. I. Korolchuk, M. Renna, S. Sarkar, M. Garcia-Arencibia, C. J. O'Kane, M. P. Murphy & D. C. Rubinsztein (2010) Antioxidants can inhibit basal autophagy and enhance neurodegeneration in models of polyglutamine disease. *Hum Mol Genet*, 19, 3413-29.
- Vega-Warner, V., R. F. Ransom, A. M. Vincent, F. C. Brosius & W. E. Smoyer (2004) Induction of antioxidant enzymes in murine podocytes precedes injury by puromycin aminonucleoside. *Kidney Int*, 66, 1881-9.
- Vogtlander, N. P., W. P. Tamboer, M. A. Bakker, K. P. Campbell, J. van der Vlag & J. H. Berden (2006) Reactive oxygen species deglycosilate glomerular alpha-dystroglycan. *Kidney Int*, 69, 1526-34.

- Vollenbroeker, B., B. George, M. Wolfgart, M. A. Saleem, H. Pavenstadt & T. Weide (2009) mTOR regulates expression of slit diaphragm proteins and cytoskeleton structure in podocytes. *Am J Physiol Renal Physiol*, 296, F418-26.
- Wada, T., J. W. Pippin, C. B. Marshall, S. V. Griffin & S. J. Shankland (2005) Dexamethasone prevents podocyte apoptosis induced by puromycin aminonucleoside: role of p53 and Bcl-2-related family proteins. *J Am Soc Nephrol*, 16, 2615-25.
- Wang, L., Q. Hong, Y. Lv, Z. Feng, X. Zhang, L. Wu, S. Cui, K. Hou, H. Su, Z. Huang, D. Wu & X. Chen (2012a) Autophagy can repair endoplasmic reticulum stress damage of the passive Heymann nephritis model as revealed by proteomics analysis. *J Proteomics*, 75, 3866-76.
- Wang, X. & C. G. Proud (2011) mTORC1 signaling: what we still don't know. *J Mol Cell Biol*, 3, 206-20.
- Wang, X. & H. Xu (2013) New insights into treatment of nephrotic syndrome in children. *Contrib Nephrol*, 181, 119-30.
- Wang, Z., X. Wei, Y. Zhang, X. Ma, B. Li, S. Zhang, P. Du, X. Zhang & F. Yi (2009) NADPH oxidase-derived ROS contributes to upregulation of TRPC6 expression in puromycin aminonucleoside-induced podocyte injury. *Cell Physiol Biochem*, 24, 619-26.
- Wang, Z., J. Zhong, H. Inuzuka, D. Gao, S. Shaik, F. H. Sarkar & W. Wei (2012b) An evolving role for DEPTOR in tumor development and progression. *Neoplasia*, 14, 368-75.

- Wei, C., C. C. Moller, M. M. Altintas, J. Li, K. Schwarz, S. Zacchigna, L. Xie, A. Henger, H. Schmid, M. P. Rastaldi, P. Cowan, M. Kretzler, R. Parrilla, M. Bendayan, V. Gupta, B. Nikolic, R. Kalluri, P. Carmeliet, P. Mundel & J. Reiser (2008a) Modification of kidney barrier function by the urokinase receptor. *Nat Med*, 14, 55-63.
- Wei, Y., S. Pattingre, S. Sinha, M. Bassik & B. Levine (2008b) JNK1-mediated phosphorylation of Bcl-2 regulates starvation-induced autophagy. *Mol Cell*, 30, 678-88.
- Weide, T. & T. B. Huber (2011) Implications of autophagy for glomerular aging and disease. *Cell Tissue Res*, 343, 467-73.
- Weil, E. J., K. V. Lemley, C. C. Mason, B. Yee, L. I. Jones, K. Blouch, T. Lovato, M. Richardson, B. D. Myers & R. G. Nelson (2012) Podocyte detachment and reduced glomerular capillary endothelial fenestration promote kidney disease in type 2 diabetic nephropathy. *Kidney Int*, 82, 1010-7.
- Welsh, G. I. & M. A. Saleem (2012) The podocyte cytoskeleton--key to a functioning glomerulus in health and disease. *Nat Rev Nephrol*, 8, 14-21.
- Williams, A., S. Sarkar, P. Cuddon, E. K. Ttofi, S. Saiki, F. H. Siddiqi, L. Jahreiss, A. Fleming, D. Pask, P. Goldsmith, C. J. O'Kane, R. A. Floto & D. C. Rubinsztein (2008) Novel targets for Huntington's disease in an mTOR-independent autophagy pathway. *Nat Chem Biol*, 4, 295-305.
- Wirawan, E., S. Lippens, T. Vanden Berghe, A. Romagnoli, G. M. Fimia, M. Piacentini & P. Vandenabeele (2012) Beclin1: a role in membrane dynamics and beyond. *Autophagy*, 8, 6-17.

- Wiza, C., E. B. Nascimento & D. M. Ouwens (2012) Role of PRAS40 in Akt and mTOR signaling in health and disease. *Am J Physiol Endocrinol Metab*, 302, E1453-60.
- Wolf, G. & R. A. Stahl (2003) CD2-associated protein and glomerular disease. *Lancet*, 362, 1746-8.
- Wong, A. S., R. H. Lee, A. Y. Cheung, P. K. Yeung, S. K. Chung, Z. H. Cheung & N. Y. Ip (2011) Cdk5-mediated phosphorylation of endophilin B1 is required for induced autophagy in models of Parkinson's disease. *Nat Cell Biol*, 13, 568-79.
- Wu, L., Z. Feng, S. Cui, K. Hou, L. Tang, J. Zhou, G. Cai, Y. Xie, Q. Hong, B. Fu & X. Chen (2013) Rapamycin upregulates autophagy by inhibiting the mTOR-ULK1 pathway, resulting in reduced podocyte injury. *PLoS One*, 8, e63799.
- Xiong, X., R. Xie, H. Zhang, L. Gu, W. Xie, M. Cheng, Z. Jian, K. Kovacina & H. Zhao (2014) PRAS40 plays a pivotal role in protecting against stroke by linking the Akt and mTOR pathways. *Neurobiol Dis*, 66, 43-52.
- Yadav, A., S. Vallabu, S. Arora, P. Tandon, D. Slahan, S. Teichberg & P. C. Singhal (2010) ANG II promotes autophagy in podocytes. *Am J Physiol Cell Physiol*, 299, C488-96.
- Yamamoto, T., N. A. Noble, A. H. Cohen, C. C. Nast, A. Hishida, L. I. Gold & W. A. Border (1996) Expression of transforming growth factor-beta isoforms in human glomerular diseases. *Kidney Int*, 49, 461-9.

- Yamamoto, T., T. Watanabe, N. Ikegaya, Y. Fujigaki, K. Matsui, H. Masaoka, M. Nagase & A. Hishida (1998) Expression of types I, II, and III TGF-beta receptors in human glomerulonephritis. *J Am Soc Nephrol*, 9, 2253-61.
- Yanagida-Asanuma, E., K. Asanuma, K. Kim, M. Donnelly, H. Young Choi, J. Hyung Chang, S. Suetsugu, Y. Tomino, T. Takenawa, C. Faul & P. Mundel (2007) Synaptopodin protects against proteinuria by disrupting Cdc42:IRSp53:Mena signaling complexes in kidney podocytes. *Am J Pathol*, 171, 415-27.
- Yang, Q. & K. L. Guan (2007) Expanding mTOR signaling. *Cell Res*, 17, 666-81.
- Young, A. R. & M. Narita (2011) Spatio-temporal association between mTOR and autophagy during cellular senescence. *Autophagy*, 7, 1387-8.
- Yu, L., Q. Lin, J. Feng, X. Dong, W. Chen, Q. Liu & J. Ye (2013) Inhibition of nephrin activation by c-mip through Csk-Cbp-Fyn axis plays a critical role in Angiotensin II-induced podocyte damage. *Cell Signal*, 25, 581-8.
- Yu, L., C. K. McPhee, L. Zheng, G. A. Mardones, Y. Rong, J. Peng, N. Mi, Y. Zhao, Z. Liu, F. Wan, D. W. Hailey, V. Oorschot, J. Klumperman, E. H. Baehrecke & M. J. Lenardo (2010) Termination of autophagy and reformation of lysosomes regulated by mTOR. *Nature*, 465, 942-6.
- Yu, S. & L. Yu (2012) Dexamethasone Resisted Podocyte Injury via Stabilizing TRPC6 Expression and Distribution. *Evid Based Complement Alternat Med*, 2012, 652059.

- Yuan, H., E. Takeuchi & D. J. Salant (2002) Podocyte slit-diaphragm protein nephrin is linked to the actin cytoskeleton. *Am J Physiol Renal Physiol*, 282, F585-91.
- Zalckvar, E., H. Berissi, L. Mizrachy, Y. Idelchuk, I. Koren, M. Eisenstein, H. Sabanay, R. Pinkas-Kramarski & A. Kimchi (2009) DAP-kinase-mediated phosphorylation on the BH3 domain of beclin 1 promotes dissociation of beclin 1 from Bcl-XL and induction of autophagy. *EMBO Rep*, 10, 285-92.
- Zhang, X., S. Chen, L. Song, Y. Tang, Y. Shen, L. Jia & W. Le (2014a) MTOR-independent, autophagic enhancer trehalose prolongs motor neuron survival and ameliorates the autophagic flux defect in a mouse model of amyotrophic lateral sclerosis. *Autophagy*, 10, 588-602.
- (2014b) MTOR-independent, autophagic enhancer trehalose prolongs motor neuron survival and ameliorates the autophagic flux defect in a mouse model of amyotrophic lateral sclerosis. *Autophagy*, 10.
- Zhang, X., H. Yan, Y. Yuan, J. Gao, Z. Shen, Y. Cheng, Y. Shen, R. R. Wang, X. Wang, W. W. Hu, G. Wang & Z. Chen (2013) Cerebral ischemia-reperfusion-induced autophagy protects against neuronal injury by mitochondrial clearance. *Autophagy*, 9.
- Zhu, H., H. Wu, X. Liu, B. Li, Y. Chen, X. Ren, C. G. Liu & J. M. Yang (2009) Regulation of autophagy by a beclin 1-targeted microRNA, miR-30a, in cancer cells. *Autophagy*, 5, 816-23.
- Zhuo, C., Y. Ji, Z. Chen, K. Kitazato, Y. Xiang, M. Zhong, Q. Wang, Y. Pei, H. Ju & Y. Wang (2013) Proteomics analysis of autophagy-deficient Atg7^{-/-}

MEFs reveals a close relationship between F-actin and autophagy. *Biochem Biophys Res Commun*, 437, 482-8.

Ziyadeh, F. N. & G. Wolf (2008) Pathogenesis of the podocytopathy and proteinuria in diabetic glomerulopathy. *Curr Diabetes Rev*, 4, 39-45.

Zou, M. S., J. Yu, G. M. Nie, W. S. He, L. M. Luo & H. T. Xu (2010) 1, 25-dihydroxyvitamin D3 decreases adriamycin-induced podocyte apoptosis and loss. *Int J Med Sci*, 7, 290-9.

Zuo, Y., H. C. Yang, S. A. Potthoff, B. Najafian, V. Kon, L. J. Ma & A. B. Fogo (2012) Protective effects of PPARgamma agonist in acute nephrotic syndrome. *Nephrol Dial Transplant*, 27, 174-81.